

# **CD1d-Restricted Antigen Presentation to Natural Killer T Cells in Intestinal Homeostasis**



## **Dissertation**

zur Erlangung des Doktorgrades der Mathematisch-Naturwissenschaftlichen  
Fakultät der Christian-Albrechts-Universität zu Kiel

Vorgelegt von

**Marie Dowds**

Kiel, 2015

Erste/r Gutachter/in: Prof. Dr. med. Sebastian Zeißig

Zweite/r Gutachter/in: Prof. Dr. rer. nat. Thomas Röder

Tag der mündlichen Prüfung: 17.12.2015

Zum Druck genehmigt: 17.12.2015

gez. Prof. Dr. Wolfgang J. Duschl, Dekan

**Part I: Protective Mucosal Immunology Mediated by Epithelial CD1d and IL-10..... 1**

1	Introduction.....	1
1.1	Inflammatory Bowel Disease.....	1
1.2	Natural Killer T cells and Their Role in Intestinal Homeostasis .....	1
2	Publication .....	6
3	Discussion .....	25

**Part II: Genetically Engineered CD1d Proteins for the Investigation of the CD1d-Associated Lipid Repertoire ..... 27**

1	Introduction.....	27
1.1	CD1d Structure and Trafficking.....	27
1.2	CD1d-Associated Lipids.....	28
1.3	Constructs for the Analysis of the CD1d-associated Lipidome.....	31
2	Materials .....	35
2.1	Antibodies .....	35
2.2	Bacteria.....	35
2.3	Buffers and Solutions.....	35
2.4	Cell Lines .....	37
2.5	Cell Culture Reagents.....	37
2.6	Chemicals and Reagents.....	38
2.7	Consumables .....	39
2.8	Enzymes and Substrates .....	40
2.9	Kits.....	40
2.10	Lipids .....	41
2.11	Instruments.....	41
2.12	Plasmids and DNA constructs .....	43

2.13	Software .....	43
2.14	Primers .....	44
3	Methods.....	45
3.1	Molecular Biological Methods .....	45
3.1.1	Polymerase Incomplete Primer Extension Polymerase Chain Reaction (PIPE PCR) .....	45
3.1.2	Agarose Gel Electrophoresis.....	46
3.1.3	Restriction Digest .....	47
3.1.4	Ligation.....	48
3.1.5	Bacterial Transformation of Chemically Competent <i>E. coli</i> Strains.....	48
3.1.6	DNA Isolation from Bacterial Cells .....	49
3.1.7	TEV Protease Digest.....	49
3.1.8	Sortase A (SrtA) Digest .....	50
3.2	Cell Biological Methods.....	51
3.2.1	Cultivation of Immortalized Cell Lines.....	51
3.2.2	Thawing of Cells Frozen for Long Term Storage.....	51
3.2.3	Freezing Cells for Long Term Storage.....	51
3.2.4	Transfection of Adherent Cells Using Lipofectamine .....	52
3.2.5	Transfection of Adherent Cells Using Turbofect .....	52
3.2.6	Cell Killing Curve .....	53
3.2.7	Generation of Stably Transfected Cell Lines .....	53
3.3	Immunological Methods .....	54
3.3.1	Staining of Cells for Flow Cytometry (FACS).....	54
3.3.2	mCD1d Enzyme Linked Immunosorbent Assay (ELISA).....	55
3.3.3	mIL-2 ELISA .....	56
3.3.4	Antigen Presentation Assay .....	56
3.3.5	Statistical Analysis.....	56
4	Results.....	57

4.1	Expression of Secreted and TEV Protease-Cleavable mCD1d.....	57
4.2	TEV Protease for Enzymatic Release of CD1d.....	61
4.3	Investigation of different buffer systems and alternative TEV proteases....	64
4.4	Glycine-Serine Spacers Do Not Promote TEV Protease Dependent Cleavage of h $\beta$ <sub>2</sub> m_mCD1d_TEV .....	66
4.5	Sortase A for proteolytic release of CD1d.....	68
4.6	Increased LPETG_CD1d Expression Through Use of an Alternative Plasmid Backbone.....	71
4.7	CD1d-Dependent Antigen Presentation Is Affected by Gly-Ser Spacers ...	74
5	Discussion .....	77
5.1	H $\beta$ <sub>2</sub> m_mCD1d_TEV Protease Does Not Allow for Proteolytic Release of Cell Surface CD1d.....	77
5.2	Sortase A-Mediated Release of Cell Surface CD1d.....	79
5.3	Conclusion and Outlook.....	82
6	Summary .....	84
7	Zusammenfassung .....	86
8	Bibliography.....	88
9	Appendix.....	100
9.1	Figure Index.....	100
9.2	Table Index .....	101
9.3	Plasmid Maps .....	102
	<b>Acknowledgments.....</b>	<b>110</b>
	<b>Curriculum Vitae.....</b>	<b>111</b>
	<b>Erklärung.....</b>	<b>113</b>

## Abbreviations

$\alpha$ GalCer	$\alpha$ -galactosylceramide
$\alpha$ GalGalCer	galactosyl- $\alpha$ 1-2-galactosylceramide
AP	adaptor protein
APC	antigen presenting cell
$\beta_2$ m	$\beta_2$ -microglobulin
$\beta$ GalCer	$\beta$ -galactosylceramide
$\beta$ GlcCer	$\beta$ -glucosylceramide
CD	Crohn's Disease
CD1	cluster of differentiation 1
DMEM	Dulbecco's Modified Eagle Medium
DN	double negative
DP	double positive
<i>E.coli</i>	<i>Escherichia coli</i>
eLPA	ether bonded lysophosphatidic acid
ER	endoplasmic reticulum
Fig.	figure
<i>g</i>	gravitational force
g	grams
GILT	$\gamma$ -interferon inducible lysosomal thioreductase
Gly	glycine
GPL	glycerophospholipid
GSL	glycosphingolipid
h	hour
hCD1d	human CD1d
HBSS	Hank's Balanced Salt Solution
HSP110	heat shock protein 110
IBD	Inflammatory Bowel Disease
IEC	intestinal epithelial cell
IEL	intraepithelial lymphocyte
iGb3	isoglobotrihexosylceramide
IL-...	interleukin-...

iNKT cell	invariant natural killer T cell
LPC	lysophosphatidylcholine
LPE	lysophosphatidylethanolamine
LPL	lamina propria lymphocyte
min	minute
MHC	major histocompatibility complex
mCD1d	mouse CD1d
ml	milliliter
MTP	microsomal triglyceride transfer protein
NKT cell	natural killer T cell
niNKT cell	non-invariant natural killer T cell
pLPE	plasmalogen lysophosphatidylethanolamine
RPMI 1640	Roswell Park Memorial Institute medium 1640
Ser	serine
s	second
<i>S.aureus</i>	<i>Staphylococcus aureus</i>
Srt A	sortase A
TEV	tobacco etch virus
TCR	T cell receptor
TD	tail deleted
TMD	transmembrane domain
UC	ulcerative colitis
Vol	volume
WT	wild type
X	random amino acid
Y	tyrosine
ϕ	bulky, hydrophobic amino acid

## **Part I: Protective Mucosal Immunology Mediated by Epithelial CD1d and IL-10**

### **1 Introduction**

#### **1.1 Inflammatory Bowel Disease**

Inflammatory Bowel Disease (IBD) is a collective term for chronic remittent or progressive inflammatory disorders of the intestine. There are two major forms of IBD. Crohn's Disease (CD) can affect the entire gastrointestinal tract, but most commonly involves the small intestine and the colon. It is characterized by transmural inflammation that usually occurs in patches and is sometimes associated with fistulas or granulomas. Ulcerative colitis (UC) is limited to the rectum and colon and is characterized by inflammation of the superficial colonic mucosa. Though there are familial cases of IBD, intestinal inflammation most commonly occurs sporadically. Further, both forms are associated with an increased risk for intestinal or colorectal cancer.<sup>1-3</sup> While the precise mechanisms behind the development of IBD remain widely elusive, three essential components have been identified: the homeostasis of the intestinal immune system, host-microbe interactions and genetic factors.<sup>1</sup>

A common hypothesis for the development of IBD is that environmental stimuli induce uncontrolled intestinal inflammation in genetically susceptible individuals.<sup>1</sup> The human intestinal tract houses a multitude of commensal bacteria that co-exist with the host's immune system in a mutually beneficial relationship.<sup>4</sup> In patients with IBD, the immune system shows an inadequate, excessive response, which is in part directed against the commensal microbiota and is associated with severe intestinal inflammation.<sup>1-3</sup> While both the innate and adaptive immune system contribute to the pathogenesis of IBD, recent data suggest a critical involvement of CD1d-restricted, lipid-reactive Natural Killer T (NKT) cells in the initiation and promotion of intestinal inflammation in human UC.<sup>5,6</sup>

#### **1.2 Natural Killer T cells and Their Role in Intestinal Homeostasis**

NKT cells are a subset of T cells that were originally characterized by the co-expression of an  $\alpha\beta$  T cell receptor (TCR) and the NK cell marker NK1.1.<sup>7</sup> This definition has since been redefined to describe lipid-reactive T cells that are restricted



by the atypical major histocompatibility complex (MHC) class I molecule CD1d (cluster of differentiation 1 d).<sup>8</sup>

NKT cell development begins in the thymus with a double negative (DN) stage, which develops into a CD4<sup>+</sup>CD8<sup>+</sup> double positive (DP) stage upon expression of the TCR. During this DP stage, NKT cells undergo positive selection upon interaction with CD1d molecules loaded with endogenous, agonistic lipid antigens, expressed on other DP thymocytes. The lipid antigens involved in this positive selection remain to be identified. Unlike conventional T cells, NKT cells undergo multiple rounds of expansion in the thymus, during which they develop an effector/memory phenotype, before emigrating to the periphery.<sup>9–11</sup>

There are two subsets of NKT cells: Type I NKT cells, or invariant NKT (iNKT) cells, use a limited set of TCR genes to form a semi-invariant TCR. In mice, this TCR is composed of a *Vα14-Jα18* α-chain, preferentially combined with a *Vβ8.2*, *Vβ7* or *Vβ2* β-chain. Human iNKT cells express a TCR consisting of a *Vα24J-α18* α-chain, which preferentially assembles with a *Vβ11* β-chain. Type II NKT cells, or non-invariant NKT (niNKT) cells, have a broader TCR repertoire and are less well understood compared to iNKT cells. Despite the limited variability of the iNKT TCR, iNKT cells are capable of detecting a range of lipids presented by CD1d.<sup>12</sup> One of the most agonistic lipids identified to date is α-galactosylceramide (αGalCer), which was originally isolated from a marine sponge.<sup>13</sup> The use of CD1d tetramers loaded with αGalCer allows for the highly specific detection of iNKT cells<sup>8,10,14</sup> In contrast, a specific and universal method for the detection of niNKT cells has not been described so far, although a subset of niNKT cells can be successfully detected using sulfatide-loaded CD1d tetramers.<sup>15</sup>

Due to their versatility, iNKT cells have been named a “Swiss Army Knife” by *Matsuda* and colleagues.<sup>11</sup> By rapid secretion of copious amounts of various cytokines and chemokines, iNKT cells act on many other cells of the innate and adaptive immune system, thereby acting as an important mediator between innate and adaptive immunity (Figure 1).<sup>9</sup> As such, they are involved in a multitude of immune responses, including bacterial, parasitic and viral clearance, allergies, anti-tumor responses and inflammatory conditions.<sup>12</sup> Most NKT cells express surface antigens reflective of their status as effector memory T cells. One of the most characteristic features of iNKT cells is their capacity to secrete large amounts of IL-4

and IFN $\gamma$  only hours after activation, thereby diverting the immune reaction either towards a Th1 or a Th2 response.<sup>11</sup>

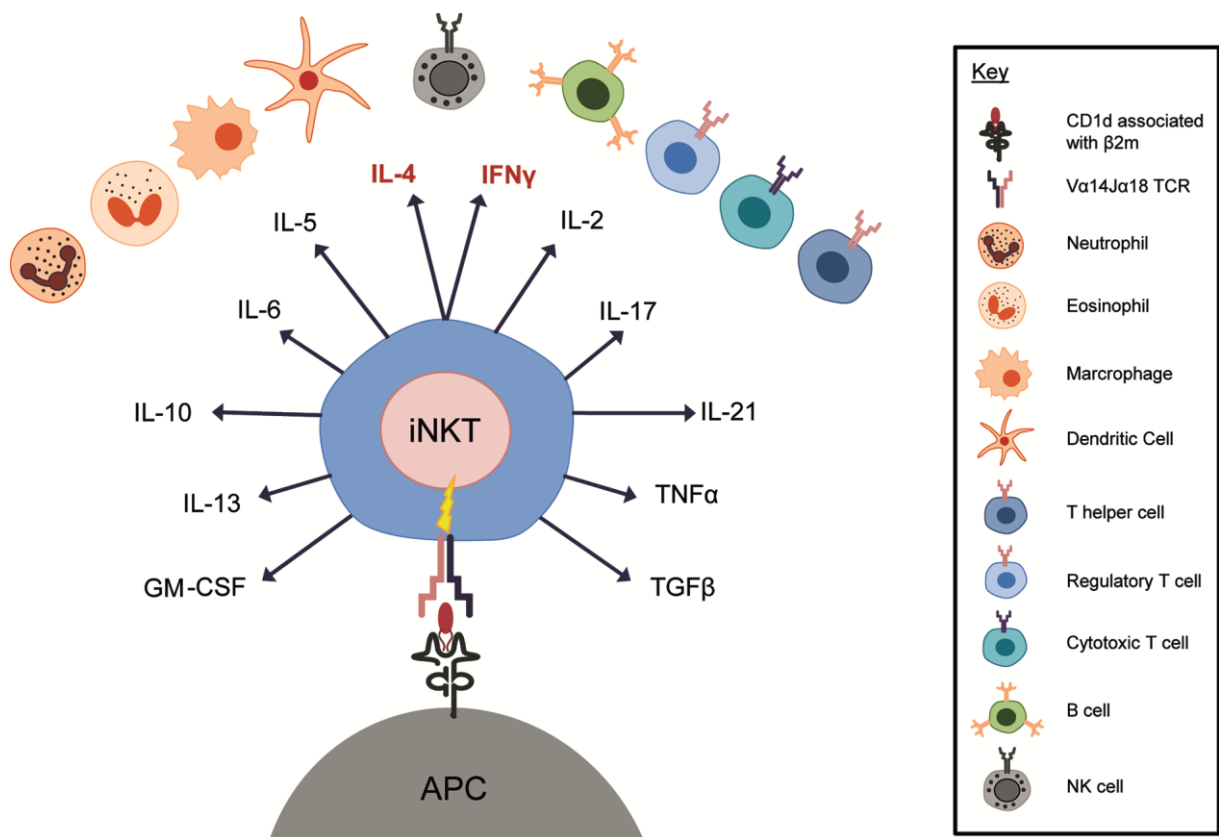


**Figure 1: NKT Cells Secrete Various Cytokines Upon Activation**

A CD1d molecule expressed on an antigen presenting cell (APC) loaded with a lipid antigen interacts with the NKT TCR, activating the NKT cell. NKT cells are capable of producing a range of cytokines and thereby influence most cells of the innate (left) and adaptive (right) immune system. Adapted from Matsuda et al. 2008.<sup>11</sup>

Studies investigating the relative frequencies of NKT cells in the intestines of mice<sup>8,16,17</sup> and humans<sup>5,18</sup> did not lead to conclusive results, most likely because the accuracy of the methods used for the detection of NKT cells varies greatly. Within older studies, NKT cells were identified based on the historic definition of CD3<sup>+</sup>/TCR $\alpha\beta$ <sup>+</sup>NK1.1<sup>+</sup> cells, the more precise  $\alpha$ GalCer-loaded CD1d tetramer has become the method of choice in more recent studies. It did become apparent, though, that iNKT cells only make up for a small fraction of lamina propria lymphocytes (LPL) and intraepithelial lymphocytes (IEL) (max. 0.5 % of LPLs in studies using the  $\alpha$ GalCer-loaded CD1d tetramer).<sup>5,17</sup> Nevertheless, this small subset of immune cells has a significant impact on the severity of intestinal inflammation in various animal models of IBD. Oxazolone colitis, a mouse model of UC induced by

rectal administration of the haptening agent oxazolone, has been shown to be strongly dependent on secretion of Th2 cytokines (IL-4 and IL-13) from iNKT cells.<sup>5,16,19</sup>  $J\alpha 18^{-/-}$  mice, which do not express the canonical iNKT TCR and therefore do not develop iNKT cells, as well as  $CD1d^{-/-}$  mice, which are devoid of all NKT cells due to impaired CD1d-restricted positive selection in the thymus, do not develop oxazolone colitis.<sup>5,16,20</sup> Studies in human UC patients also revealed CD1d-dependent secretion of epithelial barrier-disruptive IL-13, associated with NKT cell-dependent immune responses. However, contrary to observations made in mice, the T cells involved in the secretion of IL-13 did not bind the  $\alpha$ GalCer-loaded CD1d tetramer and were therefore likely niNKT cells and not iNKT cells.<sup>5,6</sup>

Conversely,  $\alpha$ GalCer-primed iNKT cells have been shown to ameliorate intestinal inflammation in Th1 driven mouse models of intestinal inflammation, such as DSS colitis, which is less dependent on the adaptive immune response than oxazolone colitis.<sup>21,22</sup> The most likely explanation for this observation is that NKT cells stimulated with  $\alpha$ GalCer robustly secrete Th2 cytokines, such as IL-4, and thereby counteract the Th1 response causing the inflammation.<sup>23</sup>

How an NKT cell reacts to antigen presentation likely depends on the lipid antigen presented and the APCs involved in this process. Since CD1d is widely expressed by a range of cell types, antigens are not only presented by professional APCs such as dendritic cells, but also by endothelial or epithelial cells.<sup>24</sup> For a long time, the intestinal epithelium was seen as a solely physical barrier between the microbiota and the intestinal immune system. However, it has become apparent that intestinal epithelial cells (IECs) can actively influence intestinal homeostasis through secretion of cytokines under constitutive conditions and upon exposure to parasites, bacteria or pro-inflammatory cytokines.<sup>25</sup> Moreover, malfunctions in IEC physiology, for instance through excessive ER stress responses, can cause spontaneous intestinal inflammation.<sup>1,26</sup> Crosslinking experiments of CD1d on intestinal epithelial cell lines *in vitro* have demonstrated the induction of heat shock protein 110 (HSP110) and IL-10 upon engagement of CD1d.<sup>27,28</sup> Both of these proteins may have a beneficial effect on intestinal inflammation, if engagement of CD1d on IECs also induces their expression *in vivo*. This raised the question of whether CD1d-mediated antigen presentation by IECs and subsequent activation of intestinal NKT cells might have a different effect on intestinal homeostasis compared to antigen presentation by

professional antigen presenting cells. Indeed, we could demonstrate in collaboration with Dr. Richard S. Blumberg's laboratory that the response of NKT cells to antigen presentation does not only depend on the antigen itself, but also on the antigen presenting cell. As such, antigen presentation by the intestinal epithelium induces a protective immune response, rather than an inflammatory response, while bone marrow-derived immune cells contribute to the pathogenesis of intestinal inflammation in a CD1d-restricted manner.<sup>29</sup> This demonstrates that lipid antigen presentation plays critical roles in NKT cell immunity and promotes beneficial as well as pathogenic NKT cell-dependent immune responses in mucosal immunity.

## 2 Publication

## LETTER

doi:10.1038/nature13150

## Protective mucosal immunity mediated by epithelial CD1d and IL-10

Torsten Olszak<sup>1\*</sup>, Joana F. Neves<sup>1\*</sup>, C. Marie Dowds<sup>2\*</sup>, Kristi Baker<sup>1</sup>, Jonathan Glickman<sup>3</sup>, Nicholas O. Davidson<sup>4</sup>, Chyuan-Sheng Lin<sup>5</sup>, Christian Jobin<sup>6</sup>, Stephan Brand<sup>7</sup>, Karl Sotlar<sup>8</sup>, Koichiro Wada<sup>9</sup>, Kazufumi Katayama<sup>9</sup>, Atsushi Nakajima<sup>10</sup>, Hiroyuki Mizuguchi<sup>11</sup>, Kunito Kawasaki<sup>12</sup>, Kazuhiro Nagata<sup>12</sup>, Werner Müller<sup>13</sup>, Scott B. Snapper<sup>1,14</sup>, Stefan Schreiber<sup>2</sup>, Arthur Kaser<sup>15</sup>, Sebastian Zeissig<sup>1,2\*</sup> & Richard S. Blumberg<sup>1\*</sup>

The mechanisms by which mucosal homeostasis is maintained are of central importance to inflammatory bowel disease. Critical to these processes is the intestinal epithelial cell (IEC), which regulates immune responses at the interface between the commensal microbiota and the host<sup>1,2</sup>. CD1d presents self and microbial lipid antigens to natural killer T (NKT) cells, which are involved in the pathogenesis of colitis in animal models and human inflammatory bowel disease<sup>3–8</sup>. As CD1d crosslinking on model IECs results in the production of the important regulatory cytokine interleukin (IL)-10 (ref. 9), decreased epithelial CD1d expression—as observed in inflammatory bowel disease<sup>10,11</sup>—may contribute substantially to intestinal inflammation. Here we show in mice that whereas bone-marrow-derived CD1d signals contribute to NKT-cell-mediated intestinal inflammation, engagement of epithelial CD1d elicits protective effects through the activation of STAT3 and STAT3-dependent transcription of IL-10, heat shock protein 110 (HSP110; also known as HSP105), and CD1d itself. All of these epithelial elements are critically involved in controlling CD1d-mediated intestinal inflammation. This is demonstrated by severe NKT-cell-mediated colitis upon IEC-specific deletion of IL-10, CD1d, and its critical regulator microsomal triglyceride transfer protein (MTP)<sup>12,13</sup>, as well as deletion of HSP110 in the radioresistant compartment. Our studies thus uncover a novel pathway of IEC-dependent regulation of mucosal homeostasis and highlight a critical role of IL-10 in the intestinal epithelium, with broad implications for diseases such as inflammatory bowel disease.

To examine the function of CD1d in the intestinal epithelium, we generated mice with tamoxifen-inducible IEC-specific deletion of MTP, a lipid transfer protein encoded by *Mttp* and required for CD1d function<sup>12,13</sup> (Villin-CreER<sup>T2</sup> (ref. 14) × *Mttp*<sup>fl/fl</sup> (ref. 15); hereafter referred to as *Mttp*<sup>ΔIEC</sup>). *Mttp*<sup>ΔIEC</sup> mice exhibited no evidence of epithelial lipid accumulation (Extended Data Fig. 2a) and endoplasmic reticulum (ER) stress (Extended Data Fig. 2b), but showed decreased IEC-mediated, CD1d- but not major histocompatibility complex (MHC)-class-I-dependent antigen presentation despite unimpaired CD1d expression (Extended Data Fig. 3a, b, c left). *Mttp*<sup>ΔIEC</sup> mice exhibited increased sensitivity to oxazolone-induced colitis, a CD1d- and NKT-cell-dependent colitis model<sup>4</sup>, as shown by increased mortality (Fig. 1a, left), weight loss (Fig. 1a, right) and histological injury (Fig. 1b and Extended Data Fig. 3d), in comparison with wild-type littermates (Villin-CreER<sup>T2</sup>-negative *Mttp*<sup>fl/fl</sup> mice). Increased severity of colitis was not caused by primary epithelial barrier defects (Extended Data Fig. 4a) but was due to loss of function

of intestinal epithelial CD1d. Thus, bone marrow chimaeras with selective deficiency of CD1d in the radioresistant compartment exhibited severe mortality and morbidity in the oxazolone model (Fig. 1c, d), increased production of pathogenic IL-13 and IL-1β in colon explants (Fig. 1e) and purified CD11b<sup>+</sup> lamina propria cells (Extended Data Fig. 4b), and reduced secretion of protective IL-10 (Fig. 1e). In accordance with a protective role of intestinal epithelial CD1d, its expression was upregulated in response to oxazolone colitis in wild-type, but not *Mttp*<sup>ΔIEC</sup> mice (Extended Data Fig. 3c, right). Intriguingly, pathogenic signals were similarly CD1d-dependent but emanated from non-epithelial cells in a manner dependent on adaptive immune cells. Thus, *Mttp*<sup>ΔIEC</sup> mice on a *Rag1*<sup>-/-</sup> or *Cd1d1*<sup>-/-</sup> *Cd1d2*<sup>-/-</sup> (CD1d-knockout) background were protected from oxazolone colitis (Extended Data Fig. 4c, d). Consistent with a role of non-epithelial cells in the delivery of pathogenic CD1d signals, antibody-mediated neutralization of (non-epithelial) CD1d in *Mtp*<sup>ΔIEC</sup> mice reduced the severity of oxazolone-induced colitis (Fig. 1f, g). Thus, intestinal epithelial CD1d- and MTP-dependent lipid antigen presentation protects from oxazolone colitis, whereas CD1d- and NKT-cell-mediated inflammation emanates from non-epithelial cells, presumably bone-marrow-derived lamina propria cells.

To investigate directly the role of epithelial CD1d, we developed mice with inducible, IEC-specific deletion of CD1d (Villin-CreER<sup>T2</sup> × *Cd1d*<sup>fl/fl</sup>, hereafter referred to as *Cd1d*<sup>ΔIEC</sup>) (Extended Data Fig. 5a). Tamoxifen-treated *Cd1d*<sup>ΔIEC</sup> mice exhibited normal numbers of invariant (i)NKT cells and lacked intestinal epithelial expression of CD1d and CD1d- but not MHC-class-I-mediated antigen presentation by IECs (Extended Data Fig. 5b–e). Oxazolone-challenged *Cd1d*<sup>ΔIEC</sup> mice, like *Mtp*<sup>ΔIEC</sup> mice, exhibited increased mortality (Fig. 1h, left), weight loss (Fig. 1h, right), histopathological injury (Fig. 1i), colon shortening (Extended Data Fig. 5f) and elevated secretion of IL-13 and IL-1β, as well as impaired secretion of IL-10 from colon explant cultures (Fig. 1j). Moreover, colonic iNKT cells from *Cd1d*<sup>ΔIEC</sup> mice showed increased IL-13 and IFN-γ expression in oxazolone colitis (Fig. 1k). Thus, intestinal epithelial CD1d protects from intestinal inflammation.

To gain insight into the mechanisms underlying protection by intestinal epithelial CD1d, we performed transcriptional profiling of intestinal mucosal scrapings from wild-type and *Mtp*<sup>ΔIEC</sup> mice in the oxazolone model (Extended Data Table 1 and data not shown). HSP110, encoded by *Hsp110*, exhibited decreased expression in *Mtp*<sup>ΔIEC</sup> mice (Fig. 2a), which was of interest given its known role in induction of epithelial CD1d expression<sup>16</sup>. In line with a potential MTP- and CD1d-dependent role of

<sup>1</sup>Division of Gastroenterology, Hepatology, and Endoscopy, Brigham and Women's Hospital, Harvard Medical School, Boston, Massachusetts 02115, USA. <sup>2</sup>Department of Internal Medicine I, University Medical Center Schleswig-Holstein, 24105 Kiel, Germany. <sup>3</sup>GI Pathology, Miraca Life Sciences, Newton, Massachusetts 02464, USA. <sup>4</sup>Division of Gastroenterology, Washington University School of Medicine, St Louis, Missouri 63110, USA. <sup>5</sup>Herbert Irving Comprehensive Cancer Center, Columbia University, New York, New York 10032, USA. <sup>6</sup>Department of Medicine, Department of Infectious Diseases & Pathology, University of Florida, Gainesville, Florida 32611, USA. <sup>7</sup>Department of Medicine II-Grosshadern, Ludwig Maximilians University, Munich 81377, Germany. <sup>8</sup>Institute of Pathology, Ludwig Maximilians University, Munich 80337, Germany. <sup>9</sup>Department of Pharmacology, Graduate School of Dentistry, Osaka University, Osaka 565-0871, Japan. <sup>10</sup>Gastroenterology Division, Yokohama City University School of Medicine, Yokohama, Kanagawa 236-0027, Japan. <sup>11</sup>Laboratory of Biochemistry and Molecular Biology, Graduate School of Pharmaceutical Sciences, Osaka University, Osaka 565-0871, Japan. <sup>12</sup>Department of Molecular Biosciences, Faculty of Life Sciences, Kyoto Sangyo University, Motoyama, Kamigamo, Kita-ku, Kyoto 603-8555, Japan. <sup>13</sup>Faculty of Life Sciences, University of Manchester, Manchester M13 9PL, UK. <sup>14</sup>Division of Pediatric Gastroenterology, Hepatology, and Nutrition, Department of Medicine, Children's Hospital Boston, Boston, Massachusetts 02115, USA. <sup>15</sup>Division of Gastroenterology, Addenbrooke Hospital, University of Cambridge, Cambridge CB2 0QQ, UK.

\*These authors contributed equally to this work.

RESEARCH LETTER

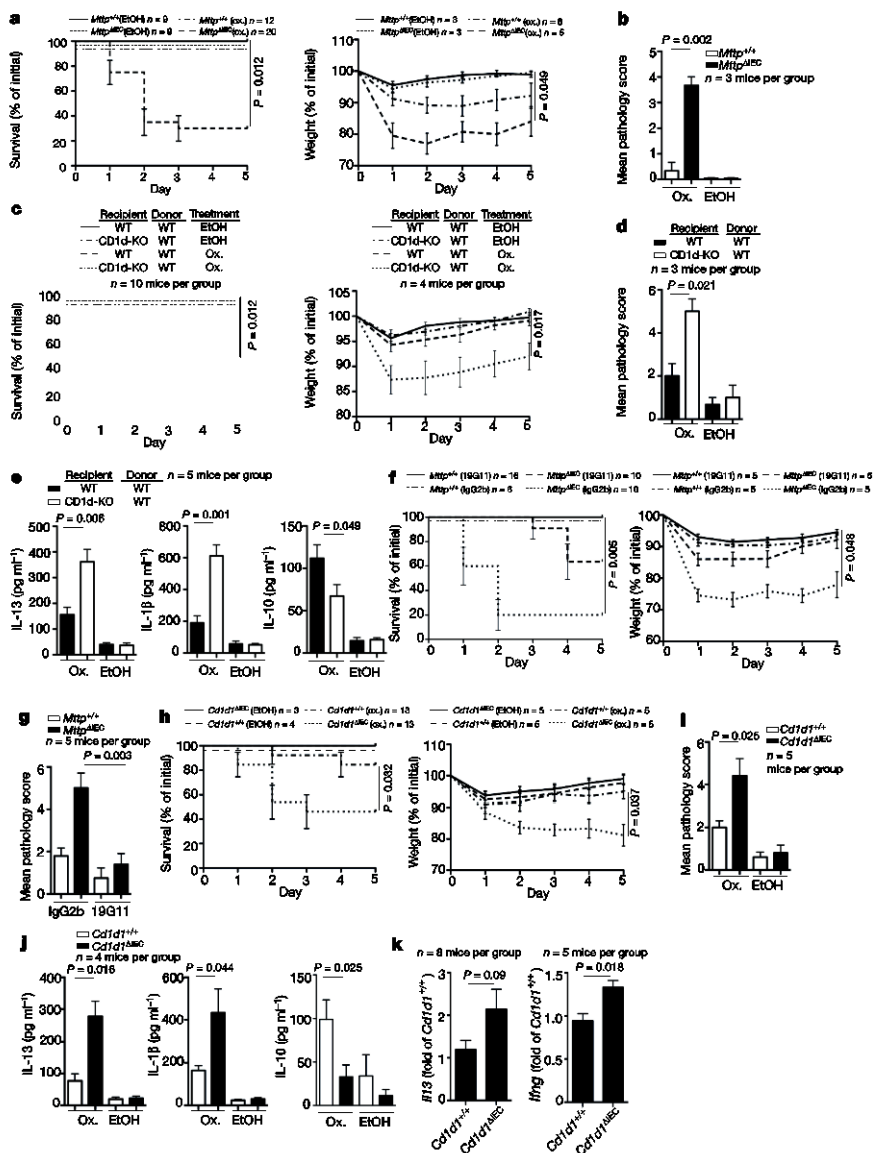


**Figure 1 | Intestinal epithelial MTP and CD1d protect from oxazolone colitis.** a–k, Survival (a, left, c, left, f, left, h, left), body weight (a, right, c, right, f, right, h, right), histopathology (b, d, g, i), cytokine secretion (enzyme-linked immunosorbent assay (ELISA)) in colon explant cultures (e, j), and cytokine expression (quantitative polymerase chain reaction (qPCR)) of sorted colonic iNKT cells combined from intraepithelial and lamina propria compartments (k) of the indicated mice upon rectal challenge with oxazolone (ox, a–k) or vehicle (ethanol (EtOH, a–e, h–j)). c–e, Wild-type (WT) and CD1d-knockout (CD1d-KO) mice were reconstituted with wild-type bone marrow. f, g, 19G11 (anti-CD1d) or isotype control antibody (IgG2b) were administered. Results representative of three independent experiments are shown. Mean ± standard error of the mean (s.e.m.) of the indicated number of mice is shown. j, Right, Mann–Whitney *U*-test was applied. In all other panels, Student’s *t*-test or log-rank test (survival) were applied.

HSP110 in intestinal inflammation, HSP110 messenger RNA (Fig. 2b, left) and protein expression (Extended Data Fig. 6a) were increased in IECs from wild-type but not *Mtp*<sup>AIEC</sup> mice upon oxazolone challenge. Similar observations were made for *Cd1d*<sup>AIEC</sup> mice (Fig. 2b, right). In addition, intestinal epithelial but not lamina propria HSP110 expression was reduced in active and inactive human ulcerative colitis compared with healthy controls (Fig. 2c and Extended Data Fig. 6b), which is in accordance with impaired epithelial CD1d expression in inflammatory bowel disease, as previously reported<sup>19</sup>. Furthermore, consistent with regulation of CD1d expression by HSP110 (ref. 16), oxazolone colitis was associated with induction of CD1d expression in wild-type but not *Mtp*<sup>AIEC</sup> IECs (Extended Data Fig. 3c, right). Together, these data indicate that IEC CD1d and MTP are required for epithelial HSP110 upregulation during oxazolone-induced colitis and that alterations in this pathway are observed in human ulcerative colitis.

To understand better the functional consequences of epithelial HSP110 deficiency observed in *Mtp*<sup>AIEC</sup> and *Cd1d*<sup>AIEC</sup> mice, bone marrow chimaeras of HSP110-knockout (HSP110-KO) or wild-type mice receiving wild-type bone marrow were studied. Compared with wild-type recipients, HSP110-knockout recipients of wild-type bone marrow exhibited increased mortality and weight loss (Fig. 2d), microscopic injury (Fig. 2e) and increased IL-13 and IL-1β secretion (Fig. 2f) in the oxazolone model. Morbidity and mortality in HSP110-knockout recipients of wild-type bone marrow reflected that observed for conventional HSP110-knockout mice, suggesting critical, protective effects of HSP110 in the radioresistant compartment, including IECs (Extended Data Fig. 6c). Antibody-mediated neutralization of CD1d reduced the severity of colitis in HSP110-knockout bone marrow chimaeras, in line with pathogenic CD1d-dependent signals originating from non-epithelial lamina propria cells (Fig. 2d, f). Together, these studies indicate

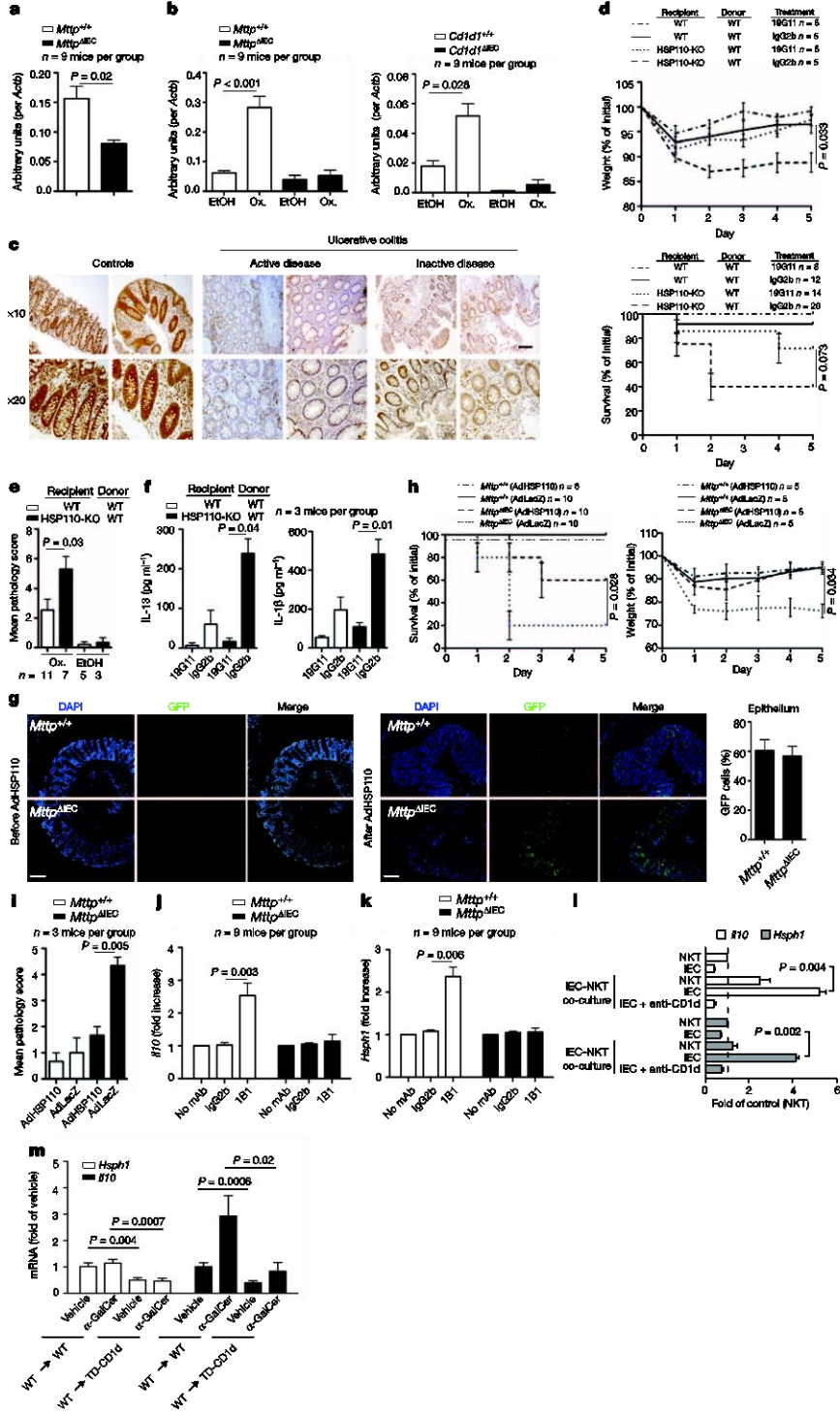


**Figure 2 | HSP110 elicits protective effects downstream of intestinal epithelial CD1d.** a, b, *Hsph1* expression (qPCR) in purified IECs of the indicated mouse strains at baseline (a) or on day 5 after rectal oxazolone (Ox.) or ethanol (EtOH) (b). c, HSP110 immunohistochemistry in colon of human ulcerative colitis and controls. d–i, Survival (d, bottom, h, left), body weight (d, top, h, right), histopathology (e, i), and cytokine secretion in colon explants (ELISA) (f) in the oxazolone model. d, f, Wild-type (WT) and HSP110-KO recipients of wild-type bone marrow received 19G11 anti-CD1d or isotype control antibody. g–i, Mice received adenoviruses expressing HSP110 (AdHSP110) or β-galactosidase (AdLacZ). g, Immunofluorescence of colonic GFP after AdHSP110-IRES2-eGFP administration. DAPI, 4',6-diamidino-2-phenylindole. j–l, MODE-K *Hsph1* and *I10* (qPCR) after antibody-mediated CD1d crosslinking (19G11) (j–k) or α-GalCer presentation to iNKT cells (2A7 hybridoma) in the presence/absence of neutralizing CD1d antibodies (19G11) (l). mAb, monoclonal antibody. m, *Hsph1* and *I10* (qPCR) in purified small intestinal IECs from wild-type and TD-CD1d recipients of wild-type bone marrow after injection with vehicle or α-GalCer (6 mice per group). c, g, Scale bars, 50 μm. Results representative of two or three independent experiments are shown. Means ± s.e.m. of the indicated number of mice or triplicate cultures (l) are indicated. Student's *t*-test or log-rank test (survival) were applied.

that reduced HSP110 expression in the absence of functional epithelial CD1d may contribute to severe oxazolone colitis. Consistent with this hypothesis, reconstitution of HSP110 expression by adenoviruses targeting IECs (Fig. 2g) ameliorated oxazolone-induced colitis in *Mtpp*<sup>ΔIEC</sup> mice, as shown by decreased mortality (Fig. 2h, left), weight loss (Fig. 2h, right) and microscopic injury (Fig. 2i). It is noteworthy that adenoviruses also

RESEARCH LETTER

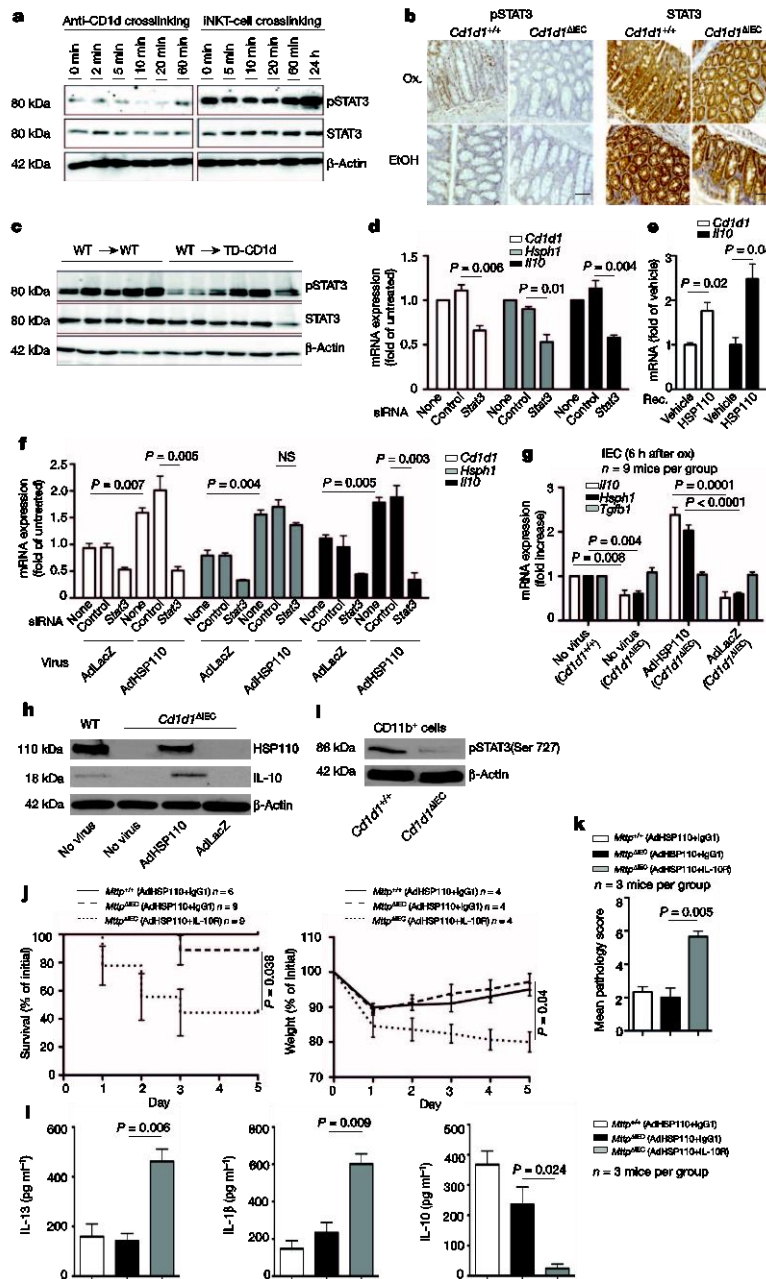


**Figure 3 | Epithelial CD1d induces STAT3-dependent expression of IL-10 and HSP110.** a, MODE-K pSTAT3 after CD1d-crosslinking (1B1 monoclonal antibody clone) or iNKT (2A.7 hybridoma) co-culture. b, Colonic pSTAT3 immunohistochemistry 5 days after rectal oxazolone (Ox.) or ethanol (EtOH). Scale bar, 50  $\mu$ m. c, pSTAT3 in purified small intestinal IECs from the indicated bone marrow chimaeras (IECs from one mouse per lane). d–f, *Cd1d1*, *Hsph1* and *Il10* (qPCR) in MODE-K cells after treatment with recombinant HSP110 (e) or *Stat3*/control siRNA knockdown (d, f) followed by viral transduction at a multiplicity of infection (MOI) of 5 (f). g, *Il10*, *Hsph1* and *Tgfb* in purified IECs (qPCR) 6 h after rectal oxazolone in the presence or absence of viral infection. The fold change compared to oxazolone-treated *Cd1d1*<sup>+/+</sup> mice without virus is indicated. h, Western blot of IECs 24 h after rectal oxazolone. i, Survival (j, left), body weight (j, right), histopathology (k) and cytokine secretion by colon explants (ELISA; l) of the indicated oxazolone-challenged mice with or without viral infection and antibody treatment as indicated. Results representative of three independent experiments are shown. Means  $\pm$  s.e.m. of the indicated number of mice or triplicate cultures (d–f) are indicated. Student's *t*-test or log-rank test (survival) were applied. NS, not significant.

targeted lamina propria cells (Fig. 2g), which may have contributed to protection from intestinal inflammation.

As mice with an IEC-specific deficiency in MTP and CD1d exhibited impaired epithelial expression of HSP110, we tested whether engagement of epithelial CD1d supports HSP110 expression. To this end, we investigated HSP110 in purified (Extended Data Fig. 7) colonic IECs after antibody-mediated CD1d crosslinking, a treatment previously shown to induce production of barrier-protective IEC-derived IL-10 (ref. 9). CD1d crosslinking led to increased expression of *Il10* (Fig. 2j) and *Hsph1* (Fig. 2k) in IECs from wild-type but not *Mtp*<sup>AIEC</sup> mice. Similar observations

were made upon *in vitro* co-culture of NKT cells with a mouse IEC line (Fig. 2l). Previous studies in a cultured human IEC line suggested that epithelial IL-10 production upon CD1d crosslinking is elicited through retrograde signalling dependent on the cytoplasmic tail of CD1d<sup>9</sup>. We therefore investigated whether bone marrow chimaeras with selective deletion of the cytoplasmic CD1d tail (hereafter referred to as tail-deleted (TD)-CD1d) in radioresistant cells exhibit impaired expression of *Il10* and *Hsph1* in purified IECs. Indeed, IECs obtained from these mice showed impaired expression of *Il10* and *Hsph1* under constitutive conditions and reduced expression after administration of the CD1d-binding



iNKT-cell-activating lipid  $\alpha$ -galactosylceramide ( $\alpha$ -GalCer) (Fig. 2m). These data demonstrate that engagement of epithelial CD1d induces expression of HSP110 and IL-10, presumably through retrograde CD1d signalling. Additional effects of the CD1d cytoplasmic tail, such as regulation of intracellular CD1d trafficking<sup>17</sup> and potential effects on NKT cell homing<sup>5</sup>, may further contribute to protection from intestinal inflammation.

As the *Il10*, *Hsph1* and *Cd1d1* genes contain STAT sites in their promoters (ref. 18 and T.O. *et al.*, unpublished observations), and as *Hsph1* and *Cd1d1* exhibit reduced expression in *Stat3*-deficient IECs (Gene Expression Omnibus accession number GSE15955)<sup>19</sup>, we reasoned that STAT3 may contribute to *Il10* and *Hsph1* expression downstream of CD1d. Indeed, epithelial STAT3 became phosphorylated in response to CD1d engagement by antibody crosslinking (Fig. 3a, left) and iNKT-cell co-culture (Fig. 3a, right, and Extended Data Fig. 8a). Moreover, impaired epithelial STAT3 phosphorylation was observed in *Cd1d1*<sup>ΔIEC</sup> mice (Fig. 3b) and TD-CD1d recipients of wild-type bone marrow (Fig. 3c). Furthermore, short interfering RNA (siRNA)-mediated knockdown of *Stat3* in the IEC line MODE-K (Extended Data Fig. 8b) led to reduced expression of *Cd1d1*, *Hsph1* and *Il10* (Fig. 3d). Together, these data demonstrate that STAT3 acts downstream of epithelial CD1d to induce expression of *Il10*, *Hsph1* and *Cd1d1*.

IL-10 and HSP110 do not only exhibit STAT3-dependent expression but also signal via STAT3 (refs 18, 20) and may thus further contribute to sustained activation of epithelial STAT3 and STAT3-dependent expression of *Cd1d1*, *Il10* and *Hsph1*. Consistent with this concept, both recombinant and adenoviral HSP110 induced epithelial expression of *Il10* and *Cd1d1* in MODE-K cells, which was abrogated upon siRNA-mediated knockdown of *Stat3* (Fig. 3e, f). Similar findings were made *in vivo*, as adenoviruses expressing HSP110, but not LacZ, restored epithelial expression of IL-10 in *Cd1d1*<sup>ΔIEC</sup> mice in the oxazolone model

(Fig. 3g, h). These data demonstrate that HSP110 acts in a STAT3-dependent manner to support the expression of IL-10 and CD1d by IECs.

Given HSP110-dependent regulation of epithelial IL-10 expression, we investigated whether the protective effects of HSP110 are dependent on IL-10. CD11b<sup>+</sup> lamina propria cells from *Cd1d1*<sup>ΔIEC</sup> mice showed decreased phosphorylated (p)STAT3 expression in oxazolone colitis, consistent with decreased IL-10 production by IECs and IL-10 receptor (IL-10R) signalling by lamina propria cells (Fig. 3i). Moreover, antibody-mediated IL-10R blocking prevented adenoviral HSP110-dependent amelioration of colitis (Fig. 3j–l). To investigate further the role of epithelial IL-10, we generated *Il10*<sup>-/-</sup> bone marrow chimaeras. *Il10* deletion in the radioresistant compartment resulted in increased mortality (Fig. 4a) and colonic IL-13 production (Fig. 4b) in the oxazolone model. Moreover, a similar trend was observed in mice with *Il10* deletion in the radiosensitive compartment (Fig. 4a, b). These data thus reveal that, in addition to the established role of bone-marrow-derived cells in IL-10-mediated control of intestinal inflammation<sup>21,22</sup>, IL-10 derived from radioresistant cells provides an additional, non-redundant pathway required for regulation of intestinal inflammation. To address whether protective IL-10 originates from the intestinal epithelium, we investigated oxazolone colitis in mice with inducible, epithelial-specific deletion of *Il10* (*Villin-CreER*<sup>T2</sup> × *Il10*<sup>fl/fl</sup>; hereafter referred to as *Il10*<sup>ΔIEC</sup>). Similar to mice with IEC-specific deletion of *Mtpp* and *Cd1d1* and mice with deletion of *Hsph1* and *Il10* in the radioresistant compartment, *Il10*<sup>ΔIEC</sup> mice exhibited increased mortality (Fig. 4c), weight loss (Fig. 4d) and histopathological inflammation (Fig. 4e) in the oxazolone model. Furthermore, in accordance with STAT3-mediated signalling by IL-10 (ref. 18) and STAT3-dependent expression of *Hsph1* and *Cd1d1* (Fig. 3d), IEC-specific *Il10* deletion was associated with reduced epithelial expression of *Hsph1* and a trend towards a reduction in *Cd1d1* expression in the oxazolone model (Fig. 4f). These results demonstrate that IEC-derived

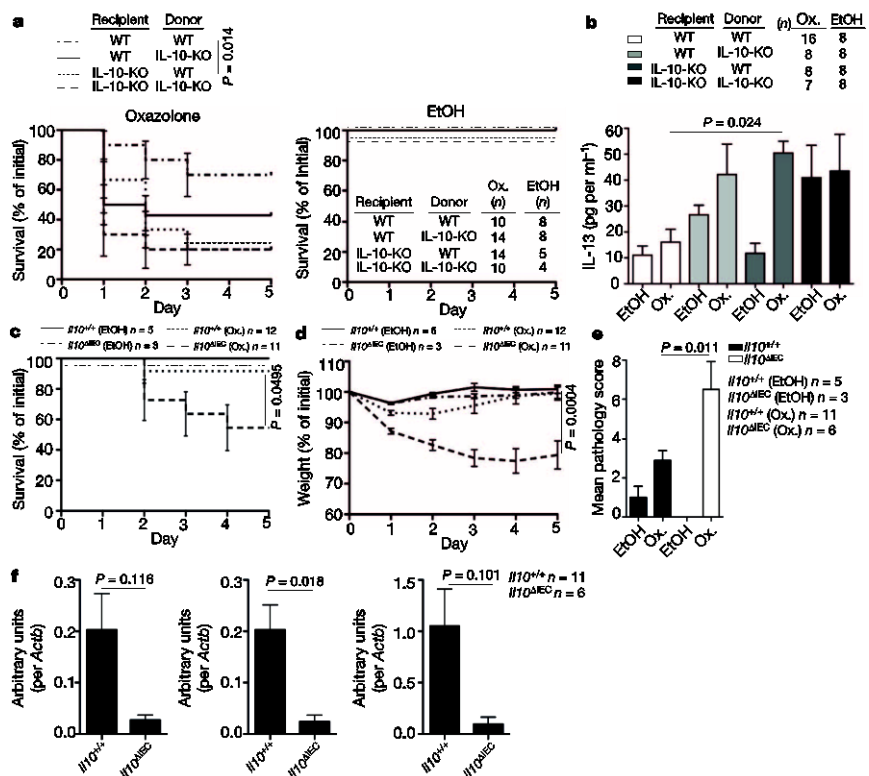


**Figure 4 | Epithelial IL-10 is critical for control of intestinal inflammation.** a–f, Survival (a, c), IL-13 production in colon explants on day 1 after rectal oxazolone (Ox.) or ethanol (EtOH) (b), body weight (d), histopathology (e), and *Il10* (left), *Hsph1* (middle) and *Cd1d1* (right) expression (qPCR; f) in colonic IECs 5 days after rectal oxazolone challenge in the indicated mouse strains. Results representative of three (a, b) or two (c–f) independent experiments are shown. Means ± s.e.m. of the indicated number of mice are shown. Student's t-test or log-rank test (survival) were applied.

## RESEARCH LETTER

IL-10, downstream of epithelial CD1d, HSP110 and STAT3 is critical for regulation of intestinal inflammation.

NKT cells are central mediators of intestinal inflammation<sup>3,4</sup>. In studies aiming to identify the cellular origin of pathogenic lipid antigen presentation in oxazolone colitis, we made the unanticipated observation that intestinal epithelial CD1d protects from intestinal inflammation in a manner dependent on STAT3, IL-10 and HSP110, whereas pathogenic NKT-cell activation emanates from bone-marrow-derived cells in a CD1d-restricted fashion (Extended Data Fig. 1a). As further outlined in the Supplementary Discussion and Extended Data Fig. 9, such opposing roles of CD1d-restricted presentation by bone-marrow-derived and epithelial cells are at least partially dependent on the expression of co-stimulatory molecules such as CD40. Our findings highlight the role of the intestinal epithelium as a key regulator of mucosal immunity and underscore the important role of intestinal epithelial CD1d and IL-10 in determining the host's response to environmental stimuli, which activate CD1d-restricted NKT cells<sup>5</sup>.

## METHODS SUMMARY

Mice were housed in a specific pathogen-free (SPF) barrier facility. HSP110-KO (ref. 23), *Cd1d*<sup>-/-</sup> *Cd1d2*<sup>-/-</sup> (ref. 24), TD-CD1d (ref. 17), *Ii10*<sup>-/-</sup> (ref. 25), Villin-CreER<sup>T2</sup> (ref. 14), *Mtpp*<sup>ΔIEC</sup> (ref. 15), *Ii10*<sup>ΔIEC</sup> (ref. 26), and *Rag1*<sup>-/-</sup> (ref. 27) mice have been described. For *Cd1d*<sup>ΔIEC</sup> mice, please refer to Methods. To activate Cre recombinase, 4–5-week-old Villin-CreER<sup>T2</sup> mice were orally gavaged daily with 1 mg tamoxifen for a total of 5 days. For bone marrow chimeras, recipients received total body irradiation of 1,100 rad in two separate doses 4 h apart. The next day 0.5 × 10<sup>6</sup> bone marrow cells were delivered intravenously. Oxazolone colitis was induced as described previously<sup>6</sup> and as outlined in Methods. Where indicated, mice received 1 mg of neutralizing antibodies against IL-10R (R&D), CD1d (19G11, BioXcell) or isotype control intraperitoneally (i.p.), or 5 × 10<sup>8</sup> adenoviruses in PBS i.p., each before skin sensitization and before and 2 days after rectal oxazolone challenge. For a schematic overview of procedures please refer to Extended Data Fig. 1b.

**Online Content** Any additional Methods, Extended Data display items and Source Data are available in the online version of the paper; references unique to these sections appear only in the online paper.

Received 1 October 2012; accepted 17 February 2014.

Published online 6 April 2014.

- Kaser, A., Zeissig, S. & Blumberg, R. S. Inflammatory bowel disease. *Annu. Rev. Immunol.* **28**, 573–621 (2010).
- Saenz, S. A., Taylor, B. C. & Artis, D. Welcome to the neighborhood: epithelial cell-derived cytokines license innate and adaptive immune responses at mucosal sites. *Immunol. Rev.* **226**, 172–190 (2008).
- Fuss, I. J. *et al.* Nonclassical CD1d-restricted NKT cells that produce IL-13 characterize an atypical Th2 response in ulcerative colitis. *J. Clin. Invest.* **113**, 1490–1497 (2004).
- Heller, F., Fuss, I. J., Nieuwenhuis, E. E., Blumberg, R. S. & Strober, W. Oxazolone colitis, a Th2 colitis model resembling ulcerative colitis, is mediated by IL-13-producing NK-T cells. *Immunity* **17**, 629–638 (2002).
- Olszak, T. *et al.* Microbial exposure during early life has persistent effects on natural killer T cell function. *Science* **336**, 489–493 (2012).
- Wingender, G. & Kronenberg, M. Role of NKT cells in the digestive system. IV. The role of canonical natural killer T cells in mucosal immunity and inflammation. *Am. J. Physiol. Gastrointest. Liver Physiol.* **294**, G1–G8 (2008).
- Heller, F. *et al.* Interleukin-13 is the key effector Th2 cytokine in ulcerative colitis that affects epithelial tight junctions, apoptosis, and cell restitution. *Gastroenterology* **129**, 550–564 (2005).
- Liao, C. M. *et al.* Dysregulation of CD1d-restricted type II natural killer T cells leads to spontaneous development of colitis in mice. *Gastroenterology* **142**, 326–334 (2012).
- Colgan, S. P., Hershberg, R. M., Furuta, G. T. & Blumberg, R. S. Ligation of intestinal epithelial CD1d induces bioactive IL-10: critical role of the cytoplasmic tail in autocrine signaling. *Proc. Natl. Acad. Sci. USA* **96**, 13938–13943 (1999).
- Perera, L. *et al.* Expression of nonclassical class I molecules by intestinal epithelial cells. *Inflamm. Bowel Dis.* **13**, 298–307 (2007).
- Blumberg, R. S. *et al.* Expression of a nonpolymorphic MHC class I-like molecule, CD1d, by human intestinal epithelial cells. *J. Immunol.* **147**, 2518–2524 (1991).
- Brozovic, S. *et al.* CD1d function is regulated by microsomal triglyceride transfer protein. *Nature Med.* **10**, 535–539 (2004).
- Zeissig, S. *et al.* Primary deficiency of microsomal triglyceride transfer protein in human abetalipoproteinemia is associated with loss of CD1 function. *J. Clin. Invest.* **120**, 2889–2899 (2010).
- El Marjou, F. *et al.* Tissue-specific and inducible Cre-mediated recombination in the gut epithelium. *Genesis* **39**, 186–193 (2004).
- Raabe, M. *et al.* Analysis of the role of microsomal triglyceride transfer protein in the liver of tissue-specific knockout mice. *J. Clin. Invest.* **103**, 1287–1298 (1999).
- Colgan, S. P. *et al.* Intestinal heat shock protein 110 regulates expression of CD1d on intestinal epithelial cells. *J. Clin. Invest.* **112**, 745–754 (2003).
- Chiu, Y. H. *et al.* Multiple defects in antigen presentation and T cell development by mice expressing cytoplasmic tail-truncated CD1d. *Nature Immunol.* **3**, 55–60 (2002).
- Saraiva, M. & O'Garra, A. The regulation of IL-10 production by immune cells. *Nature Rev. Immunol.* **10**, 170–181 (2010).
- Pickert, G. *et al.* STAT3 links IL-22 signaling in intestinal epithelial cells to mucosal wound healing. *J. Exp. Med.* **206**, 1465–1472 (2009).
- Yamagishi, N., Fujii, H., Saito, Y. & Hatayama, T. Hsp105 $\beta$  upregulates *hsp70* gene expression through signal transducer and activator of transcription-3. *FEBS J.* **276**, 5870–5880 (2009).
- Chaudhry, A. *et al.* Interleukin-10 signaling in regulatory T cells is required for suppression of Th17 cell-mediated inflammation. *Immunity* **34**, 566–578 (2011).
- Rubtsov, Y. P. *et al.* Regulatory T cell-derived interleukin-10 limits inflammation at environmental interfaces. *Immunity* **28**, 546–558 (2008).
- Nakamura, J. *et al.* Targeted disruption of Hsp110/105 gene protects against ischemic stress. *Stroke* **39**, 2853–2859 (2008).
- Smiley, S. T., Kaplan, M. H. & Grusby, M. J. Immunoglobulin E production in the absence of interleukin-4-secreting CD1-dependent cells. *Science* **275**, 977–979 (1997).
- Kühn, R., Lohler, J., Rennick, D., Rajewsky, K. & Müller, W. Interleukin-10-deficient mice develop chronic enterocolitis. *Cell* **75**, 263–274 (1993).
- Roers, A. *et al.* T cell-specific inactivation of the interleukin 10 gene in mice results in enhanced T cell responses but normal innate responses to lipopolysaccharide or skin irritation. *J. Exp. Med.* **200**, 1289–1297 (2004).
- Mombaerts, P. *et al.* RAG-1-deficient mice have no mature B and T lymphocytes. *Cell* **68**, 869–877 (1992).

**Supplementary Information** is available in the online version of the paper.

**Acknowledgements** The authors thank H.-C. Hung for technical assistance with microinjection, Y. Xie for performing osmium staining, A. Bedynek and M. Friedrich for performing immunohistochemistry of the human biopsies, F. A. Zhu for assistance with antigen presentation assays, D. Shouval, M. Sablon and D. Perez for animal care and husbandry, K. Tashiro for technical assistance with adenovirus preparation, V. M. Thiele for technical assistance, J. Cusick for help with manuscript preparation, and S. E. Plevy for discussions and reagents. This work was supported by: National Institutes of Health (NIH) (grants DK044319, DK051362, DK053056, DK088199) and the Harvard Digestive Diseases Center (DK0034854) (R.S.B.); the European Research Council (ERC Starting Grant agreement no. 336528), the Deutsche Forschungsgemeinschaft (DFG) (ZE 814/4-1, ZE 814/5-1, ZE 814/6-1), the Crohn's and Colitis Foundation of America (Postdoctoral Fellowship Award), the European Commission (Marie Curie International Reintegration Grant no. 256363) and the DFG Excellence Cluster "Inflammation at Interfaces" (S.Z.); the DFG (OL 324/1-1) (T.O.); HL38180, DK56260, Washington University DDRCC P30DK52574 (morphology core) (N.O.D.); HDCC Pilot and Feasibility Grant (K.B.); NCI P30CA013696 (C.-S.L.), the DFG (BR 1912/6-1) and the Else Kroener-Fresenius-Stiftung (Else Kroener-Exzellenzstipendium 2010\_EKES.32) (S.B.); Grant-in-Aid for Challenging Exploratory Research 24659823 from Japan Society for Promotion of Science (K.W.); the ERC under the European Community's Seventh Framework Programme (FP7/2007-2013/ERC Grant agreement no. 260961), the National Institute for Health Research Cambridge Biomedical Research Centre, the Austrian Science Fund and Ministry of Science P21530-B18 and START Y446-B18, Innsbruck Medical University (MF1 2007-407) and the Addenbrooke's Charitable Trust, CicRA (A.K.); the European Community's Seventh Framework Programme (FP7/2007-2013) under grant agreement SysmedIBD (no. 305564) (W.M., S.S.); the NIH (grants HL59561, DK034854, AI50950), the Helmsley Charitable Trust and the Wolpov Family Chair in IBD Treatment and Research (S.B.S.). PBS57-loaded and unloaded mouse CD1d tetramer was obtained through the NIH Tetramer Facility. The authors thank M. A. Exley and S. P. Colgan for discussions.

**Author Contributions** T.O., J.F.N., C.M.D. and K.B. performed *in vitro* and *in vivo* experiments and analysed the results; N.O.D. performed osmium tetroxide staining; J.G. obtained and scored histopathologies; C.-S.L. generated *Cd1d*<sup>ΔIEC</sup> mice; C.J. contributed to the analysis of CD1d<sup>ΔIEC</sup> mice; S.B. and K.S. contributed to the immunohistochemical analysis of ulcerative colitis patients; K.W., K. Katayama, A.N. and H.M. generated adenoviruses; K. Kawasaki and K.N. provided HSP110-KO mice; W.M. and S.B.S. provided and participated in the analysis of the *Ii10*<sup>ΔIEC</sup> mice; S.S. contributed to the coordination of experimental studies; A.K. contributed to *Mtpp*<sup>ΔIEC</sup> studies and to the analysis of microarray data; R.S.B. and S.Z. designed the study, coordinated the experimental work and wrote the manuscript with input from co-authors. All authors discussed the results and commented on the manuscript.

**Author Information** Reprints and permissions information is available at [www.nature.com/reprints](http://www.nature.com/reprints). The authors declare no competing financial interests. Readers are welcome to comment on the online version of the paper. Correspondence and requests for materials should be addressed to R.S.B. ([rlblumberg@partners.org](mailto:rlblumberg@partners.org)) or S.Z. ([szeissig@1.med.uni-kiel.de](mailto:szeissig@1.med.uni-kiel.de)).

## METHODS

**Mice.** Mice (C57BL/6J unless indicated otherwise) were housed in a specific pathogen-free (SPF) barrier facility. *Cd1d1<sup>-/-</sup> Cd1d2<sup>-/-</sup>* (ref. 24), TD-CD1d (ref. 17), *Il10<sup>-/-</sup>* (ref. 25), Villin-CreER<sup>22</sup> (ref. 14), *Il10<sup>fl/fl</sup>* (ref. 26), *Rag1<sup>-/-</sup>* (ref. 27), HSP110-KO (ref. 23) (C57BL/6N) and *Mtpp<sup>fl/fl</sup>* (ref. 15) (C57BL/6J129) mice have been described. To generate the floxed/neo *Cd1d1* allele, a LoxP (L83) site at 10310 and a FNFL (Frt-Neo-Frt-LoxP) cassette at 12190 was inserted to flank exon 2, 3 and 4 (about 1.9 kb) of the *Cd1d1* gene. A gene-targeting vector was constructed by retrieving one 5 kb long homology arm (5' to L83), one 1.9 kb sequence containing exon 2/3/4, FNFL cassette, and one 2 kb short homology arm (end of FNFL to 3'). The FNFL cassette conferred G418 resistance during gene targeting in PTL1 (129B6 hybrid) embryonic stem (ES) cells. The *Cd1d1* allele was PCR amplified and sequenced to confirm the targeted C57BL/6J allele based on the C57BL/6J-specific mutation in *Cd1d2* allele<sup>28</sup>. Three targeted ES cells with targeted C57BL/6J allele were injected into C57BL/6J blastocysts to generate chimaeras. Male chimaeras were bred to bACTPpe females or Ella-Cre females to transmit the floxed *Cd1d1* allele (*Cd1d1<sup>fl/+</sup>*) (with neo cassette removed by FpIe recombinase) and *Cd1d1*-null allele (*Cd1d1<sup>-/-</sup>*) (with exon 2/3/4 and neo cassette removed by Cre recombinase) through the germ line. Mice carrying floxed *Cd1d1* alleles were crossed to Villin-CreER<sup>22</sup> mice (ref. 14) expressing Cre recombinase.

To activate Cre recombinase, 4–5-week-old Villin-CreER<sup>22</sup> mice were orally gavaged daily with 1 mg tamoxifen for a total of 5 days. For bone marrow chimaeras, recipients received total body irradiation of 1,100 rad in two separate doses 4 h apart. The next day,  $0.5 \times 10^6$  bone marrow cells were delivered intravenously. For  $\alpha$ -GalCer studies, mice were injected with 2  $\mu$ g of  $\alpha$ -GalCer (KRN7000, Avanti Polar Lipids) intraperitoneally (i.p.) 8 weeks after bone marrow reconstitution and RNA was isolated from Percoll-purified IECs (see later) 12 h after injection. For oxazolone colitis, mice were pre-sensitized by abdominal skin application of 3% (w/v) oxazolone in 100% ethanol, followed by rectal administration of 1% oxazolone in 50% ethanol after 5 days. Where indicated, mice received 1 mg of neutralizing antibodies against IL-10R (R&D), CD1d (19G11, BioXcell) or isotype control i.p., or  $5 \times 10^8$  adenoviruses in PBS i.p., each before skin sensitization and before and 2 days after rectal oxazolone challenge. Body weight, rectal bleeding and stool consistency were analysed on a daily basis. Tissues were examined for evidence of colitis by five established criteria for colitis activity in a blinded fashion by a pathologist (J.G.): hypervascularization, presence of mononuclear cells, epithelial hyperplasia, epithelial injury, and presence of granulocytes. For a schematic overview of procedures please refer to Extended Data Fig. 1b.

Animal studies were conducted in a gender- and age-matched manner using littermates for each experiment. Both male and female mice were used and were 8 weeks of age at the time of experiments (11–16 weeks of age for bone marrow chimaera studies). The number of animals used per group was based on previous experimental results and observed variability. Histopathology analysis was performed in a blinded manner. For all other *in vitro* and *in vivo* analyses, investigators were not blinded to treatment allocation. Animal studies were performed in compliance with ethical regulations and were approved by the ethics committees of Harvard Medical School and the Christian Albrechts University.

**Patients.** Human studies were approved by the ethics committee of the Ludwig Maximilians University. All subjects provided written informed consent. Immunohistochemical staining was performed on intestinal biopsies from ten healthy controls (patients undergoing screening colonoscopy without detection of malignancy), four patients with active ulcerative colitis, and five patients with inactive ulcerative colitis.

**Isolation of IECs and lymphocytes, flow cytometry, and sorting.** To isolate IECs, the intestines were opened, washed in cold PBS, cut into pieces, and transferred into tubes containing HBSS without calcium and magnesium. After the addition of dithiothreitol (DTT) at 1 mM (Sigma), intestines were shaken at 250 r.p.m. for 10 min at room temperature to remove mucus. After washing in PBS, tissues were incubated in RPMI-1640 with  $1 \text{ U ml}^{-1}$  Dispase (Roche) for 30–40 min at 37 °C at 250 r.p.m. After filtering through a 100  $\mu$ m strainer and centrifugation for 5 min at 1,500 r.p.m., the pellet was resuspended in 5 ml of 100% Percoll and placed beneath 8 ml of 40% Percoll. After centrifugation for 20 min at 1,500 r.p.m. the top layer was removed, washed three times in PBS and used as IECs.

To isolate intraepithelial (IEL) and lamina propria lymphocytes, large intestines were collected, fat tissue removed, the intestines cut longitudinally and washed in PBS in order to remove faecal content, cut into 30 mm pieces, and shaken in RPMI-1640 containing 20 mM HEPES, 1 mM DTT and 5 mM EDTA for 30 min at 37 °C. To isolate IELs, cells derived from the epithelial compartment were resuspended in 4 ml of 40% Percoll and layered on top of 2 ml of 75% Percoll. After centrifugation for 20 min at 2,000 r.p.m. the middle layer was removed, washed in 2% FBS in PBS and the IELs were obtained. For lamina propria lymphocytes, the non-epithelial compartment was washed in PBS, cut into smaller pieces and incubated in RPMI-1640 containing 5% FBS,  $1.5 \text{ mg ml}^{-1}$  collagenase type II and  $0.5 \text{ mg ml}^{-1}$  dispase (GIBCO) for 1 h at 37 °C under constant horizontal shaking (250 r.p.m.). The digested

tissues were filtered through a 40  $\mu$ m strainer and, after Percoll gradient centrifugation and washing as described earlier, were used as lamina propria lymphocytes in flow cytometry. Where indicated, CD11b<sup>+</sup> lamina propria cells were purified using magnetic beads according to the manufacturer's instructions (Miltenyi Biotec). Liver lymphocytes were prepared as described before<sup>29</sup>.

Primary iNKT cells were sorted by double staining with PBS57-loaded CD1d tetramers and CD3e using a BD FACSAria II SORP UV sorter. RNA samples were prepared using an RNeasy Micro Kit and cDNAs were synthesized using the Omniscript RT Kit (Qiagen).

PBS57-loaded or -unloaded CD1d tetramers were obtained from the NIH Tetramer Core Facility. Flow cytometry antibodies were obtained from eBiosciences. Flow cytometry was performed using a MACSQuant (Miltenyi Biotec) and a BD FACSVers (BD Biosciences) and data were analysed with FlowJo software (TreeStar).

**Antigen presentation assays.** Freshly isolated IECs, MODE-K cells<sup>30</sup>, and CD11c-magnetic-bead-purified (Miltenyi Biotec) splenic dendritic cells were incubated with 100 ng ml<sup>-1</sup>  $\alpha$ -GalCer for 4 h, washed three times with PBS, and aliquoted into 96-well plates at  $1 \times 10^5$  cells per well. NKT-cell hybridomas (24.7, DN32.D3 and 14S.6 (ref. 31)) were added at a 1:1 ratio. Where indicated, soluble, stimulatory CD28 antibody was added (1  $\mu$ g ml<sup>-1</sup>; clone 37.51; eBioscience). In addition, where indicated, cells were transfected with expression plasmids or siRNA 24 h and 72 h, respectively, before co-culture with NKT cells. Mouse IL-2, IL-10, IL-12p70, IL-13 and IL-1 $\beta$  production were assessed by ELISA (OptEIA; BD Biosciences) in supernatants after 24 h of co-culture.

**Cell stimulation by crosslinking.** CD1d crosslinking on freshly isolated clonic IECs was achieved as described previously<sup>32</sup> using plate-bound anti-mCD1d antibody (1B1, BD). In the case of MODE-K cells, surface CD1d was crosslinked by addition of soluble anti-mCD1d antibody (1B1, 10  $\mu$ g ml<sup>-1</sup>, 60 min) followed by washing and addition of secondary goat anti-rat IgG (Biological, 10  $\mu$ g ml<sup>-1</sup>) for the indicated time as well as subsequent cell lysis (see later). MODE-K STAT3 phosphorylation in response to iNKT-cell engagement was investigated after co-culture with the iNKT-cell hybridoma 24.7 for the indicated time, removal of non-adherent iNKT cells by thorough washing, and cell lysis. Where indicated, MODE-K cells were pre-treated with 19G11 anti-CD1d antibody for blocking of CD1d (10  $\mu$ g ml<sup>-1</sup>, BioXcell).

**Adenoviruses.** Type 5, E1/E3-deleted adenoviruses expressing murine HSP110 (AdHSP110) or *Escherichia coli*  $\beta$ -galactosidase (AdLacZ) under the control of the cytomegalovirus promoter, were constructed according to the *in vitro* ligation method<sup>33,34</sup>. Briefly, murine *Hsp110* (NM-013559) was isolated and amplified by PCR from mouse intestinal cDNA using the following primers, cloned into NheI and EcoRI sites of pIRES2-eGFP (Clontech), sequenced, and the resulting plasmid was called pHSP110-IRES2-eGFP. Forward primer: ATAAAGCTAGCGCCACCatgtcgggtgtgggctag, containing an NheI site and a Kozak-like sequence; reverse primer: AATTAGAAATTCCTAgtcaggctgtgtgacagag, containing an EcoRI site (the sequence complementary to *Hsp110* cDNA is shown in lower case). An NheI-HSP110-KpnI or NheI-HSP110-IRES2-eGFP-NotI fragment from pHSP110-IRES2-eGFP was transferred into pHMCMV6 (pHMCMV6-HSP110 and pHMCMV6-HSP110-IRES2-eGFP, respectively). Subsequently, pAdHM15RGD-CMV6-HSP110 and pAdHM15RGD-CMV6-HSP110-IRES2-eGFP were constructed by ligating I-CeuI/PI-SceI-digested pAdHM15-RGD and pHMCMV6-HSP110-IRES2-eGFP or pHMCMV6-HSP110. To prepare the virus, a PacI fragment of pAdHM15-RGD-CMV-HSP110 or pAdHM15-RGD-CMV-HSP110 was transfected into 293 cells. The adenoviruses were purified by two rounds of caesium chloride density centrifugation and dialysed against Tris-HCl (pH 7.5). The concentrations of plaque-forming units (p.f.u.) of individual stocks were determined from the tissue culture infectious dose 50 titre.

**Colon organ culture.** Standardized segments (1 cm  $\times$  1 cm) of the transverse colon were washed in cold PBS supplemented with penicillin and streptomycin (GIBCO) and cultured in 24-well flat-bottom culture plates (Falcon) in RPMI 1640 media (GIBCO) for 24 h at 37 °C. Supernatants were analysed for cytokines IL-10, IL-13 and IL-1 $\beta$  by ELISA (all BD).

**Western blotting.** Protein extraction and western blotting were performed as described previously<sup>35</sup>. The following antibodies were used: anti-IL10 (R&D), anti-HSP110 (BD), anti-STAT3 (Cell signaling), anti-pSTAT3 (Cell signaling) and anti- $\beta$ -actin (Cell Signaling).

**Real-time RT-PCR.** RNA samples were prepared using an RNeasy Mini Kit and cDNAs were synthesized using the Omniscript RT Kit (Qiagen). Real-time RT-PCR was performed using SYBR Green I Master Mix (Roche) and a CFX96 Real-Time System (Bio-Rad). Values were normalized to  $\beta$ -actin. The following primer sets were used:  $\beta$ -actin, 5'-GATGCTCCCGGGCTGTATT-3' and 5'-GGGGTATTCAGGGTCAGGA-3'; *Hsp110*, 5'-CAGGTACAAACTGATGGTCAACA-3' and 5'-TGAGGTAAGTTCAGGTGAAGG-3'; *Il10*, 5'-GAGAGCTGACGGGCCTTTGC-3' and 5'-CTCCCTGGTTTCTCTCCCAAGACC-3'; *Tgfb*, 5'-TGTACGGCAGTGGCTGAACCA-3' and 5'-TGTACAAAGACAGTGTAGCGCT-3'.

## RESEARCH LETTER

*Cd1d1*, 5'-GCAGCCAGTACGCTCTTTTC-3' and 5'-ACAGCTTGTTTCTGGCAGGT-3'; *Stat3*, 5'-CCCGTACCTGAAGACCAAGT-3' and 5'-ACACTCCGAGGTCAGATCCA-3'; *Il13*, 5'-AGCATGGTATGGAGTGTGGACCTG-3' and 5'-CAGTTGCTTTGTGTAGCTGAGCAG-3'; *Irfng* 5'-TCAGCAACAGCAAGCGAAAAAGG-3' and 5'-CCACCCCGAATCAGCAGCGA-3'.

**Transfection, siRNA treatment and recombinant HSP110.** Where indicated, MODE-K cells were transfected with mouse CD40 or CD1d (in pSR $\alpha$ -neo), with SignalSilence *Stat3* siRNA II or with SignalSilence Control siRNA (Cell Signaling Technology) using Lipofectamine 2000 (Life Technologies) according to the manufacturer's instructions. *Il10* siRNA was obtained from Invitrogen and transduced by Amaxa Nucleofector technology (Lonza) according to the manufacturer's instructions. Cells were used for antigen presentation assays after 72 h or were incubated with the indicated adenoviruses after 48 h at a MOI of 5 before RNA preparation after another 24 h as described earlier. Where indicated, recombinant HSP110 was added at a final concentration of 6  $\mu\text{g ml}^{-1}$  to MODE-K cells 24 h before RNA extraction.

**XBP1 splicing assay.** The assay was performed as described previously<sup>36</sup>.

**In vivo permeability assay.** *In vivo* intestinal permeability was measured using the FITC-labelled dextran (FD-4) method as described previously<sup>37,38</sup> with modifications. Mice were administered 150  $\mu\text{l}$  of FD-4 (50 mg ml<sup>-1</sup>) by oral gavage before and 18 h after rectal challenge with oxazolone. Serial dilutions of FD-4 were made to generate a standard curve and serum concentrations of FD-4 were determined using a BioTek FLx800 Fluorescence Microplate Reader (BioTek) with an excitation wavelength of 490 nm and emission wavelength of 530 nm.

**Immunohistochemistry and immunofluorescence.** A polyclonal rabbit anti-HSP110 antibody (anti-mouse 1:250, anti-human 1:500; Sigma-Aldrich), an anti-STAT3 (anti-mouse 1:900) and anti-pSTAT3 antibody (anti-mouse 1:350), both from Cell Signaling, as well as a rabbit polyclonal anti-GFP antibody conjugated to FITC (1:1,000) (Novus Biologicals) were used. All images were taken by a digital camera on a Nikon Eclipse Ti microscope.

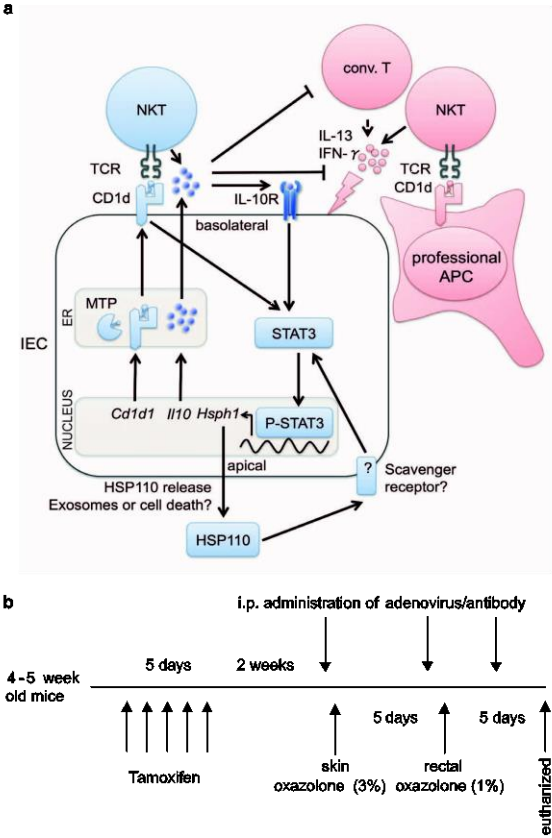
**Osmium tetroxide staining of intracellular lipid droplets.** Intestinal tissue was fixed in 10% neutral buffered formalin and transferred into 1% osmium tetroxide with periodic shaking. The tissue was rinsed with distilled water and incubated in 0.5% periodic acid, washed and counterstained with haematoxylin and eosin.

**Microarray analysis.** *Mtth* <sup>$\Delta\text{IEC}$</sup>  and littermate wild-type mice were skin sensitized with oxazolone, and IECs were harvested via colonic epithelial scraping as described previously<sup>35</sup>, either before administration of rectal oxazolone ( $n = 2$  per group) or

6 h thereafter ( $n = 4$  per group). Isolated RNAs were pooled for each condition and subjected to transcriptomic analysis with mouse genome 430 2.0 array (Affymetrix) at the Biopolymers Core Facility (Harvard Medical School). Data analysis was performed with Agilent GeneSpring GX and Affymetrix GCOS software under default parameter settings with GC-RMA normalization.

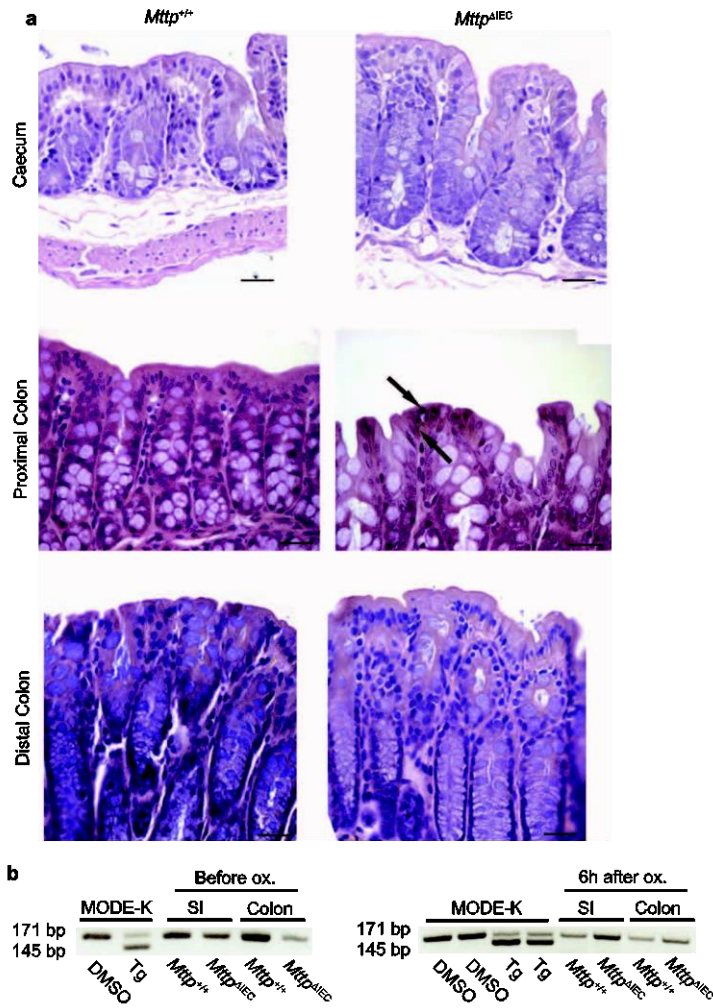
**Statistical analysis.** Statistical testing was performed using the unpaired Student's *t*-test unless otherwise indicated. The Mann-Whitney *U*-test was applied when data were demonstrated to not follow a Gaussian distribution, which is indicated in the respective figures legends. Comparisons of mortality were made by analysing Kaplan-Meier survival curves, and the log-rank test was used to assess differences in survival. All *P* values were two-tailed, and statistical significance was assumed at  $P < 0.05$ .

28. Park, S. H., Roark, J. H. & Bendelac, A. Tissue-specific recognition of mouse CD1 molecules. *J. Immunol.* **160**, 3128–3134 (1998).
29. Zeissig, S. *et al.* Hepatitis B virus-induced lipid alterations contribute to natural killer T cell-dependent protective immunity. *Nature Med.* **18**, 1060–1068 (2012).
30. Vidal, K., Grosjean, I., Revillard, J.-P., Gespach, C. & Kaiserlian, D. Immortalization of mouse intestinal epithelial cells by the SV40-large T gene. Phenotypic and immune characterization of the MODE-K cell line. *J. Immunol. Methods* **166**, 63–73 (1993).
31. Behar, S. M., Podrebarac, T. A., Roy, C. J., Wang, C. R. & Brenner, M. B. Diverse TCRs recognize murine CD1. *J. Immunol.* **162**, 161–167 (1999).
32. Yue, S. C., Shaulov, A., Wang, R., Balk, S. P. & Exley, M. A. CD1d ligation on human monocytes directly signals rapid NF- $\kappa$ B activation and production of bioactive IL-12. *Proc. Natl Acad. Sci. USA* **102**, 11811–11816 (2005).
33. Katayama, K. *et al.* A novel PPAR $\gamma$  gene therapy to control inflammation associated with inflammatory bowel disease in a murine model. *Gastroenterology* **124**, 1315–1324 (2003).
34. Mizuguchi, H. & Kay, M. A. A simple method for constructing E1- and E1/E4-deleted recombinant adenoviral vectors. *Hum. Gene Ther.* **10**, 2013–2017 (1999).
35. Chen, Z., Chen, L., Qiao, S. W., Nagaishi, T. & Blumberg, R. S. Carcinoembryonic antigen-related cell adhesion molecule 1 inhibits proximal TCR signaling by targeting ZAP-70. *J. Immunol.* **180**, 6085–6093 (2008).
36. Kaser, A. *et al.* XBP1 links ER stress to intestinal inflammation and confers genetic risk for human inflammatory bowel disease. *Cell* **134**, 743–756 (2008).
37. Furuta, G. T. *et al.* Eosinophils alter colonic epithelial barrier function: role for major basic protein. *Am. J. Physiol. Gastrointest. Liver Physiol.* **289**, G890–G897 (2005).
38. Furuta, G. T. *et al.* Hypoxia-inducible factor 1-dependent induction of intestinal trefoil factor protects barrier function during hypoxia. *J. Exp. Med.* **193**, 1027–1034 (2001).



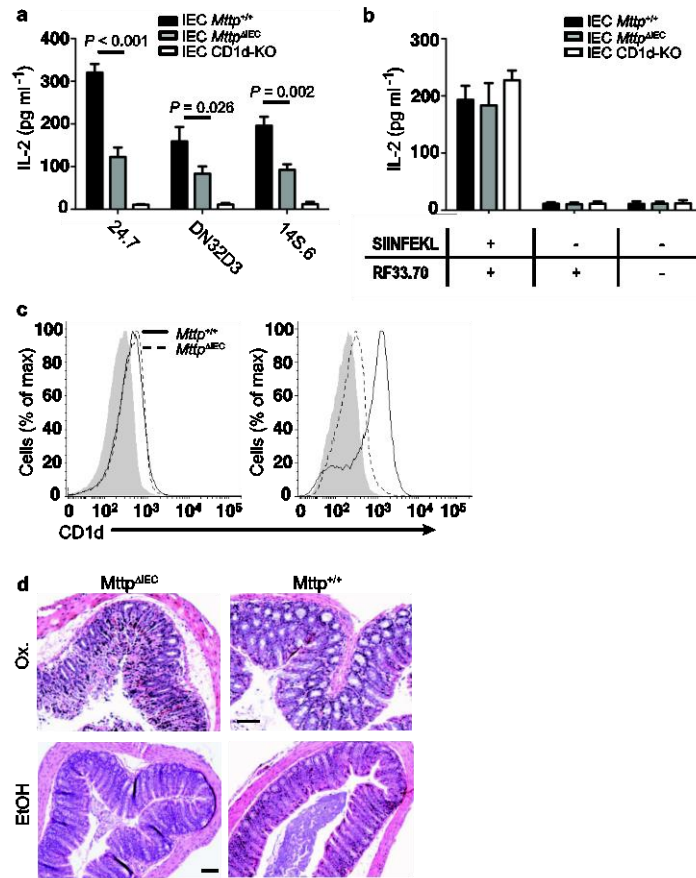
**Extended Data Figure 1 | Proposed model of CD1d signalling in polarized intestinal epithelia and overview of experimental procedures.** a. The proposed model of protective (blue) and pathogenic (red) effects of lipid antigen presentation in intestinal inflammation. Bone-marrow-derived antigen-presenting cells (APCs) contribute to oxazolone colitis in a CD1d- and iNKT-cell-dependent manner. By contrast, engagement of intestinal epithelial CD1d elicits protective functions through cytoplasmic CD1d tail-dependent activation of STAT3, and STAT3-dependent transcription of *Cd1d1*, *Il10* and *Hsp110*. Epithelial IL-10 and HSP110 support this protective self-reinforcing pathway through STAT3-dependent signalling. Interference with any of the elements involved in this regulatory pathway (MTP, CD1d, IL-10 or HSP110) is associated with uncontrolled intestinal inflammation, thus highlighting a critical role of this pathway in the control of intestinal inflammation. Conv., conventional. b. Overview of experimental procedures.

RESEARCH LETTER



**Extended Data Figure 2 | Absence of enterocyte lipid accumulation and ER stress in *Mttp<sup>AIEC</sup>* mice.** a, Absence of lipid accumulation in *Mttp<sup>AIEC</sup>* mice as shown in representative haematoxylin and eosin and rare osmium tetroxide (arrows) staining in the caecum, proximal, and distal colon. Scale bar, 25  $\mu$ m. b, *Xbp1* splicing in small intestinal (SI) and colonic IECs of the indicated mice

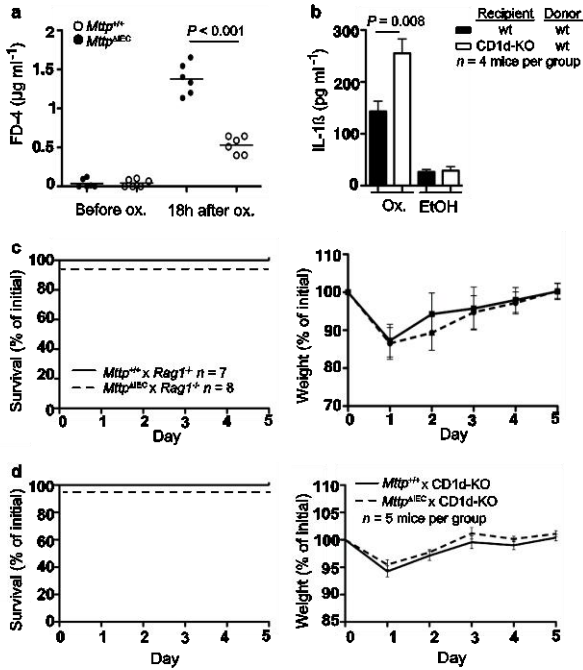
before (left) ( $n = 5$  mice per group) and 6 h after rectal challenge with oxazolone (Ox., right) ( $n = 5$  mice per group). MODE-K cells were treated with either thapsigargin (Tg) or vehicle (DMSO) as positive and negative controls, respectively. Results representative of three independent experiments are shown.



**Extended Data Figure 3 | Impaired CD1d- but not MHC-class I-restricted antigen presentation in *Mttp*<sup>ΔIEC</sup> mice.** **a**, CD1d-mediated presentation of the exogenous lipid antigen  $\alpha$ -GalCer to the invariant NKT-cell hybridomas 24.7 and DN32.D3 and of endogenous lipid antigens (autoreactivity) to the non-invariant NKT-cell hybridoma 14S.6 by IECs from CD1d-knockout (CD1d-KO) mice, *Mttp*<sup>ΔIEC</sup> mice and wild-type littermates (*Mttp*<sup>+/+</sup>) ( $n = 5$  mice per group). **b**, Presentation of H2-K<sup>b</sup>-restricted SIINFEKL by the indicated IECs (see **a**) to the SIINFEKL-responsive hybridoma RF33.70.

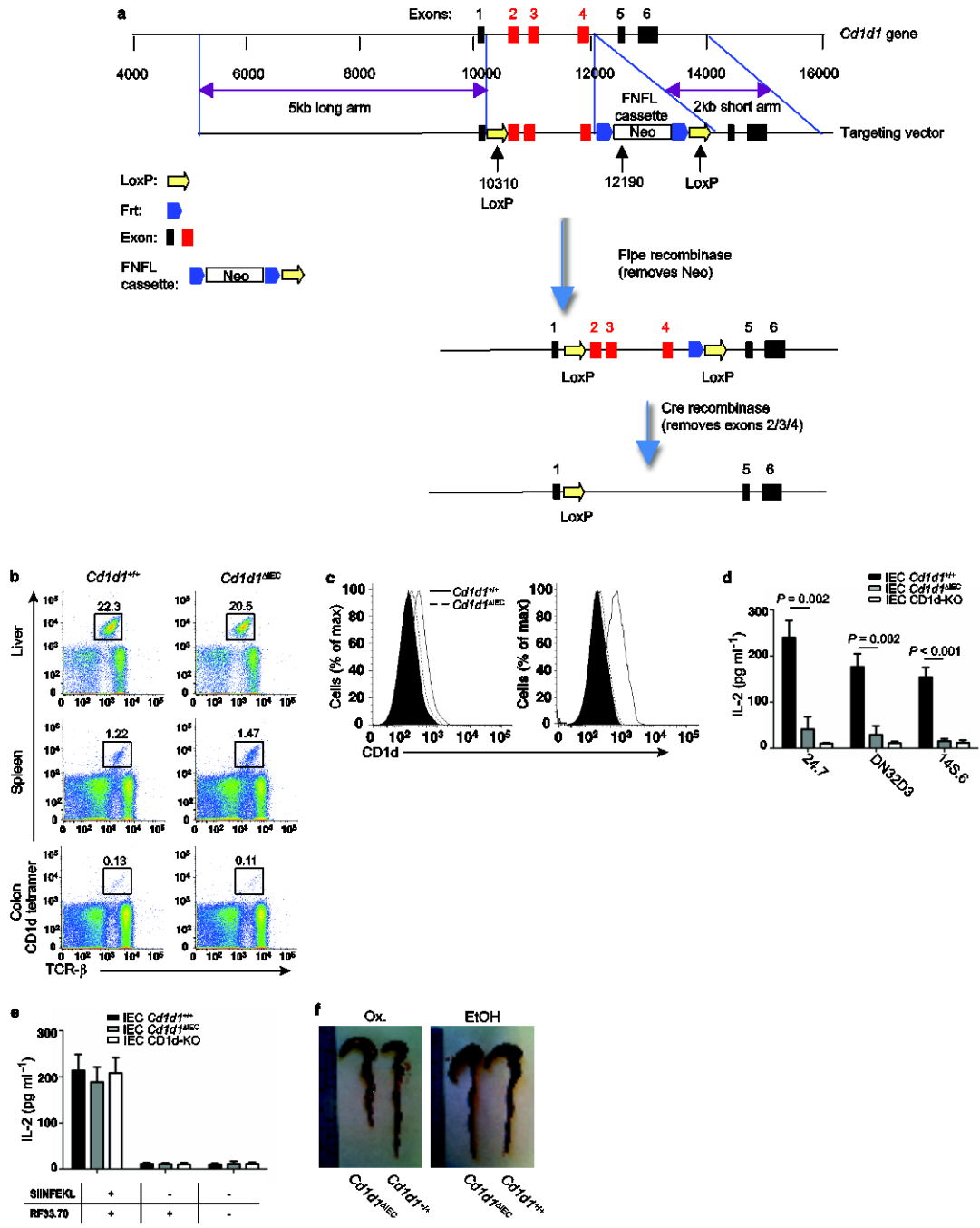
**c**, Representative histograms of CD1d cell surface expression as determined by flow cytometry of colonic IECs of the indicated mouse strains before (left,  $n = 5$  mice per group) and 6 h after (right,  $n = 5$  mice per group) rectal oxazolone challenge. **d**, Representative haematoxylin and eosin stainings of the indicated mouse strains upon rectal challenge with oxazolone (Ox.) or vehicle (ethanol (EtOH)). Scale bar, 40  $\mu$ m. Results representative of three independent experiments are shown. Mean  $\pm$  s.e.m. of triplicate cultures are shown. Student's *t*-test was applied.

RESEARCH LETTER



**Extended Data Figure 4 | Increased morbidity and mortality in oxazolone-challenged *Mtp<sup>ALBEC</sup>* mice is due to CD1d-restricted components of the adaptive immune system.** a, Intestinal permeability as determined by FD-4 before and 18 h after rectal challenge with oxazolone (ox.) in the indicated mouse strains. Each symbol represents a single mouse. b, IL-1 $\beta$  secretion by CD11b<sup>+</sup> cells from colonic lamina propria of the indicated bone marrow chimaeras. CD11b<sup>+</sup> cells were isolated using magnetic microbeads 24 h after rectal challenge with oxazolone or ethanol and cultured for 24 h before measurement of IL-1 $\beta$  in culture supernatants by ELISA. Mean  $\pm$  s.e.m. of triplicate cultures are shown. c, d, Survival and body weight of the indicated mouse strains at the indicated days after rectal oxazolone challenge. Results representative of three independent experiments are shown. Mean  $\pm$  s.e.m. of the indicated number of mice are shown. Student's *t*-test was applied.

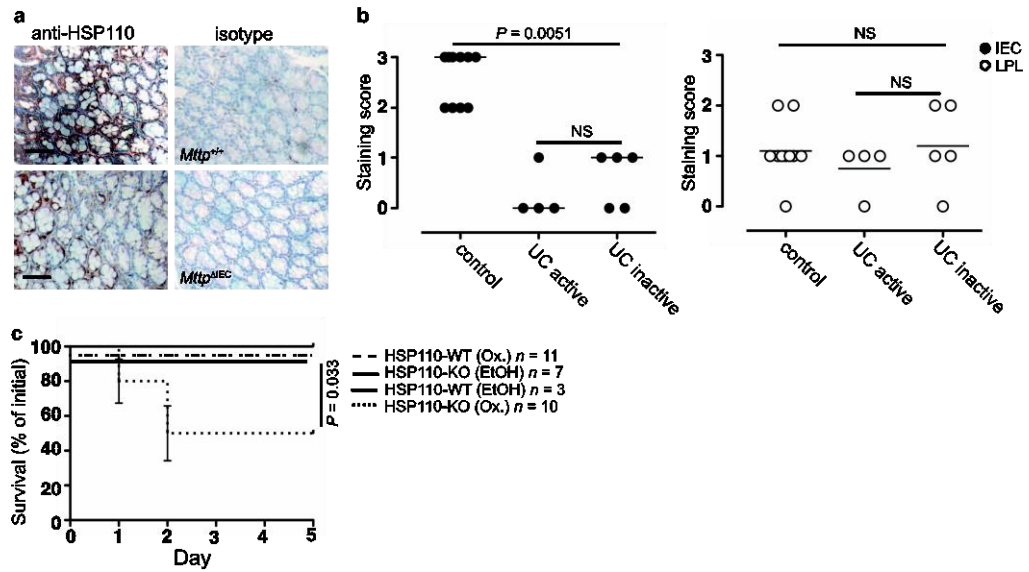




## RESEARCH LETTER

**Extended Data Figure 5 | Development and characterization of mice with IEC-specific *Cd1d1* deletion.** **a**, Schematic map of the targeting strategy for generation of *Cd1d1*<sup>fl/fl</sup> mice. A LoxP (L83) site was inserted at 10310 and a FNFL (Frt-Neo-Frt-LoxP) cassette at 12190 to flank exons 2, 3, and 4 (about 1.9 kb) of the *Cd1d1* gene to generate the 'floxed/neo' *Cd1d1* allele. A gene-targeting vector was constructed by retrieving one 5 kb long homology arm (5' to L83), one 1.9 kb sequence containing exon 2/3/4, FNFL cassette, and one 2 kb short homology arm (end of FNFL to 3'). The FNFL cassette conferred G418 resistance during gene targeting in PTL1 (129B6 hybrid) embryonic stem (ES) cells. The targeted *Cd1d1* allele was PCR amplified and sequenced to confirm the targeted *C57BL/6* allele based on the *C57BL/6*-specific mutation in the *Cd1d2* allele. Three targeted ES cells with targeted *C57BL/6* allele were injected into *C57BL/6* blastocysts to generate chimaeric mice. Male chimaeras were bred to bACTFpe females or EIIa-Cre females to transmit the floxed *Cd1d1* allele (*Cd1d1*<sup>fl/+</sup>) (with neo cassette removed by FpIe recombinase) through the germ line. Mice carrying the floxed *Cd1d1* allele were crossed to tissue-specific VillinCre-ER<sup>T2</sup> and exons 2, 3 and 4 and Frt-LoxP were removed by Cre recombinase in intestinal epithelial cells. **b–e**, Impaired CD1d- but not

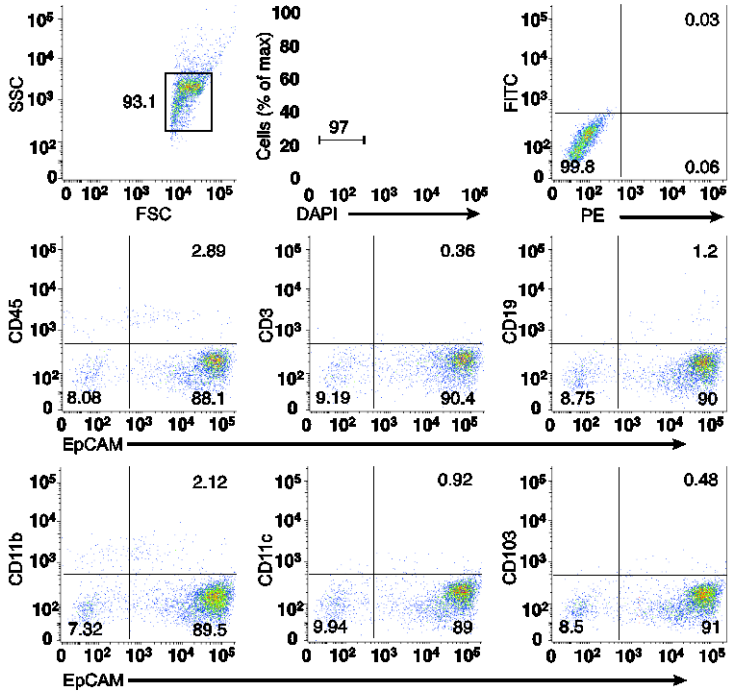
MHC-class I-restricted antigen presentation in *Cd1d1*<sup>ΔIEC</sup> mice. **b**, *Cd1d1*<sup>ΔIEC</sup> mice exhibit normal numbers of invariant NKT cells in liver, spleen and colonic lamina propria as determined by flow cytometry using  $\alpha$ -GalCer/CD1d tetramers ( $n = 4$  mice per group). **c**, Representative histograms of CD1d cell surface expression on colonic IECs of the indicated mouse strains before (left,  $n = 5$  mice per group) and 6 h after (right,  $n = 5$  mice per group) rectal oxazolone challenge. **d**, CD1d-mediated antigen presentation by colonic IECs of the indicated mouse strains ( $n = 5$  mice per group). Presentation of the model glycolipid antigen  $\alpha$ -GalCer to invariant NKT-cell hybridomas 24.7 and DN32.D3 and of endogenous antigens (autoreactivity) to the non-invariant NKT-cell hybridoma 14S.6 is shown. **e**, Presentation of H2-K<sup>b</sup>-restricted SIINFEKL presentation by the indicated IECs ( $n = 5$  mice per group) to the SIINFEKL-responsive hybridoma RF33.70. Results representative of three independent experiments are shown **b–e**, Mean  $\pm$  s.e.m. of triplicate cultures are shown. Student's *t*-test was applied. **f**, Intestinal epithelial CD1d is protective in oxazolone colitis. Representative macroscopic colon images of *Cd1d1*<sup>ΔIEC</sup> and wild-type littermates upon rectal challenge with oxazolone (Ox.,  $n = 5$  mice per group) or vehicle (ethanol (EtOH),  $n = 4$  mice per group).



**Extended Data Figure 6 | Epithelial HSP110 expression is decreased in *Mttp*<sup>ΔIEC</sup> mice and in human ulcerative colitis.** **a**, HSP110 immunohistochemistry in mice with IEC *Mttp* deletion (bottom) as compared with wild-type littermates (top) 6 h after rectal oxazolone challenge. **b**, HSP110 immunohistochemistry in the colonic intestinal epithelium and the lamina propria of healthy controls and patients with active and inactive ulcerative colitis. Signal intensity was scored on a scale from 0 to 3 in a blinded fashion.

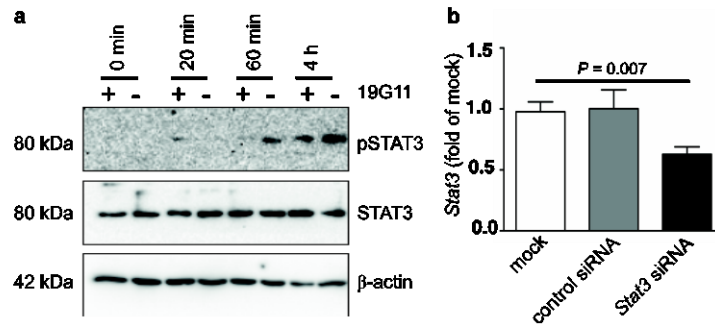
Each symbol represents a single patient. The median and significance level as determined by the Mann-Whitney *U*-test are shown. **c**, Mortality in conventional HSP110-knockout mice in the oxazolone colitis model. Results representative of three independent experiments are shown. Mean  $\pm$  s.e.m. of the indicated number of mice is shown. Student's *t*-test and the log-rank test (survival) were applied. NS, not significant.

RESEARCH LETTER



**Extended Data Figure 7 | Purity of isolated IECs.** After isolation of colonic IECs, potential contamination with haematopoietic cells was investigated by flow cytometry. The major population of cells was gated (upper left), was shown to contain viable cells (upper middle), and to contain largely EpCAM-positive

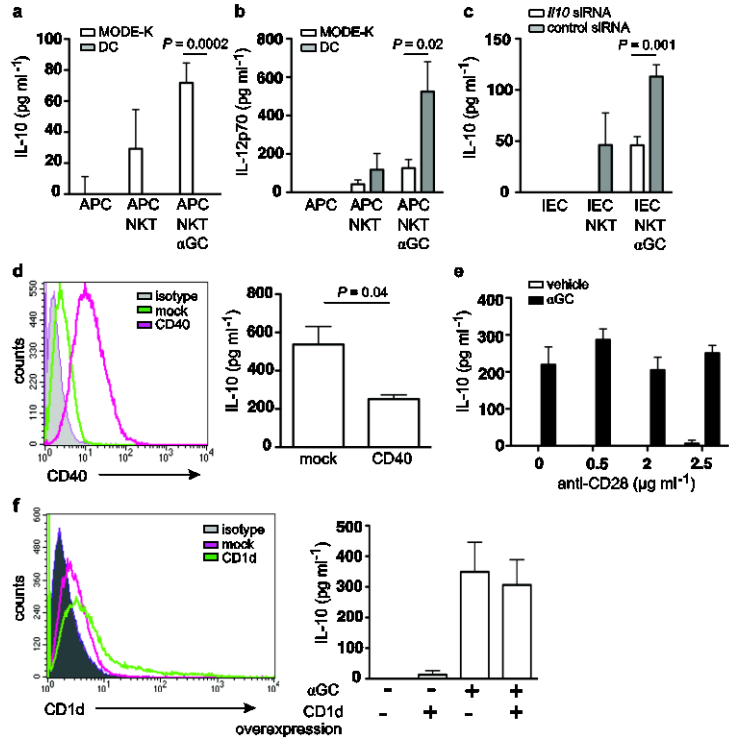
epithelial cells that do not stain with leukocyte markers (middle and bottom). The upper right panel shows isotype control staining. Results representative of three independent experiments ( $n = 5$  mice per experiment) are shown.



**Extended Data Figure 8 | CD1d-dependent STAT3 phosphorylation upon co-culture of IECs and iNKT cells.** a, STAT3 phosphorylation in IECs upon co-culture with iNKT cells is CD1d-dependent. Expression of pSTAT3, STAT3 and β-actin as determined by western blotting of MODE-K cells at the indicated time after addition of the iNKT-cell hybridoma 24.7. Where indicated, MODE-K cells were pre-incubated with a monoclonal blocking

antibody directed against CD1d (19G11; +) or an isotype control (-). b, siRNA-mediated knockdown of *Stat3* in MODE-K cells as determined 68 h after siRNA transfection. Results representative of three independent experiments are shown. Means ± s.e.m. of triplicates are shown. Student's *t*-test was applied.

RESEARCH LETTER



**Extended Data Figure 9 | CD1d-mediated cytokine production is dependent on the APC and expression of co-stimulatory molecules. a-f, IL-10 (a, c-f) and IL-12p70 (b) secretion of co-cultures of the IEC line MODE-K or splenic dendritic cells (DCs) together with the iNKT-cell hybridoma 24.7. APCs were loaded with α-GalCer (αGC; 100 ng ml<sup>-1</sup>) before washing and co-culture with iNKT cells. c, MODE-K cells (IEC) were transfected with control siRNA or siRNA directed against *Il10* before co-culture with iNKT cells.**

**d, f, MODE-K cells were transfected with CD40 (d) and CD1d (f) as indicated. Histograms demonstrated increased expression of CD40 (d) and CD1d (f) after transfection. e, Stimulatory anti-CD28 antibody was added during co-culture of MODE-K and iNKT cells. Means ± s.e.m. of quadruplicate cultures are shown. Student's *t*-test was applied. Results are representative of two independent experiments.**

Extended Data Table 1 | Genes downregulated in expression in oxazolone-challenged *Mttp*<sup>ΔIEC</sup> mice

Fold Change*	GeneID	Description
8.721	<i>Irf202b</i>	interferon activated gene 202B
3.878	<i>Eya3</i>	eyes absent 3 homolog (Drosophila)
3.7	<i>Sipa111</i>	signal-induced proliferation-associated 1 like 1
3.661	<i>Gna14</i>	AV230778 RIKEN full-length enriched, 0 day neonate skin Mus musculus cDNA clone 4632401H08 3', mRNA sequence.
3.534	<i>Cd79b</i>	CD79B antigen
3.347	<i>Mapk14</i>	mitogen activated protein kinase 14
3.347	<i>Aasdhppt</i>	aminoadipate-semialdehyde dehydrogenase-phosphopantetheinyl transferase
3.259	<i>Marcks</i>	myristoylated alanine rich protein kinase C substrate
3.216	<i>Tgtp</i>	T-cell specific GTPase
3.216	<i>Rbmx</i>	RNA binding motif protein, X chromosome
3.178	<i>Tcl1b3</i>	T-cell leukemia/lymphoma 1B, 3
3.162	<i>Clu</i>	clusterin
3.134	<i>Indo</i>	indoleamine-pyrrole 2,3 dioxygenase
3.12	<i>Ncl</i>	uy94h11.x1 NCI_CGAP_Mam5 Mus musculus cDNA clone IMAGE:3667269 3' similar to SW:NUCL_MOUSE P09405 NUCLEOLIN ; mRNA sequence.
3.101	<i>Hspa4</i>	heat shock protein 4
3.068	<i>Gbp2</i>	guanylate nucleotide binding protein 2
3.057	<i>Ncbp2</i>	nuclear cap binding protein subunit 2
3.034	<i>Mcm5</i>	minichromosome maintenance deficient 5, cell division cycle 46 (S. cerevisiae)
<b>3.024</b>	<b><i>Hsph1</i></b>	<b>heat shock protein 110</b>

\* Fold change: *Mttp*<sup>+/+</sup> / *Mttp*<sup>ΔIEC</sup>Genes downregulated by more than threefold in intestinal mucosal scrapings of *Mttp*<sup>ΔIEC</sup> mice compared with wild-type littermates 6 h after rectal challenge with oxazolone.

### 3 Discussion

In this study we could reveal an epithelial signaling pathway critical for intestinal homeostasis, involving intestinal epithelial CD1d, HSP110 and IL-10. To this end we show that mice with impaired CD1d-mediated antigen presentation by IECs (*Cd1d1<sup>ΔIEC</sup>*, *Mttp<sup>ΔIEC</sup>* mice) were significantly more susceptible to oxazolone colitis than WT mice, which was due to impaired epithelial expression of HSP110 and IL-10. It was previously demonstrated that epithelial CD1d can promote the production of IL-10.<sup>27</sup> This study further suggested that CD1d-dependent expression and secretion of IL-10 is dependent on retrograde signaling of CD1d through its cytoplasmic tail.<sup>26</sup> To test whether similar principles apply to IECs *in vivo*, we performed cross-linking experiments on purified IECs from mice expressing “tail-deleted” CD1d, lacking the intracellular C-terminus of CD1d (*TD-CD1d*). Indeed, IECs obtained from these mice exhibited reduced expression of *Hsph1* and *Ii10* mRNA under constitutive conditions and also after sensitization of the mice with the iNKT cell agonist  $\alpha$ GalCer, thus supporting the notion that retrograde CD1d signaling promotes the expression of IL-10 by IECs. STAT3, which can bind to STAT sites in the promoters of the *Cd1d1*, *Hsph1* and *Ii10* genes, was identified as potential downstream target of CD1d.<sup>30</sup> siRNA-mediated knockdown of *Stat3* in an intestinal epithelial cell line indeed resulted in reduced transcription of *Cd1d1*, *Hsph1* and *Ii10* mRNA. Additionally, reduced STAT3 phosphorylation was observed in IECs of *Cd1d1<sup>ΔIEC</sup>* and *TD-Cd1d* mice, confirming its role as integrating factor in the described protective CD1d-dependent signaling pathway in IECs. These results are in accordance with preceding studies demonstrating the importance of the activation of intestinal epithelial STAT3 in the regulation of intestinal homeostasis and wound healing during colitis.<sup>31,32</sup> Interestingly, IL-10 and HSP110 themselves can signal through STAT3 and thereby further increase their own expression, along with that of CD1d, thus generating a positive feedback loop.

However, constantly activated STAT3 is also involved in the development of colorectal cancer and acts downstream of IL-6 and IL-11 signaling during chronic inflammation.<sup>33,34</sup> It is therefore possible, that the described feedback loop, while protecting from acute intestinal inflammation, may promote the development of colorectal cancer.<sup>35</sup> This needs to be investigated further, as does the exact mechanism behind retrograde CD1d signaling. Nevertheless, our studies clearly



demonstrate the importance of IEC-derived IL-10 downstream of STAT3 in the amelioration of intestinal inflammation.

Another interesting aspect which was not explored during the course of these studies is the repertoire of lipids associated with intestinal epithelial CD1d and their effect on retrograde CD1d signaling. CD1d is capable of binding a range of endogenous lipid species, including phospholipids and glycosphingolipids, of which only few have been identified as NKT cell antigens.<sup>12,36-41</sup> Multiple studies have established that inflammatory responses can affect cellular lipid metabolism and thus CD1d-mediated antigen presentation.<sup>12</sup> Also, a recent publication by *Iyer et al.* established that STAT3 is involved in the expression of an enzyme required for the biosynthesis of glycosphingolipids. STAT3-deficient APCs exhibited reduced presentation of endogenous antigens to NKT cells, while the presentation of exogenous antigens was not impaired.<sup>42</sup> With respect to our study this may suggest that epithelial lipid metabolism - and thus potentially CD1d-mediated antigen presentation to NKT cells - may not only be influenced by the inflammatory conditions in the intestine during colitis, but also by STAT3-dependent processes upon retrograde CD1d signaling.

However, the investigation of CD1d-associated lipids is laborious and has been of limited success because classical protein isolation methods involving detergents cannot be utilized for the isolation of CD1d-lipid complexes. We thus set out to establish genetically engineered CD1d proteins, which can be enzymatically cleaved from the cell surface of eukaryotic cells instead of requiring extraction from the plasma membrane (Part II). Cell-surface cleavable CD1d proteins would be an invaluable asset for the investigation of CD1d-associated lipids *in vitro* and *in vivo* and would help to address the question of whether cell-intrinsic differences in the CD1d-associated lipid repertoire provide the basis for APC-specific effects of CD1d in intestinal inflammation.

## Part II: Genetically Engineered CD1d Proteins for the Investigation of the CD1d-Associated Lipid Repertoire

### 1 Introduction

#### 1.1 CD1d Structure and Trafficking

CD1d is a member of the CD1 (cluster of differentiation 1) family of proteins, which is separated into group 1 (CD1a, CD1b, CD1c) and group 2 (CD1d). Since group 1 CD1 proteins are not expressed by mice, CD1d is the most extensively researched CD1 protein.<sup>12,43</sup> By presenting antigens to lipid-reactive T cells, such as NKT cells, CD1 proteins play important roles in immune homeostasis.

CD1 proteins are structurally similar to classical MHC class I proteins, bearing three N-terminal extracellular domains ( $\alpha_{1-3}$ ), a single transmembrane domain (TMD) and an intracellular C-terminal domain. However, unlike classical MHC class I and II molecules, CD1 family members do not bind peptide antigens, but lipids.<sup>44</sup> This can be attributed to deeper, largely hydrophobic antigen binding pockets (A' and F' pockets and additional C' and T' pockets in CD1b). These accommodate the fatty acyl tails of the lipids and leave the headgroups accessible for presentation to CD1-restricted T cells.<sup>43</sup> Antigen-binding groove volumes vary between the CD1 isoforms, allowing for presentation of distinct lipid antigens by different molecules (Figure 2).<sup>45</sup>

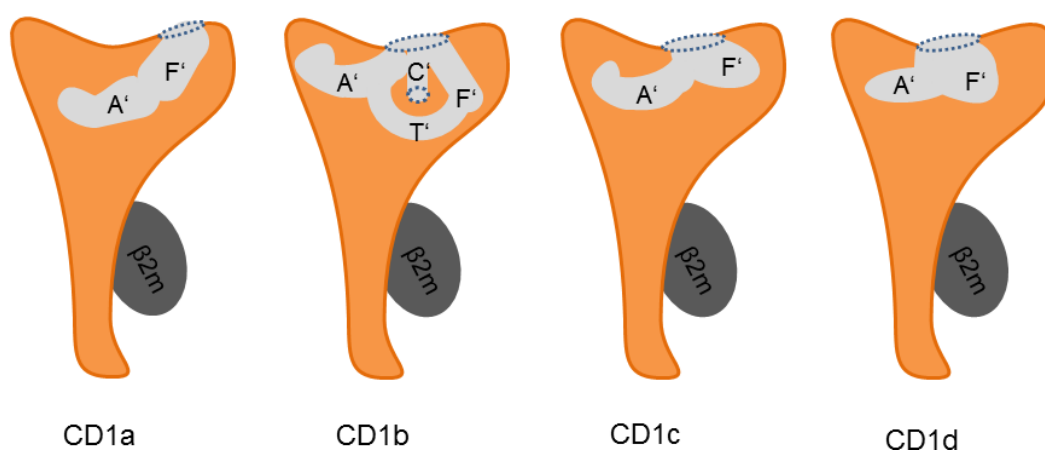


**Figure 2: Schematic Depiction of the Antigen-Binding Grooves of the CD1 Isoforms**

CD1a, c and d have two antigen-binding pockets (A' and F'), while CD1b has two additional loops (C' and T'). Adapted from De Libero and Mori, 2010<sup>46</sup>.

CD1d synthesis depends on ER chaperones such as calnexin, calreticulin and the thiol oxidoreductase ERp57, which support correct folding and disulfide bond formation of the CD1d heavy chain. Once CD1d is in its correct conformation, it leaves the ER as a free heavy chain or as a heterodimer, non-covalently associated with  $\beta_2$ -microglobulin ( $\beta_2m$ ) at the  $\alpha_3$  domain.<sup>44,47,48</sup> CD1d passages along the secretory pathway and is believed to load lipids in each of the compartments: from the ER through the Golgi complex to the plasma membrane, where it presents lipid antigens to CD1d-restricted NKT cells.<sup>43</sup> Continuing on from the plasma membrane, human (h) and mouse (m) CD1d undergo different internalization pathways. While hCD1d only passes through early endosomes and the endocytic recycling compartment, mCD1d additionally passes through late endosomes and lysosomes before recycling back to the plasma membrane.<sup>45</sup> Internalization of human and mouse CD1d is clathrin-dependent and is mediated by interaction of adaptor proteins (AP) with a tyrosine-based sorting motif (YXX $\phi$ ) in the cytoplasmic tail of the CD1d heavy chain. This sequence of two random amino acids (X) which are framed by a tyrosine (Y) and a bulky hydrophobic amino acid ( $\phi$ ) binds to the  $\mu$  domain of AP2, mediating entry into early endosomes.<sup>49-52</sup> The mCD1d YXX $\phi$  motif additionally associates with the  $\mu$ 3A subunit of AP3, which targets the protein to lysosomes (Figure 3).<sup>43,53</sup>

## 1.2 CD1d-Associated Lipids

Different studies have demonstrated that defects in the trafficking of and lipid transfer onto CD1d influence its antigen presentation and thereby the development and function of NKT cells.<sup>52-56</sup> While passaging through the cell, CD1d loads and exchanges a range of self- and non-self-lipids. Lipid loading onto CD1d in the ER is facilitated by lipid transfer proteins, such as the microsomal triglyceride transfer protein (MTP). It is believed that MTP-mediated ligand binding stabilizes the CD1d heavy chain before its departure from the ER.<sup>57-59</sup> *En route* through the secretory pathway, CD1d mainly loads glycosphingolipids (GSLs), glycerophospholipids (GPLs) and sphingolipids, which are presented to CD1d-restricted T cells at the cell surface.<sup>60-62</sup> Within the endolysosomal compartments, these lipids are exchanged for other endogenous or exogenous lipids (of microbial or environmental origin). This exchange is mediated by low pH values, which stabilize the conformation of CD1d.<sup>59</sup> Also, endolysosomal lipid transfer proteins, such as members of the saposin family,

extract lipids from membranes and load them onto CD1d in a manner not fully understood.<sup>51,56,63,64</sup> These newly loaded lipids have often been previously altered by endolysosomal glycosidases and lipases, which process the complex glycolipid headgroups and lipid tails, respectively, thereby modifying lipid antigenicity.<sup>37,56,65,66</sup> Recycling of CD1d through the endolysosomal compartments allows the presentation of different lipids by the same CD1d molecule (Figure 3).

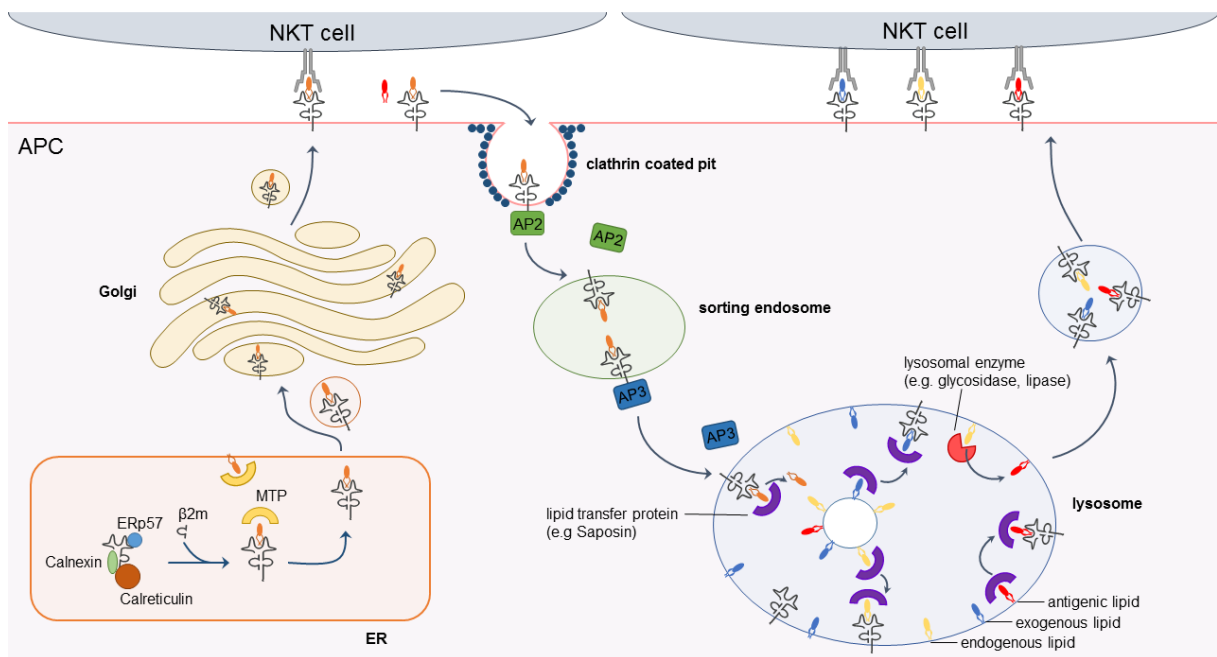


**Figure 3: Trafficking of mCD1d**

CD1d is synthesized in the ER of the antigen presenting cell (APC), where it is folded under the influence of the ER chaperones calnexin, calreticulin and ERp57.  $\beta_2m$  loosely associates with the CD1d heavy chain and endogenous lipid is transferred onto CD1d by microsomal triglyceride transfer protein (MTP). Following trafficking through the Golgi apparatus and presentation of endogenous lipids at the cell surface, CD1d is endocytosed in a clathrin-dependent fashion. Adaptor protein (AP) 2 mediates the transfer of CD1d into sorting endosomes, from where AP3 recruits CD1d into lysosomes. Endogenous lipids are exchanged for other endogenous or foreign antigens by means of lipid transfer proteins, such as saposins. Endogenous lipids are often modified by lysosomal enzymes such as glycosidases or lipases, CD1d is recycled to the cell membrane, where it presents the antigens loaded in lysosomes to CD1d-restricted NKT cells.

Experiments using modified CD1d molecules, which are either retained in the ER (ER-CD1d), secreted at the plasma membrane (secreted CD1d) or undergo normal trafficking through the endolysosomal compartments, revealed trafficking-dependent differences in the spectrum of CD1d-associated lipids. For instance, ER-retained CD1d mostly bound GPLs, while lipid extractions from CD1d molecules which had

passed through the ER and Golgi contained GPLs, GSLs and sphingolipids.<sup>60–62,67</sup> The majority of self-lipids associated with CD1d most likely exhibit limited to no antigenicity.<sup>36,37,41,68</sup> However, some *bona fide* self-derived iNKT antigens have been identified, including glycosphingolipids such as isoglobotrihexosylceramide (iGb3), and phospholipids such as lysophosphatidylcholine (LPC), plasmalogen lysophosphatidylethanolamine (pLPE) or ether bonded lysophosphatidic acid (eLPA). Antigens for nI NKT cells include (lyso)sulfatide and LPE, which are also antigens for iNKT cells (Figure 4).<sup>12,36–39,41,56</sup> Previously, the GSLs  $\beta$ -galactosylceramide ( $\beta$ GalCer) and  $\beta$ -glucosylceramide ( $\beta$ GlcCer) were believed to be antigens for iNKT cells.<sup>68</sup> However, recent studies have suggested that mammalian cells may also produce small quantities of  $\alpha$ -linked glucosylceramides, which cannot be differentiated from  $\beta$ -linked glucosylceramides through conventional lipidomics analysis. These recent studies propose that the antigenic lipids previously identified as  $\beta$ GalCer and  $\beta$ GlcCer are actually mammalian  $\alpha$ GalCer and  $\alpha$ GlcCer (Figure 4).<sup>69,70</sup> Microbes and inflammatory responses can influence the cellular lipid metabolism, thereby altering the ratio of antigenic to non-antigenic self-lipids and thus increasing the likelihood of NKT cell activation.<sup>12,37,60,71,72</sup>

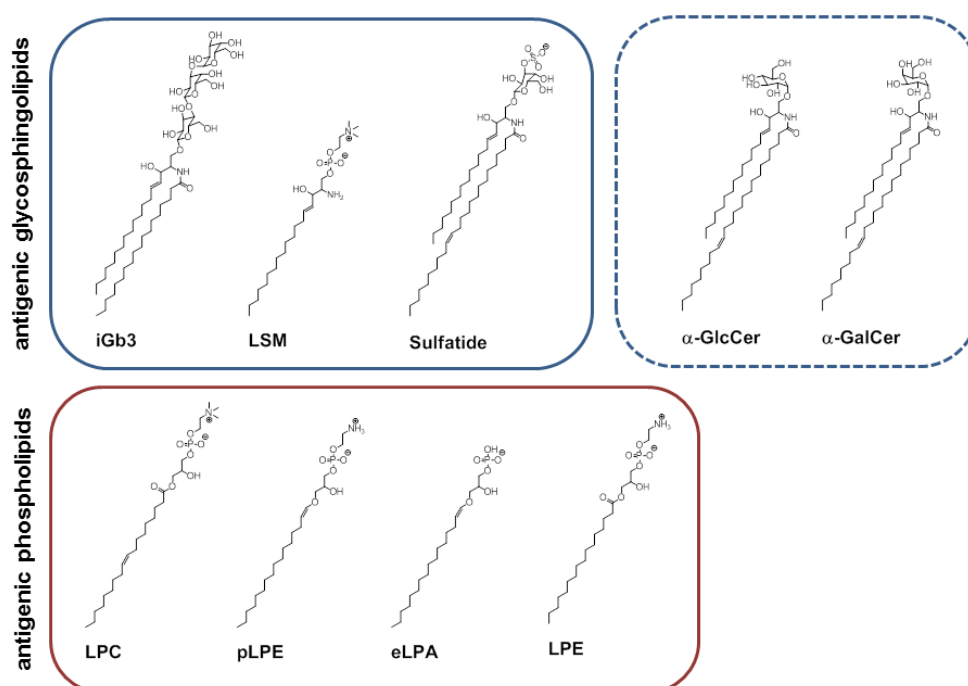


**Figure 4: Antigenic Self-Lipids**

Examples of known (solid frame) and putative (dashed frame) self-lipid antigens for invariant and/or non-invariant NKT cells. Adapted from Dowds, Kornell, Blumberg, Zeissig; 2014.<sup>12</sup>

The range of exogenous CD1d-associated lipids is even broader. NKT cell-activating lipids include  $\alpha$ -linked GSLs, phospholipids, glycolipids and lipophosphoglycans derived from various bacteria and protozoans. These lipids either associate with CD1d at the cell surface or during recycling through the endolysosomal compartment.<sup>12,73–77</sup>

Considering the dimension of lipids generated and modified by eukaryotic and prokaryotic cells, which could theoretically be bound and presented by CD1d, this small number of identified lipids is likely a minor part of the complete spectrum of CD1d-associated lipids. Identifying NKT-activating lipids and understanding their origin therefore remains an important, but technically challenging, aspect of immunological research.

### 1.3 Constructs for the Analysis of the CD1d-associated Lipidome

Different research groups have generated modified CD1d molecules to investigate the CD1d-associated lipid repertoire. Adding retention signals such as a KDEL sequence (ER-CD1d), deleting the transmembrane and C-terminal domain (secreted CD1d) or deleting the last seven amino acids required for CD1d endocytosis (TD-CD1d) have provided insight into the significance of different cellular compartments for CD1d and NKT cell physiology.<sup>52,53,60–62,78</sup>

To fully characterize the CD1d-associated lipidome and thus its role in NKT cell physiology, it would be crucial to investigate wild type (WT) CD1d, which undergoes trafficking through the secretory pathway and the endolysosomal compartments. However, this is associated with technical difficulties, as chemical (detergents) or physical (freeze-thaw cycles) methods used for the isolation of transmembrane proteins, such as CD1d, are associated with the dissociation of lipids bound by the protein. A promising alternative was presented by *Yuan* and colleagues, as well as by *Muindi* and colleagues, who developed enzymatically cleavable CD1d constructs, which undergo trafficking through the secretory pathway and endolysosomal compartments.<sup>60,61</sup> Both groups inserted a short peptide sequence between the TMD and the  $\alpha_3$  domain of the CD1d heavy chain. One peptide sequence was the cleavage site associated with premature  $\gamma$ -IFN-inducible lysosomal thioreductase (GILT), which is proteolytically cleaved into its mature form in lysosomes. *Yuan* and colleagues anticipated that endogenous lysosomal cleavage of their engineered

CD1d protein would result in spontaneous release of CD1d once it reached the lysosome. However, cleavage was inefficient and the concentration of released CD1d therefore too low for mass spectrometry (MS)-based analysis of CD1d-associated lipids.<sup>61</sup>

Another strategy investigated was based on tobacco etch virus (TEV) protease.<sup>60,79</sup> Due to its high sequence specificity, TEV protease is commonly used for controlled intracellular proteolysis of fusion proteins in prokaryotic cells or cleavage of purified fusion proteins.<sup>80,81</sup> Large quantities of the enzyme can be generated through transformation of yeast or *E. coli* strains with TEV protease expression plasmids, making it an attractive tool in biotechnology. Moreover, mutated, more stable forms of the protease are commercially available from different vendors.<sup>82</sup> *Muindi* and colleagues therefore engineered a CD1d protein containing two TEV protease recognition sites in the juxtamembrane part of the extracellular domain of CD1d. However, the authors observed limited to no TEV-induced cleavage of CD1d, while spontaneous release of CD1d was observed. They were able to analyze glycans bound to the cleavable CD1d, but noted that the quantity was lower than that of secreted CD1d and thus information about rare lipid species may have been lost.<sup>60</sup> Thus, CD1d constructs which undergo unimpaired subcellular trafficking and can be proteolytically released at the cell surface in quantities sufficient for MS analysis do not exist at present.

An interesting alternative for TEV protease might be sortase A (SrtA), a bacterial transpeptidase involved in the anchoring of bacterial cell wall proteins.<sup>83,84</sup> SrtA-mediated cleavage occurs in two sequential reactions. First, SrtA cleaves the threonine-glycine bond of an LPXTG sequence, forming an acyl-enzyme intermediate. This intermediate can then be attacked by a substrate containing an N-terminal amino group, which is subsequently linked to the C-terminal threonine, generating a fusion protein (Figure 5). Researchers have used this strategy to label proteins with fluorophores or affinity tags such as biotin or streptavidin.<sup>85-87</sup> If no nucleophilic substrate is available, the protein can be released from the enzyme complex by spontaneous hydrolysis. Hence, SrtA could be used as an alternative for TEV protease for proteolytic release of CD1d from the plasma membrane (Figure 5).

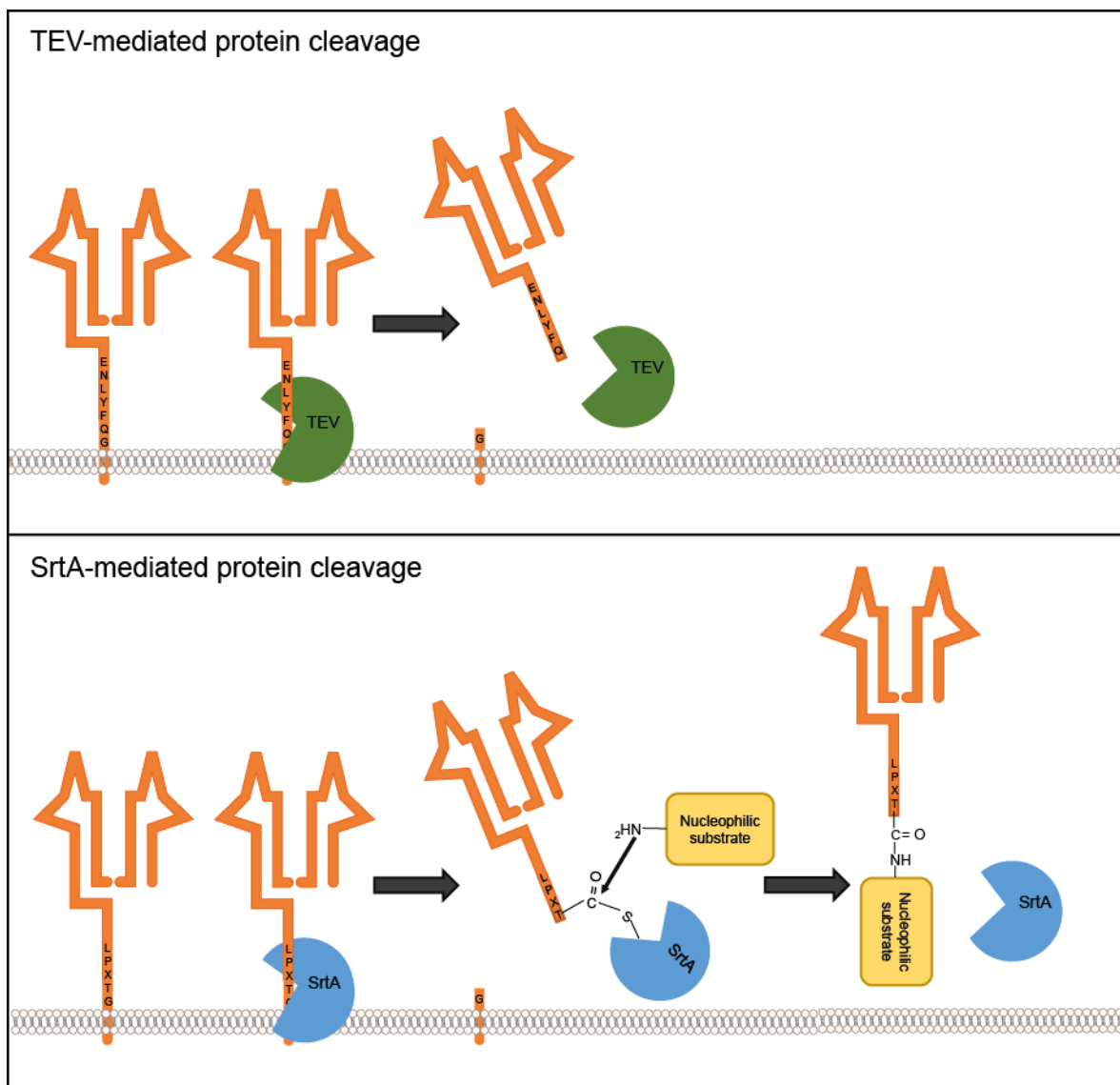


**Figure 5: Schematic Depiction of TEV Protease- and Sortase A-Mediated Protein Cleavage**

TEV protease recognizes the amino acid motif ENLYFQG and cleaves the peptide bond between threonine and glycine, thereby releasing the extracellular domain of the transmembrane protein. Sortase A transpeptidase recognizes an LPXTG amino acid motif, cleaves the peptide bond between threonine and glycine and then forms an acyl-enzyme intermediate. This intermediate can be attacked by a nucleophilic molecule containing an N-terminal amino group, which is then linked to the C-terminal threonine, resulting in release of the fusion protein from the enzyme.

CD1d constructs amenable to proteolytic release at the cell surface may provide a critical, novel approach to the study of CD1d-associated lipids. These constructs would enable the analysis of lipids bound to a fully functional CD1d protein with unimpaired subcellular trafficking, which could be released at a given time using specific enzymes in the absence of detergents. Such CD1d constructs, once established, could be used for a range of experiments, both *in vitro* and *in vivo*.



Besides experiments with cultured cells, integrating these constructs into the genome of model organisms would allow for the investigation of spatial and temporal variations, as well as tissue- and disease-specific changes in the spectrum of CD1d-associated lipids. Such strategies would provide unique insight into the lipid antigens involved in protective and pathogenic NKT cell responses and may provide the basis for future therapeutic approaches targeting NKT cells in human disease. Therefore, we aimed to establish engineered CD1d molecules, which are susceptible to specific proteolytic release at the cell surface and display unimpaired trafficking, lipid loading and antigen presentation.

## 2 Materials

### 2.1 Antibodies

**Table 1: Antibodies**

Antigen	Clone	Host	Source	Concentration
$\alpha$ -mouse mCD1d	19G11	rat	BioXCell, West Lebanon, USA	10 mg/ml
$\alpha$ -mouse mCD1d	1B1 biotinylated	rat	Biologend, London, UK	10 mg/ml
$\alpha$ -mouse mCD1d	1B1 PE- Labeled	rat	Biologend, London, UK	0.25 mg/ml
$\alpha$ -human mCD1d	51.1 PE- labeled	rat	Biologend, London, UK	0.25 mg/ml

### 2.2 Bacteria

DH5 $\alpha$  Chemically Competent *E. coli*

New England Biolabs, Frankfurt am  
Main, Germany

Top10 Chemically Competent *E. coli*

New England Biolabs, Frankfurt am  
Main, Germany

### 2.3 Buffers and Solutions

DMEM complete

500 ml DMEM  
10 % FCS (v/v)  
2 mM L-glutamine  
1 % penicillin-streptomycin (v/v)

10 x DNA Loading Dye

12.5 ml Ficoll  
37.5 ml TE Buffer  
25 mg Bromophenol blue

ELISA Blocking Buffer

1 x PBS  
10 % FCS (v/v)

ELISA Washing Buffer	1 x PBS 0.05 % Tween20 (v/v)
FACS Buffer	1 x PBS 1 % FCS (v/v)
10 x Hank's Buffered Saline Solution (HBSS)	1.37 M NaCl 54 mM KCl 4.4 mM $\text{KH}_2\text{PO}_4$ 55 mM Glucose 3.4 mM $\text{Na}_2\text{HPO}_4$ anhydrous  Add 4.2 mM $\text{NaHCO}_3$ to 1 x HBSS
Luria-Bertani (LB) Medium	5 g yeast extract 10 g bacterial peptone 5 g NaCl $\text{H}_2\text{O}$ ad 1 l
LB Agar	5 g yeast extract 10 g bacterial peptone 5 g NaCl 15 g Agar-Agar $\text{H}_2\text{O}$ ad 1 l
10 x Phosphate Buffered Saline (PBS)	1.37 M NaCl 27 mM KCl 100 mM $\text{Na}_2\text{HPO}_4$ 18 mM $\text{KH}_2\text{PO}_4$  set pH to 7.4

RPMI 1640 complete	500 ml RPMI 1640 10 % FCS (v/v) 2 mM L-glutamine 1 % penicillin-streptomycin (v/v)
50 x Tris-Acetate-EDTA (TAE) Buffer	1 M Tris base 0.54 % glacial acetic acid (v/v) 10 % EDTA 0.5 M (v/v)
Tris-EDTA (TE) Buffer	10 mM Tris-HCl pH 7.5 1 mM EDTA

## 2.4 Cell Lines

24.7 cells	J. Gumperz, 2000 <sup>78</sup>
HeLa cells	G.O. Gey, 1952 <sup>88</sup>
L-cells	K.K. Sanford, 1948 <sup>89</sup>
MODE-K cells	K. Vidal, 1993 <sup>90</sup>
THP-1_hCD1d_LPETG(GGGS) <sub>3</sub> cells	Kind gift from Gijs Grotenbreg, Singapore, Singapore <sup>91</sup>

## 2.5 Cell Culture Reagents

Dulbecco's Modified Eagle Medium (DMEM)	Biochrom, Berlin, Germany
Fetal calf serum	Biochrom, Berlin, Germany
L-glutamine	Biochrom, Berlin, Germany
Lipofectamine 2000	Life Technologies, Darmstadt, Germany
Penicillin/streptomycin solution	Biochrom, Berlin, Germany
RPMI 1640	Biochrom, Berlin, Germany
10 x Trypsin-EDTA Solution	Biochrom, Berlin, Germany
TurboFect	Life Technologies, Darmstadt, Germany
Ultra-Pure water	Biochrom, Berlin, Germany

## 2.6 Chemicals and Reagents

2-Propanol	Carl Roth, Karlsruhe, Germany
Agar-Agar	Carl Roth, Karlsruhe, Germany
Agarose	Carl Roth, Karlsruhe, Germany
Ammonium chloride (NH <sub>4</sub> Cl)	Merck, Darmstadt, Germany
Ampicillin sodium salt	Sigma Aldrich, Seelze, Germany
Bacterial peptone	BD Biosciences, Heidelberg, Germany
BD Via-Probe Cell Viability Dye	BD Biosciences, Heidelberg, Germany
Bovine serum albumin (BSA)	Serva, Heidelberg, Germany
Brefeldin A	Bio-Rad, München, Germany
Bromophenol blue	Sigma Aldrich, Seelze, Germany
Disodium phosphate (Na <sub>2</sub> HPO <sub>4</sub> )	Merck, Darmstadt, Germany
EDTA 0,5 M solution pH 8.0	Applied Biosystems, Darmstadt, Germany
Ethanol 99 % p.A.	Carl Roth, Karlsruhe, Germany
Ethidium bromide solution	Bio-Rad, München, Germany
Fixable Viability Dye eFluor®450	eBioscience, Frankfurt am Main, Germany
Geneticin G418 sodium salt	Life Technologies, Darmstadt, Germany
Glucose	Merck, Darmstadt, Germany
HEPES	Sigma Aldrich, Seelze, Germany
HPLC grade water	Sigma Aldrich, Seelze, Germany
1 N Hydrochloric acid (HCl)	Merck, Darmstadt, Germany
Potassium chloride (KCl)	Merck, Darmstadt, Germany
Potassium dihydrogen orthophosphate (KH <sub>2</sub> PO <sub>4</sub> )	Merck, Darmstadt, Germany
Sodium chloride (NaCl)	Carl Roth, Karlsruhe, Germany
Sodium hydrogen carbonate (NaHCO <sub>3</sub> )	Merck, Darmstadt, Germany

Tris base	Calbiochem (Merck), Darmstadt, Germany
Tris	Calbiochem (Merck), Darmstadt, Germany
Tween 20	Merck, Darmstadt, Germany
Yeast extract	BD Difco, Heidelberg, Germany

## 2.7 Consumables

6-well cell culture dish	NUNC, Thermo Scientific, Wiesbaden, Germany
8-well RT-PCR strips	Brand, Wertheim, Germany
96-well flat bottom cell culture dish	NUNC, Thermo Scientific, Wiesbaden, Germany
Biosphere® stuffed pipet tips 200 µl	Sarstedt, Nümbrecht, Germany
Centrifuge tubes 15 ml, 50 ml	Sarstedt, Nümbrecht, Germany
Combitips Advanced® 2.5 ml, 5 ml, 10 ml	Eppendorf, Hamburg, Germany
Cryopure 1 ml cryo tube	Sarstedt, Nümbrecht, Germany
Feather disposable scalpel	pmf Medical, Köln, Germany
Flow cytometry tubes, 5 ml	Sarstedt, Nümbrecht, Germany
Kimwipes	Kimberly-Clark, Koblenz, Germany
Nalgene™ Rapid-Flow™ Bottle-Top Filter 0.22 µm	Thermo Scientific, Schwerte, Germany
Nitra-Tex® MicroTouch® gloves	Ansell, Munich, Germany
Parafilm®	Brand, Wertheim, Germany
Pasteur pipettes 230 mm	Hecht-Assistent, Sondheim, Germany
Peha-soft® powder free gloves	Hartmann, Heidenheim, Germany
Petri dish, 92x16 mm	Sarstedt, Nümbrecht, Germany
Pipet tips, 10 µl, 200 µl, 1000 µl, gel loader	Sarstedt, Nümbrecht, Germany
Reaction tubes 1.5 ml, 2 ml, 15 ml, 50 ml	Sarstedt, Nümbrecht, Germany
Serological pipet 5 ml, 10 ml, 25 ml	Sarstedt, Nümbrecht, Germany
T25 cm <sup>2</sup> , T75 cm <sup>2</sup> cell culture flask	Sarstedt, Nümbrecht, Germany

## 2.8 Enzymes and Substrates

AcTEV protease and buffer	Life Technologies, Darmstadt, Germany
Avidin-horseradish peroxidase (HRP)	Bio-Rad, München, Germany
BamHI	New England Biolabs, Frankfurt am Main, Germany
dNTPs	New England Biolabs, Frankfurt am Main, Germany
Dpnl	New England Biolabs, Frankfurt am Main, Germany
NheI	New England Biolabs, Frankfurt am Main, Germany
KpnI	New England Biolabs, Frankfurt am Main, Germany
ProTEV protease and buffer	Promega, Mannheim, Germany
Sortase A	121 Bio, Cambridge, USA
Sortase A	Kind gift of Gijbert Grotenbreg, Singapore, Singapore
T4 DNA Ligase	New England Biolabs, Frankfurt am Main, Germany
TMB substrate	Biolegend, London, UK
XbaI	New England Biolabs, Frankfurt am Main, Germany

## 2.9 Kits

Cytofix/Cytoperm™	BD Biosciences, Heidelberg, Germany
Endo-free Maxiprep Large Scale Plasmid Isolation Kit	Qiagen, Hilden, Germany
Miniprep Small Scale Plasmid Isolation Kit	Qiagen, Hilden, Germany
Mouse interleukin-2 (IL-2) ELISA Kit	BD Bioscience, Heidelberg, Germany

NucleoSpin® Gel and PCR Clean-up Kit	Macherey-Nagel, Düren, Germany
PeqGOLD Plasmid Miniprep Kit	Peqlab, Erlangen, Germany

## 2.10 Lipids

$\alpha$ -Galactosylceramide ( $\alpha$ -GalCer/KRN7000)	Avanti Polar Lipids, Alabaster, USA
Galactosyl- $\alpha$ 1-2-galactosylceramide ( $\alpha$ -GalGalCer)	Kind gift from Gurdyal Besra, Birmingham, UK

## 2.11 Instruments

Axiovert 25 Microscope	Carl Zeiss, Jena, Germany
Centrifuge Varifuge 3.0 R	Heraeus, Hanau, Germany
Centrifuge Varifuge 20 RS	Heraeus, Hanau, Germany
Chemidoc™ XRS System	Bio-Rad Laboratories, München, Germany
Dispenser Multipette® Plus	Eppendorf, Hamburg, Germany
Flex Station Multiplate Reader	Molecular Devices, Biberach and der Riß, Germany
Flow cytometer FACS Verse	BD Biosciences, Heidelberg, Germany
Flow cytometer & Cell Sorter FACSAriaII	BD Biosciences, Heidelberg, Germany
Freezer -20° C	Liebherr, Biebrach an der Riß, Germany
Freezer -80° C	Panasonic, Hamburg, Germany
Gel developing system GelDoc	Bio-Rad Laboratories, München, Germany
Gel developing system Alpha Imager	Alpha-Innotec, Kasendorf, Germany
Gel electrophoresis chamber Owl D2	Thermo Scientific, Schwerte, Germany
Horizontal shaker Unihood	Uniequip, Planegg, Germany
Ice machine	Ziegra, Isernhagen, Germany



Incubator BBD6220	Heraeus, Hanau, Germany
Laminar flow hood Herasafe	Heraeus, Hanau, Germany
Liquid nitrogen tank K Series	Taylor Wharton, Mildstedt, Germany
Magnetic stirrer Ikamag® RH	IKA, Staufen, Germany
Microwave R933	Sharp, Hamburg, Germany
Micro scale CP124-OCE	Sartorius AG, Göttingen, Germany
Multi channel pipet	Gilson, Villiers le Bel, France
Pipet Boy	Integra, Ratingen, Germany
Power pack P25	Biometra, Göttingen, Germany
Refrigerator 4° C	Liebherr, Bieberach an der Riß, Germany
Roller mixer Srt6d	Bibby Scientific Ltd, Staffordshire, UK
Roller mixer RS-TR05	Carl Roth, Karlsruhe, Germany
Single channel pipets Research Plus	Eppendorf, Hamburg, Germany
Sonication water bath 2510	Branson, Dietzenbach, Germany
Sprout mini centrifuge	Biozym, Hessisch Olendorf, Germany
Table top centrifuge Biofuge fresco	Heraeus, Hanau, Germany
Table top centrifuge Biofuge pico	Heraeus, Hanau, Germany
Table top centrifuge Labofuge 400	Heraeus, Hanau, Germany
Thermal cycler Bio-Rad MyCycler	Bio-Rad, München, Germany
Thermal cycler 2720	Applied Biosystems, Darmstadt, Germany
Thermal cycler T3000	Biometra, Göttingen, Deutschland
Vacuum pump Laboport	KNF, Freiburg, Germany
Vortex Vortexgenie 2	Scientific Industries, Schwerte, Germany
Water bath SW22	Julabo, Seelbach, Germany

## 2.12 Plasmids and DNA constructs

pcDNA3.1(+) empty	Life Technologies, Darmstadt, Germany
pcDNA3.1_m $\beta$ 2m_mCD1d_TEV	Genecust, Dudelange, Luxembourg
pcDNA3.1_h $\beta$ 2m_mCD1d_TEV	Genecust, Dudelange, Luxembourg
pcDNA3.1_h $\beta$ 2m_mCD1d_TEV(GGGS) <sub>3</sub>	generated in lab
pcDNA3.1_m $\beta$ 2m_sol_mCD1d	Genecust, Dudelange, Luxembourg
pcDNA3.1_h $\beta$ 2m_sol_mCD1d	Genecust, Dudelange, Luxembourg
mCD1d-Fc	Kind gift of Dr. Michael Brenner, Boston, USA
mCD1d-TEV-CT	Kind gift of Dr. Michael Brenner, Boston, USA
pcep4_LPETG_mCD1d(GGGS) <sub>0</sub>	Kind gift of Dr. Gijsbert Grotenbreg, Singapore, Singapore
pcep4_LPETG_mCD1d(GGGS) <sub>1</sub>	Kind gift of Dr. Gijsbert Grotenbreg, Singapore, Singapore
pcep4_LPETG_mCD1d(GGGS) <sub>2</sub>	Kind gift of Dr. Gijsbert Grotenbreg, Singapore, Singapore
pcDNA3.1_LPETG_mCD1d(GGGS) <sub>0</sub>	generated through mutagenesis
pcDNA3.1_LPETG_mCD1d(GGGS) <sub>1</sub>	generated through mutagenesis
pcDNA3.1_LPETG_mCD1d(GGGS) <sub>2</sub>	generated through mutagenesis

## 2.13 Software

Adobe Illustrator	Adobe Systems GmbH, München, Germany
BD FACSuite	BD Biosciences, Heidelberg, Germany
BD FACS Diva	BD Biosciences, Heidelberg, Germany
FlowJo	FlowJo LLC, Ashland, USA
GraphPad Prism	GraphPad Software, Inc., La Jolla, USA
Image Lab	Bio-Rad Laboratories, München,

Microsoft Excel	Germany
Microsoft Word	Microsoft, Redmond, USA
SnapGene software	Microsoft, Redmond, USA
SoftMax Pro	GSL Biotech LLC; snapgene.com
	Molecular Devices, Biberach an der Riß, Germany

## 2.14 Primers

**Table 2: Primer Sequences**

Primer name	Sequence	Use
PIPE_fwd	GGCGGCGGTAGCGGCGGTGGATCTGGAG G TTCAGGTGGAGCACCCGTGGGCCTGAT	PIPE Mutagenesis PCR
PIPE_rev	GGGTGCTCCACCTGAACCTCCAGATCCAC CGCCGCTACCGCCGCCCTGAAAATACAGG TTTTTCGC	PIPE Mutagenesis PCR
h $\beta$ <sub>2</sub> m_fwd	GGCTATCCAGCGTACTCCAAA	Sequencing cloning products
h $\beta$ <sub>2</sub> m_rev	CGGCAGGCATACTCATCTTTTT	Sequencing cloning products
mCD1d1ex23 _fwd	GAAGACTATCCCATTGAGATCC	Sequencing cloning products
mCD1d1ex3_ rev	TTTCCTTGAAATGCTACGTG	Sequencing cloning products
mCD1dseq_F	CTCACAGAGGTGATTCCTGCC	Sequencing cloning products
T7_F	TAATACGACTCACTATAGG	Sequencing cloning products

### 3 Methods

#### 3.1 Molecular Biological Methods

##### 3.1.1 Polymerase Incomplete Primer Extension Polymerase Chain Reaction (PIPE PCR)

A PIPE PCR is a type of mutagenesis PCR that allows the substitution of DNA sequences without requiring multiple PCRs or subsequent cloning steps, such as multi-enzymatic restriction digest and ligation. Primers, which contain a short binding sequence flanking the desired insertion or substitution site, and extensions complementary to each other, are used for the PCR. The PCR product is a linearized DNA sequence, including the required substitution (Figure 6).

Subsequently, the PCR product is incubated with DpnI restriction endonuclease (see 3.1.3), which only digests methylated DNA, i.e. DNA previously isolated from bacteria expressing Dam methylase, such as *E. coli*, but not the PCR product. This strongly reduces the amount of remaining original template. 5 µl of the PCR product were then transformed into chemically competent Top10 *E. coli* (3.1.5), where the linearized PCR products are circularized through intracellular ligation.

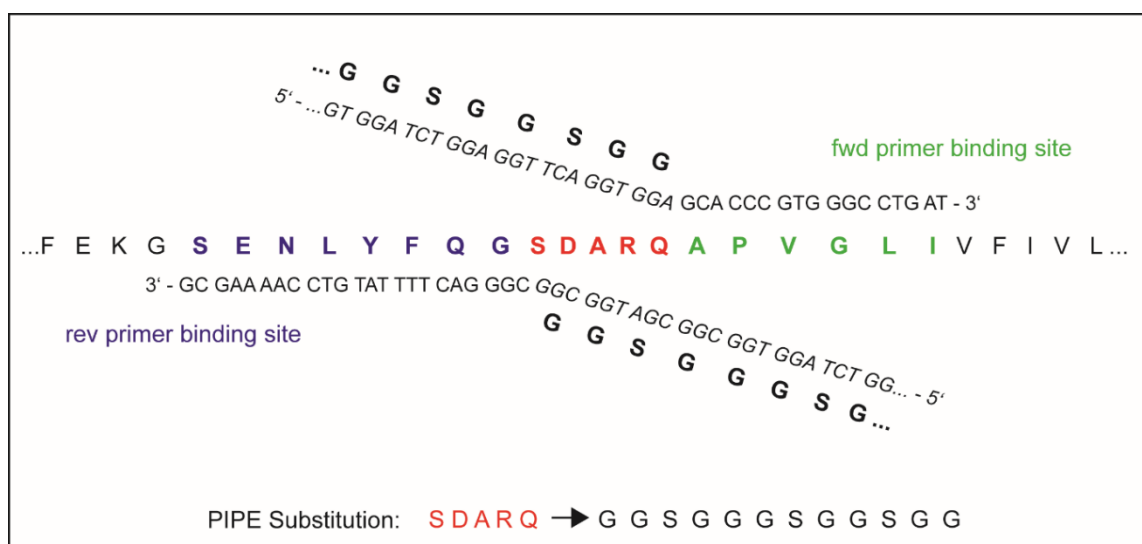


**Figure 6: Schematic Depiction of the  $h\beta_2m\_mCD1d\_TEV(GGGS)_3$  PIPE Substitution PCR.**

Primers including sequences complementary to each other flank the region chosen for substitution. The PCR results in the linearized plasmid, containing the substituted sequences introduced by the primers. By using an enzyme that leaves blunt ends, the linearized plasmid can be re-circularized by intracellular ligation during bacterial transformation. Adapted from Klock and Lesley; 2009.<sup>92</sup>

DNA amplification and modification was performed using Pfu Ultra II Fusion DNA Polymerase and the appropriate PIPE mutagenesis primers (Table 2). The reaction was set up according to table 3.

**Table 3: Composition of a PIPE-PCR Reaction**

Reagent	Composition per reaction	Volume (Vol) per reaction
10 x Pfu Ultra II Reaction Buffer	1 x	5 $\mu$ l
dNTP Mix	25 mM each	5 $\mu$ l
fwd Primer	10 $\mu$ M	1 $\mu$ l
rev Primer	10 $\mu$ M	1 $\mu$ l
Pfu Ultra II Fusion DNA Polymerase	1 $\mu$ l	1 $\mu$ l
Template	100 ng	1 $\mu$ l
HPLC H <sub>2</sub> O	ad 50 $\mu$ l	36 $\mu$ l
total Vol	50 $\mu$ l	50 $\mu$ l

**Table 4: Reaction Conditions for PIPE-PCR<sup>1</sup>**

Step	Process	Temperature	Time
1	Initial Denaturation	95° C	3 min
2	Denaturation	95° C	20 s
3	Annealing	70° C	30 s
4	Elongation	72° C	4 min
5	Final Elongation	72° C	10 min
6	Storage	4° C	$\infty$

### 3.1.2 Agarose Gel Electrophoresis

Agarose gel electrophoresis was used to visualize PCR products and separate DNA fragments by size. Depending on the size of the expected DNA fragments, gels with a concentration of 0.7 - 2 % agarose were used. The appropriate amount of agarose was dissolved in 1 x TAE buffer by boiling in a microwave, and after cooling briefly, ethidium bromide was added (final concentration of 0.25  $\mu$ g/ml). Once the gels had

<sup>1</sup> Steps 2-3 were repeated 25 times.

set, the PCR samples or restriction digest products were resuspended with the appropriate amount of 10 x DNA loading dye and 10-25  $\mu\text{l}$  of the product were loaded onto the gels. Electrophoresis was performed at 140-160 V.

DNA fragments required for further assays such as ligation or sequencing were cut from the agarose gel using a scalpel and transferred to a 1.5 ml reaction tube. The DNA was excised from the agarose using the Macherey-Nagel Nucleospin Gel and PCR Clean-up kit according to the manufacturer's protocol.

### 3.1.3 Restriction Digest

DNA can be cleaved by specific restriction endonucleases at palindromic DNA sequences of 4-8 base pairs, so-called restriction sites. DNA fragments cleaved by the same restriction enzyme can be ligated to generate new DNA sequences. Digestion was performed according to tables 5 and 6.

**Table 5: Restriction Digest of Plasmid DNA**

10 x Buffer	5 $\mu\text{l}$
Restriction Enzymes	1 $\mu\text{l}$ each
Plasmid DNA	0.1-1 $\mu\text{g}$
if required, 1 x BSA solution	5 $\mu\text{l}$
HPLC H <sub>2</sub> O	ad 50 $\mu\text{l}$

**Table 6: Restriction Digest of PCR Products**

10 x Buffer	5 $\mu\text{l}$
Restriction Enzymes	1 $\mu\text{l}$ each
PCR Product	20 $\mu\text{l}$
if required, 1 x BSA solution	5 $\mu\text{l}$
HPLC H <sub>2</sub> O	ad 50 $\mu\text{l}$

As needed, one or two restriction endonucleases were used per digest. The reaction was incubated at 37° C for 1-2 h. One half of the reaction was loaded onto an agarose gel for electrophoresis, the other half was stored at -20° C. DNA fragments required for further analysis were excised from the agarose gel and purified using the Macherey-Nagel Nucleospin Gel and PCR Clean-up kit according to manufacturer's protocol.

KpnI and XbaI were used for sub-cloning of the h $\beta_2$ m\_mCD1d\_TEV, m $\beta_2$ m\_mCD1d\_TEV, h $\beta_2$ m\_mCD1d\_TEV(GGGS)<sub>3</sub>, h $\beta_2$ m\_sol\_mCD1d and m $\beta_2$ m\_sol\_mCD1d constructs into pcDNA3.1.

For sub-cloning of pcep4\_LPETG\_mCD1d(GGGS)<sub>0-2</sub> into pcDNA3.1, NheI and BamHI restriction endonucleases were used.

#### 3.1.4 Ligation

DNA fragments restricted by the same restriction endonuclease can be joined between their 5' phosphate and 3' hydroxy groups by T4 DNA ligase. Normally, an average molar ratio of 3:1 of insert to plasmid vector is used for a ligation reaction. The required volumes were calculated based on the concentration and size of the DNA fragments. 2  $\mu$ l of 10 x T4 DNA ligase buffer and 1  $\mu$ l of T4 DNA ligase were added to the DNA fragments and the reaction was filled up to a final volume of 20  $\mu$ l using HPLC grade water. The reaction was incubated over night at 16° C and transformed into chemically competent *E. coli* the following day. Alternatively, the reaction was incubated for 3 h at room temperature (RT) and then transformed.

#### 3.1.5 Bacterial Transformation of Chemically Competent *E. coli* Strains

Top10 or DH5 $\alpha$  chemically competent *E. coli* were thawed on ice. 10-20  $\mu$ l of the ligation or 100 ng to 1  $\mu$ g of empty plasmid were added to 50  $\mu$ l of *E. coli* and mixed by careful snapping. The cells were kept on ice for 30 min and mixed gently every 10 min. After a 30 s heat shock in a water-bath at 42° C, the cells were kept on ice for an additional 2 min before being plated onto multiple LB-Agar plates (with 100  $\mu$ g/ml ampicillin) at different volumes (normally 10  $\mu$ l, 20  $\mu$ l, and 30  $\mu$ l per transformation and plate). The plates were incubated at 37° C over night and screened for colonies the following day.

### 3.1.6 DNA Isolation from Bacterial Cells

Bacterial colonies grown over night on LB-Agar plates with ampicillin were picked using sterile pipette tips and transferred to round bottom 15 ml reaction tubes containing 5 ml of LB Medium supplemented with 100 µg/ml ampicillin. After shaking at 37° C at 250 rpm in a horizontal shaker for 12-16 h, 2 ml of the bacterial suspension were transferred to 2 ml reaction tubes and bacterial cells were pelleted. The remaining cell suspension was stored at 4° C. DNA was extracted from the cells using either Miniprep Small Scale Plasmid DNA Isolation Kits from Qiagen or PeqLab, according to the manufacturer's protocol. To ensure that the correct plasmid was isolated, the DNA was analyzed by restriction digest and subsequent agarose gel electrophoresis. If the DNA fragments detected on the gel corresponded to the expected sizes, the plasmid was further analyzed by Sanger sequencing. Once the correct sequence was confirmed, 100 µl of the cell suspension for small scale DNA isolation were transferred to an Erlenmeyer flask containing 200 ml LB Medium with 100 µg/ml ampicillin and shaken at 37° C at 250 rpm for 12-16 h. Large scale DNA isolation was performed using Qiagen's Maxiprep Endotoxin Free Large Scale DNA Isolation Kit according to the manufacturer's protocol.

### 3.1.7 TEV Protease Digest

TEV protease is a cysteine protease isolated from the tobacco etch virus. Due to its high cleavage sequence specificity, it is commonly used in molecular biology for the cleavage of recombinant proteins.

Cells transfected with mCD1d\_TEV or WT\_mCD1d were treated with Brefeldin A in DMEM complete (1 µg/ml final concentration) to limit the turnover of CD1d. After incubation for 3 h at 37° C, 5 % CO<sub>2</sub> and 85 % humidity, the cells were trypsinized, transferred to 15 ml reaction tubes, washed once with DMEM complete and spun down at 330 × g for 5 min at RT before washing once with PBS. The cells were then resuspended in TEV protease reaction mix, which was set up as follows described in table 7.



**Table 7: Reaction Conditions for TEV-Mediated Cleavage of CD1d**

	AcTEV	ProTEV
20 x Reaction Buffer	15 $\mu$ l	10 $\mu$ l
100 mM DTT	3 $\mu$ l	2 $\mu$ l
TEV Protease	10-40 U	40 U
HPLC H <sub>2</sub> O	ad 300 $\mu$ l	ad 200 $\mu$ l

AcTEV protease from Invitrogen and ProTEV protease from Promega were tested and compared. The reaction was incubated at 30° C for 1-1.5 h. Cells were incubated in DMEM complete, 1 x HBSS or 1 x TEV reaction buffer without active enzyme as controls. Following centrifugation at 330 x g for 5 min at RT, the supernatants were collected and frozen at -20° C for subsequent mCD1d ELISA (3.3.2). The cells were washed twice in cold FACS buffer, centrifuged and prepared for FACS staining (3.3.1).

### 3.1.8 Sortase A (SrtA) Digest

Sortase A is a transpeptidase originally isolated from *Staphylococcus aureus*. Similar to TEV protease, it recognizes and cleaves a specific peptide motif.

Cells transfected with LPETG\_mCD1d or WT\_mCD1d were trypsinized, split into two 1.5 ml reaction tubes, washed once with DMEM complete and centrifuged for 5 min at 330 x g at RT. THP-1\_LPETG\_hCD1d(GGGS)<sub>3</sub> and untransfected THP-1 suspension cells were also split into two reaction tubes, washed once and pelleted. Cells were then resuspended in 100  $\mu$ l DMEM complete medium containing 50  $\mu$ M SrtA enzyme for half of the samples. The remaining samples were incubated in 100  $\mu$ l DMEM complete only as controls. All samples were incubated at 37° C for 1 h and centrifuged for 5 min at 330 x g. Supernatants were removed and stored at -20° C for subsequent mCD1d ELISA and the cells were washed twice in 4° C FACS buffer before FACS staining of mCD1d (3.3.1).

## 3.2 Cell Biological Methods

### 3.2.1 Cultivation of Immortalized Cell Lines

Human (HeLa)<sup>88</sup> and mouse (MODE-K, L-cells)<sup>89,90</sup> adherent cell lines were cultured in T75 cm<sup>2</sup> flasks using DMEM complete (supplemented with 10 % FCS, 2 mM L-Glutamine and 1 % penicillin/streptomycin solution) in an incubator set to 37° C, 5 % CO<sub>2</sub> and 85 % humidity. The cells were passaged twice or thrice per week, at a confluency of 80-90 % and at a rate of 1:5 or 1:10, respectively. To this end, the cells were washed once with RT 1 x PBS and 3 ml of pre-warmed 1 x trypsin-EDTA solution were added. The cells were incubated at 37° C for 30-120 s, shaken gently and pipetted up and down to generate a single cell suspension. A fraction of these cells was either transferred to 6-well plates for experiments or transferred to a new T75 cm<sup>2</sup> flask for passaging. 2 ml or 12 ml of complete DMEM were added, respectively, and cells were left to adhere in the incubator.

Mouse (24.7)<sup>78</sup> and human (THP-1)<sup>91</sup> suspension cells were kept in RPMI complete (supplemented with 10 % FCS, 2 mM L-Glutamine and 1 % penicillin/streptomycin solution) in a standing T25 cm<sup>2</sup> flask in an incubator at 37° C, 5 % CO<sub>2</sub> and 85 % humidity. Cells were passaged thrice per week at a rate of 1:10 by pipetting up and down to generate a single cell suspension.

### 3.2.2 Thawing of Cells Frozen for Long Term Storage

Cells were removed from the liquid nitrogen tank and carefully thawed at 37° C in a water bath. They were then transferred to a 50 ml tube and 40 ml of the appropriate pre-warmed cell culture medium were added slowly. The cells were then centrifuged for 5 min at 330 × *g* at RT. The supernatant was removed and the cell pellet was resuspended in 12-15 ml of the appropriate cell culture medium, transferred to a T75 cm<sup>2</sup> cell culture flask and incubated at 37° C with 5 % CO<sub>2</sub> and a humidity of 85 %.

### 3.2.3 Freezing Cells for Long Term Storage

Adherent cells grown to 70 – 90 % confluency in T75 cm<sup>2</sup> cell culture flasks were washed once with 1 x PBS, trypsinized with 3 ml 1 x trypsin-EDTA solution and transferred to a 15 ml tube containing 3 ml of the appropriate medium containing FCS to prevent further trypsin activity. Suspension cells were grown to a

concentration of  $1 \times 10^7$  cells/ml and washed once with fresh RPMI. Subsequently, the cells were counted and pelleted at  $330 \times g$  for 5 min at RT. The supernatant was discarded and the cells were gently resuspended in FCS containing 10 % DMSO, resulting in a concentration of  $4-10 \times 10^6$  cells per ml. 1 ml aliquots were transferred to cryovials and placed in a cryobox containing isopropanol to ensure slow and gentle freezing of the cells. After one night at  $-80^\circ \text{C}$ , the cells could be transferred to liquid nitrogen for long-term storage.

#### 3.2.4 Transfection of Adherent Cells Using Lipofectamine

Cells were seeded at  $5 \times 10^5 - 7.5 \times 10^5$  cells per well into a 6-well plate in the appropriate medium and left to attach over night at  $37^\circ \text{C}$ , 5 %  $\text{CO}_2$  and 85 % humidity. The following day, solution A, containing the DNA and solution B, containing the cationic lipid transfection reagent, were pipetted into two 1.5 ml reaction tubes.

**Table 8: Reaction Conditions For Transfection Using Lipofectamine**

Dish	Solution A	Solution B	Final Vol. Medium
6-well	100 $\mu\text{l}$ DMEM w/o additives + 3 $\mu\text{g}$ DNA	100 $\mu\text{l}$ DMEM w/o additives + 6 $\mu\text{l}$ Lipofectamine	2 ml

The solutions were mixed by gentle snipping and following a 5 min incubation period at RT, solution B was added to solution A and mixed gently. To allow for the formation of DNA containing liposomes, the mixture was incubated for 20 min at RT. In the meantime, the medium of the seeded cells, which were at 50-70 % confluency, was replaced with antibiotic-free medium. The DNA-lipofectamine mixture was pipetted drop-wise onto the dish and distributed by careful shaking. Following incubation over night at  $37^\circ \text{C}$ , 5 %  $\text{CO}_2$  and 85 % humidity, the medium of the cells was changed to complete medium with antibiotics and the cells were cultured until further analysis.

#### 3.2.5 Transfection of Adherent Cells Using Turbofect

Though Turbofect is also a cationic lipid transfection reagent, the transfection procedure differs slightly from that used for Lipofectamine. First, the DNA was added

to DMEM without (w/o) additives, the previously vortexed lipofection reagent was added to the same tube immediately and mixed by resuspending. The mixture was also incubated for 20 min at RT to allow for the formation of DNA-liposome complexes. In the meantime, the cells' medium was replaced by fresh DMEM complete. The transfection mix was then pipetted drop-wise onto the dish and distributed by gentle shaking. After incubation over night at 37° C, 5 % CO<sub>2</sub> and 85 % humidity, the medium was changed and the cells were grown until further analysis.

**Table 9: Reaction Conditions for Transfection Using Turbofect**

Dish	Vol. Turbofect [µl]	Conc. DNA [µg]	Final Vol. Medium
6-well	6	4 µg/400 µl DMEM	2 ml

### 3.2.6 Cell Killing Curve

Plasmid DNA often contains an antibiotic-resistance cassette, rendering successfully and stably transfected cells less sensitive to this antibiotic. The remaining cells are sensitive to this antibiotic and will undergo cell death upon drug exposure, enabling the selection of successfully and stably transfected cells. To determine the minimal concentration required to induce cell death, cells were thinly seeded to 6-well plates ( $2.5 \times 10^4$  cells/well), left to adhere and incubated with the appropriate medium containing different concentrations of antibiotic (based on the manufacturer's recommendation), including an antibiotic-free condition. The cell culture medium was changed every two to three days and cells were screened for viability by light microscopy. If the cells were still viable after one week, the antibiotic concentration was considered too low and the experiment was repeated with increased concentrations of antibiotics. If the cells were dead after two to three days of incubation, the antibiotic concentration was considered too high. Optimally, the cells treated with antibiotics would die after approximately one week, while untreated cells were still healthy.

### 3.2.7 Generation of Stably Transfected Cell Lines

Adherent cells were transfected with plasmid DNA on a pcDNA3.1 backbone as described in 3.2.4 and 3.2.5. The cells were trypsinized and one well of a 6-well-plate was divided onto four 10 cm dishes 24 h after the transfection. The cells were then incubated with the appropriate medium containing an adequate concentration of

Geneticin, as previously determined by a killing curve. The medium was changed every two to three days and cells were screened for viability. One 10 cm dish of untransfected cells was cultured with the same concentration of Geneticin and used as a reference. Once all of the untransfected cells were dead, any viable cell remaining was considered successfully transfected and left to grow. After approximately two weeks, small cell clusters had formed in the 10 cm dishes. These clusters were scraped off the dish using a 10  $\mu$ l pipet tip and transferred to a 96-well plate (one cluster per well). Alternatively, the cells were trypsinized, counted and diluted to a concentration of 5-2.5 cells per ml of medium and seeded into a 96-well plate, corresponding to a concentration of one to 0.5 cells/well. Still under antibiotic selection, the cells were grown and transferred to larger well sizes once 80 % confluency was reached. At the 6-well stage, the cells were screened for the expression of the transfected protein by flow cytometry (3.3.1).

### **3.3 Immunological Methods**

#### **3.3.1 Staining of Cells for Flow Cytometry (FACS)**

FACS is a commonly used method to determine cellular expression of a certain antigen by the use of fluorophore-coupled antibodies. To analyze extracellular antigens, cells were washed twice with 1 ml of FACS buffer and centrifuged for 5 min at 4° C at 400  $\times$  g. The cells were resuspended in 100  $\mu$ l FACS buffer containing the appropriate antibody, vortexed and incubated at 4° C in the dark for 20 min. Following one more washing step with 1 ml of FACS buffer and centrifugation at 400  $\times$  g for 5 min at 4° C, the cells were resuspended in 300  $\mu$ l of FACS buffer and analyzed using a BD FACSVerse flow cytometer. For additional staining of intracellular antigens, such as secreted CD1d, cells were washed after extracellular staining and resuspended in 250  $\mu$ l Cytifix™ solution for 20 min at 4° C in the dark for fixation. Then, the cells were washed twice with 1 ml 1 x Perm/Wash™ solution for permeabilization and incubated in 100  $\mu$ l Perm/Wash™ solution containing the appropriate quantity of antibody for 30 min at 4° C in the dark. The cells were then washed once with 1 x Perm/Wash™ solution and resuspended in 300  $\mu$ l FACS buffer for flow cytometric analysis.

### 3.3.2 mCD1d Enzyme Linked Immunosorbent Assay (ELISA)

Sandwich-ELISA is a common method to detect soluble proteins in cell culture supernatants or serum. Samples are normally measured in triplicates and the standard curve is pipetted in duplicates. First, the appropriate amount of wells of a 96-well ELISA plate were coated with 100  $\mu$ l of 10  $\mu$ g/ml mCD1d 19G11 capture antibody diluted with blocking solution (PBS + 10 % FCS) and incubated over night at 4° C. The following day, the plate was washed thrice with ELISA washing solution (PBS + 0.05 % Tween) and blocked for 1 h at RT with 200  $\mu$ l/well blocking solution to prevent nonspecific protein binding. In the meantime, the samples to be analyzed were diluted 1:2 to 1:10 in blocking solution. After washing the plate thrice, 100  $\mu$ l of the diluted samples were pipetted onto the plate in triplicates. The standard curve was pipetted beginning with 200  $\mu$ l of a 2 ng/ml top standard solution of biotinylated mCD1d monomer in blocking solution and serially diluting the top standard down to 0.03 ng/ml. Blocking solution was used as blank. Following a 2 h incubation, during which the soluble mCD1d proteins in the supernatant attached to the coating antibody, the plate was washed thrice and 100  $\mu$ l of a 10  $\mu$ g/ml solution of biotinylated 1B1 mCD1d antibody in blocking solution were pipetted into the wells previously containing the samples. Since the mCD1d monomer is already biotinylated, these wells were filled with 100  $\mu$ l blocking solution to prevent drying and excess biotinylation. After 1 h of incubation, during which the biotinylated antibody binds to the mCD1d protein, the plate was washed five times and 100  $\mu$ l of a 1:2500 dilution of Avidin HRP in blocking solution was added to each well, including the standard curve wells. The plate was incubated for 25 min at RT and washed seven times with 30 s incubation between each washing step. 100  $\mu$ l/well of TMB substrate were added/well and the plate was incubated in the dark for a maximum of 20 min. TMB solution is a substrate for the HPR bound to avidin and therefore acts as an indicator for the amount of protein present per well. With increasing protein concentration, the TMB substrate changes from a clear solution to a dark blue color. To stop the reaction, 50  $\mu$ l of 1 N HCl solution were added to each well, turning the indicator yellow, and the extinction was measured at 450 nm using a FlexStation.

### 3.3.3 mIL-2 ELISA

Based on the same principle as the mCD1d ELISA, mIL-2 can be detected via sandwich-ELISA. For this purpose, the mIL-2 ELISA kit from BD Biosciences was used according to the manufacturer's protocol.

### 3.3.4 Antigen Presentation Assay

CD1d presents lipid antigens to CD1d-restricted NKT cells. By co-culturing CD1d-expressing cells with an iNKT cell hybridoma (24.7) and investigating the supernatants after 24 h of co-culture for NKT-cell derived IL-2, it is possible to detect activation of the NKT hybridoma cells.

To this end, cells transfected with mCD1d constructs in 6-well plates on the previous day were seeded into 96-well plates at a concentration of  $5 \times 10^4$  cells/well, and left to adhere at 37° C with 5 % CO<sub>2</sub> and 85 % humidity for at least six hours. In the meantime, 1 µg α-galactosylceramide (α-GalCer) and α-GalGalCer were diluted in 500 µl of DMEM, sonicated for 10 min in a sonication water bath and then diluted to solutions with concentrations of 10 ng/ml, 20 ng/ml, 50 ng/ml and 100 ng/ml of lipid. The attached cells were washed once with DMEM complete and 100 µl of each lipid solution were added per well in triplicates and incubated over night for processing and loading onto CD1d. Three wells of each line of transfected cells were left without lipids. The next day, the cells were washed thrice with DMEM complete and  $1 \times 10^5$  24.7 cells were added to each well in a total volume of 200 µl. 24.7 cells were also seeded into three wells alone as negative controls, just as three wells of HeLa cells transfected with one of each constructs were cultured alone. After 24 h, the plate was briefly centrifuged to settle the cells and 100 µl of the supernatants were removed and stored at -20° C for subsequent IL-2 ELISA.

### 3.3.5 Statistical Analysis

Graphs were generated and analyzed using the unpaired Student's *t*-test or, in case of multiple comparisons, one- or two-way ANOVA followed by Bonferroni's post hoc analysis using GraphPad Prism software (version 5.0 for Windows; GraphPad Software, LaJolla, USA). P values  $\leq 0.05$  were considered significant and indicated as  $p \leq 0.05$  (\*),  $p \leq 0.01$  (\*\*) or  $p \leq 0.001$  (\*\*\*).

## 4 Results

### 4.1 Expression of Secreted and TEV Protease-Cleavable mCD1d

CD1d, an atypical MHC class I molecule, which is expressed by a wide range of cells presents lipid antigens to NKT cells.<sup>24</sup> Lipids are bound by CD1d during its transport through secretory and endolysosomal compartments of the cell and are presented at the cell surface. The origin and molecular nature of CD1d-associated lipid antigens has been researched extensively, but only a limited number of such antigens has been identified to date, let alone the complete spectrum of CD1d-associated lipids. The analysis of the CD1d lipidome is technically difficult, because detergents are necessary to isolate CD1d from the membrane and these cause the dissociation of the bound lipids. To avoid this, genetically engineered secreted CD1d constructs were generated recently.<sup>60–62,67,78,93</sup> Secreted CD1d constructs lack the TMD and the cytoplasmic tail of CD1d and are therefore released into the cell culture medium after passage through the ER and Golgi apparatus.<sup>60–62</sup> However, these constructs do not undergo endolysosomal trafficking and thus do not allow the investigation of lipids which associate with CD1d during its passage through these compartments. To avoid such limitations, a cell surface cleavable CD1d construct was recently engineered by Brenner and coworkers.<sup>60</sup> In contrast to secreted CD1d, this construct undergoes endolysosomal trafficking, as it has an intact cytoplasmic tail and TMD, and was designed to allow for TEV-mediated enzymatic release of CD1d at the cell surface (see 1.5 and Figure 6, Figure 7).<sup>60</sup> Surprisingly, however, the respective construct showed little TEV protease-mediated cleavage, thus limiting MS-based studies.<sup>60</sup> First analyses using this construct nevertheless demonstrated that CD1d may bind a wide range of lipids *in vitro*, which is consistent with MS-based analyses of lipids associated with secreted CD1d.<sup>12,60,78</sup>

Two constructs were received from the laboratory of Dr. Michael Brenner (Brigham and Women's Hospital, Harvard Medical School, Boston, MA, USA): A secreted (mCD1d-Fc) and a TEV-cleavable (mCD1d-TEV-CT) version of mCD1d. Both constructs have previously been published.<sup>60,78</sup> The soluble mCD1d-Fc construct was generated as a single-chain construct with h $\beta_2$ m covalently linked to the N-terminus of mCD1d by a glycine-serine (Gly-Ser) spacer. The transmembrane domain and cytoplasmic tail of mCD1d were substituted by the Fc portion of murine IgG<sub>2a</sub> and covalently linked to the extracellular domain by another Gly-Ser spacer.<sup>78</sup> The cell



surface-cleavable construct had h $\beta_2m$  covalently linked to the N-terminus of full length mCD1d by a Gly-Ser spacer and contained two TEV cleavage sites inserted just N-terminal of the transmembrane domain and C-terminal of the  $\alpha_3$  domain of CD1d (Figure 7).<sup>60</sup> Under physiological conditions,  $\beta_2m$  non-covalently associates with the CD1d heavy chain in the ER.<sup>44,48</sup> It has been shown that the association with  $\beta_2m$  is important for glycosidase processing of CD1d in the Golgi apparatus and that CD1d heavy chains which traffic without  $\beta_2m$  show an immature glycosylation pattern at the cell surface.<sup>94</sup> As  $\beta_2m$  expression may limit the formation of heterodimers upon overexpression of CD1d, covalent linkage to CD1d was applied in the constructs investigated here.

Based on the publication by *Muindi* and colleagues, it appeared that the mCD1d-TEV-CT cell surface cleavable construct underwent spontaneous cleavage rather than enzyme-mediated shedding, since significant concentrations of CD1d could be detected in the supernatant of cells incubated with TEV buffer in the absence of active TEV enzyme.<sup>60</sup> We therefore modified the sequence provided by Dr. Brenner's laboratory by substituting one of two TEV cleavage sites with a Strep-tag ii for protein purification (h $\beta_2m$ \_mCD1d\_TEV). The secreted mCD1d-Fc construct was also modified by adding an 8  $\times$  His tag and Strep-tag ii to mCD1d C-terminally, replacing the Fc portion of murine IgG<sub>2a</sub> (h $\beta_2m$ \_sol\_mCD1d). Additionally, to avoid possible side effects from the association of human  $\beta_2m$  with mouse CD1d, secreted and cell surface cleavable single chain m $\beta_2m$ \_mCD1d constructs were generated (m $\beta_2m$ \_sol\_mCD1d and m $\beta_2m$ \_mCD1d\_TEV) (Figure 7).

To determine whether the species of  $\beta_2m$  associated with mCD1d influences construct expression in a mouse small intestinal epithelial cell line (MODE-K)<sup>90</sup>, cells were transfected with each construct and analyzed by flow cytometry. Cells transfected with secreted CD1d were treated with Brefeldin A for three hours prior to flow cytometric analysis. Additionally, supernatants (SN) were assayed for CD1d via ELISA 24 h after transfection, to analyze the secretion of the secreted CD1d constructs and possible spontaneous shedding of the cell surface-cleavable constructs.

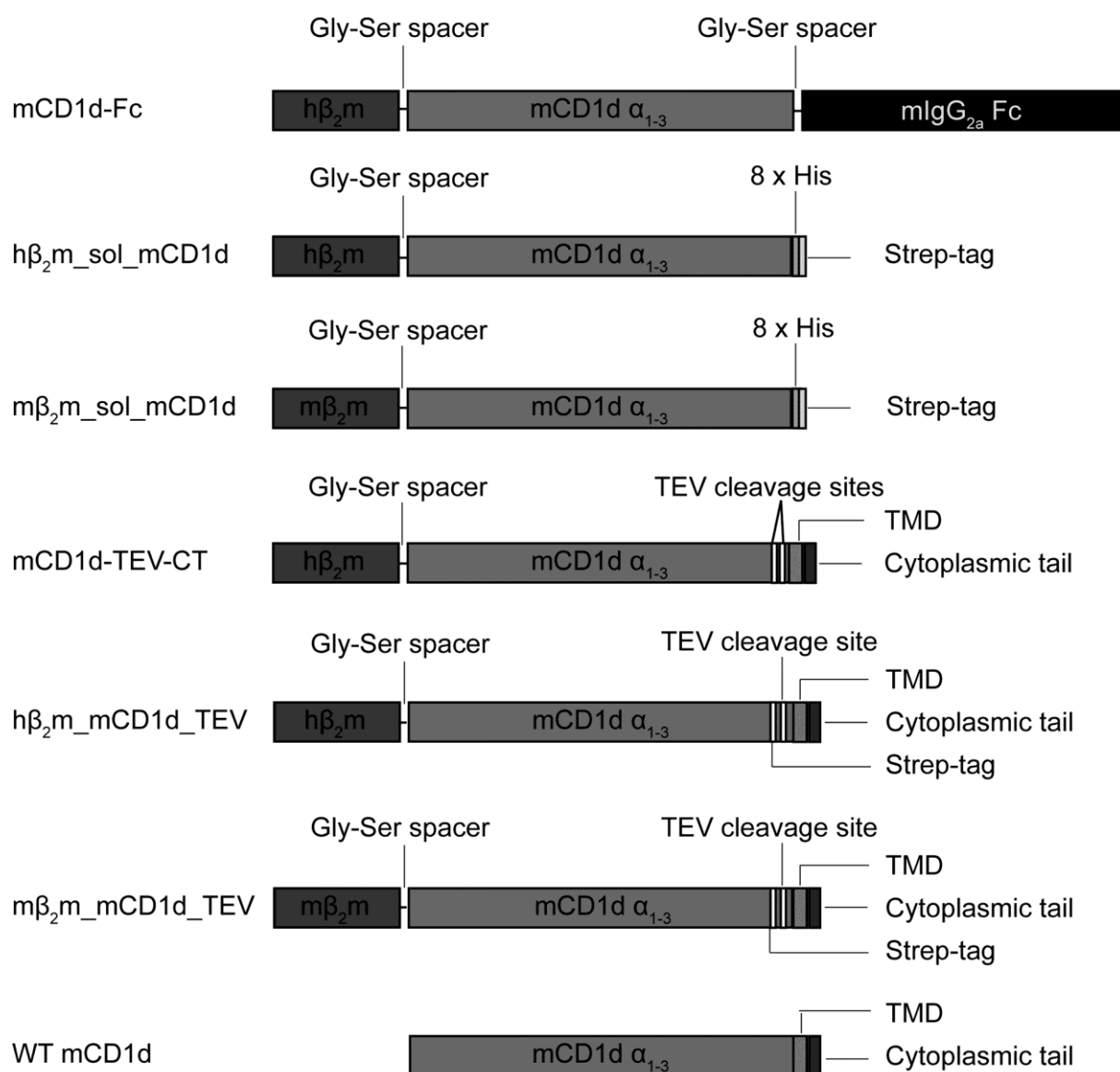


**Figure 7: Schematic overview of mCD1d constructs**

The highest expression rate among the mCD1d constructs was recorded for h $\beta_2$ m\_mCD1d\_TEV (20 %), followed by m $\beta_2$ m\_mCD1d\_TEV (15 %) and h $\beta_2$ m\_sol\_mCD1d (12 %). mCD1d-Fc had the lowest expression rate in accordance with it being the largest construct due to the C-terminal Fc sequence (5 %) (Figure 7, Figure 8). These observations correlated with CD1d expression per cell, as determined by the mean fluorescence intensity (MFI) of CD1d expressing cells (Figure 8).

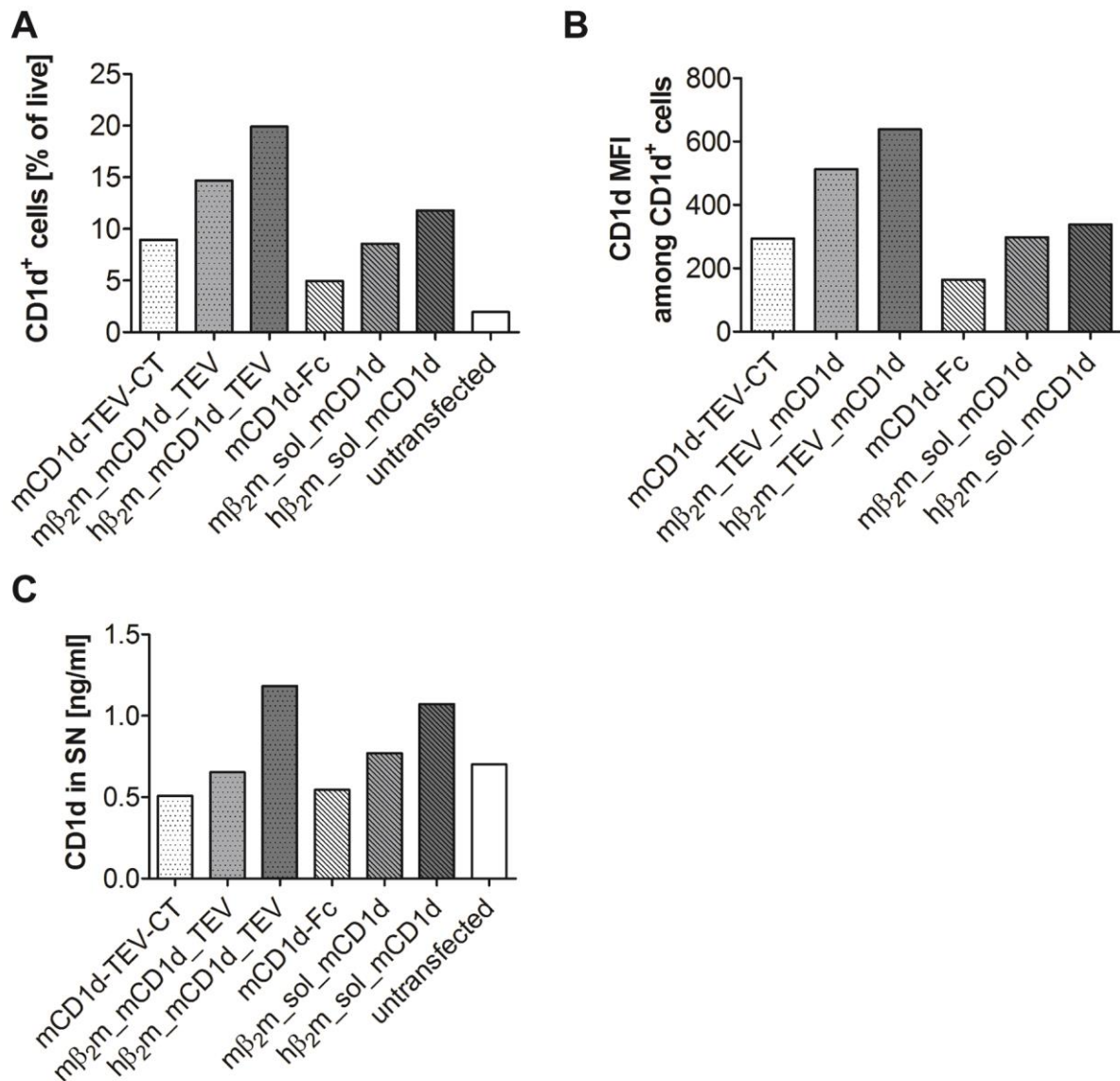


**Figure 8: Comparison of the Expression of Different Genetically Modified mCD1d Constructs in MODE-K cells**

(A) Relative number of cells expressing CD1d, given as a percentage of live cells 24 h after lipofection of the indicated mCD1d constructs into MODE-K cells. Cells transfected with secreted CD1d constructs were treated with Brefeldin A for three hours prior to analysis. (B) Mean fluorescence intensity (MFI) of CD1d in the subset of CD1d-expressing MODE-K cells treated as described in (A). (C) Mean mCD1d levels in the supernatants (SN) of MODE-K cells treated as described in (A) (measured in triplicates). ELISA results in (C) were not normalized to CD1d expression (A, B). This experiment was performed once, analyzing  $2 \times 10^5$  cells per construct.

While results could not be normalized to cellular CD1d expression, quantification of mCD1d spontaneously released into the supernatant of transfected MODE-K cells demonstrated that CD1d was only secreted into the medium by MODE-K cells transfected with hβ<sub>2</sub>m\_mCD1d\_TEV and hβ<sub>2</sub>m\_sol\_mCD1d (Figure 8). Though this observation indicated spontaneous cleavage of the hβ<sub>2</sub>m\_mCD1d\_TEV fusion

protein, we decided to proceed with h $\beta_2$ m\_mCD1d\_TEV and h $\beta_2$ m\_sol\_mCD1d, based on their expression rates.

#### 4.2 TEV Protease for Enzymatic Release of CD1d

For the establishment of a TEV cleavage protocol, we decided to generate cells stably expressing TEV-cleavable CD1d. To this end, we decided to transfect L cells, a mouse fibroblast cell line<sup>89</sup>, with h $\beta_2$ m\_mCD1d\_TEV (L-TEV-cells). L cells, which are stably transfected with WT mCD1d, were used as control since WT CD1d is not sensitive to TEV-mediated proteolytic cleavage (L-WT-cells).

L-TEV-cells cells and L-WT-cells cells were incubated for three hours with Brefeldin A<sup>95</sup>, an antibiotic that interferes with anterograde trafficking of proteins from the ER to the Golgi, to arrest trafficking of newly synthesized CD1d to the cell surface. We used the manufacturer's protocol for AcTEV protease (Invitrogen) as a reference for our experimental setup, estimating the concentration of cleavable protein and using AcTEV at a concentration four times higher than required (1  $\mu$ l). The transfected cells were trypsinized, washed, and incubated for 1 h at 30° C, according to the manufacturer's recommendation for optimal TEV activity. Either DMEM complete or AcTEV buffer, a Tris-based buffer provided with TEV protease, were used as reaction buffers - with or without DTT and with or without active enzyme.

Noteworthy, only 20 % of cells stably transduced with h $\beta_2$ m\_mCD1d\_TEV showed detectable levels of CD1d at the cell surface, whereas more than 90 % of the L-WT-cells cells were positive for CD1d. While the molecular basis for these observations was not investigated, previous studies using mouse embryonic stem cells and CHO cells expressing recombinant proteins have demonstrated transcriptional silencing by epigenetic modification of the CMV promoter, as well as progressive loss of gene copies during cell culture.<sup>96,97</sup> It is therefore possible that such mechanisms may have contributed to limited h $\beta_2$ m\_mCD1d\_TEV expression in our experiments.

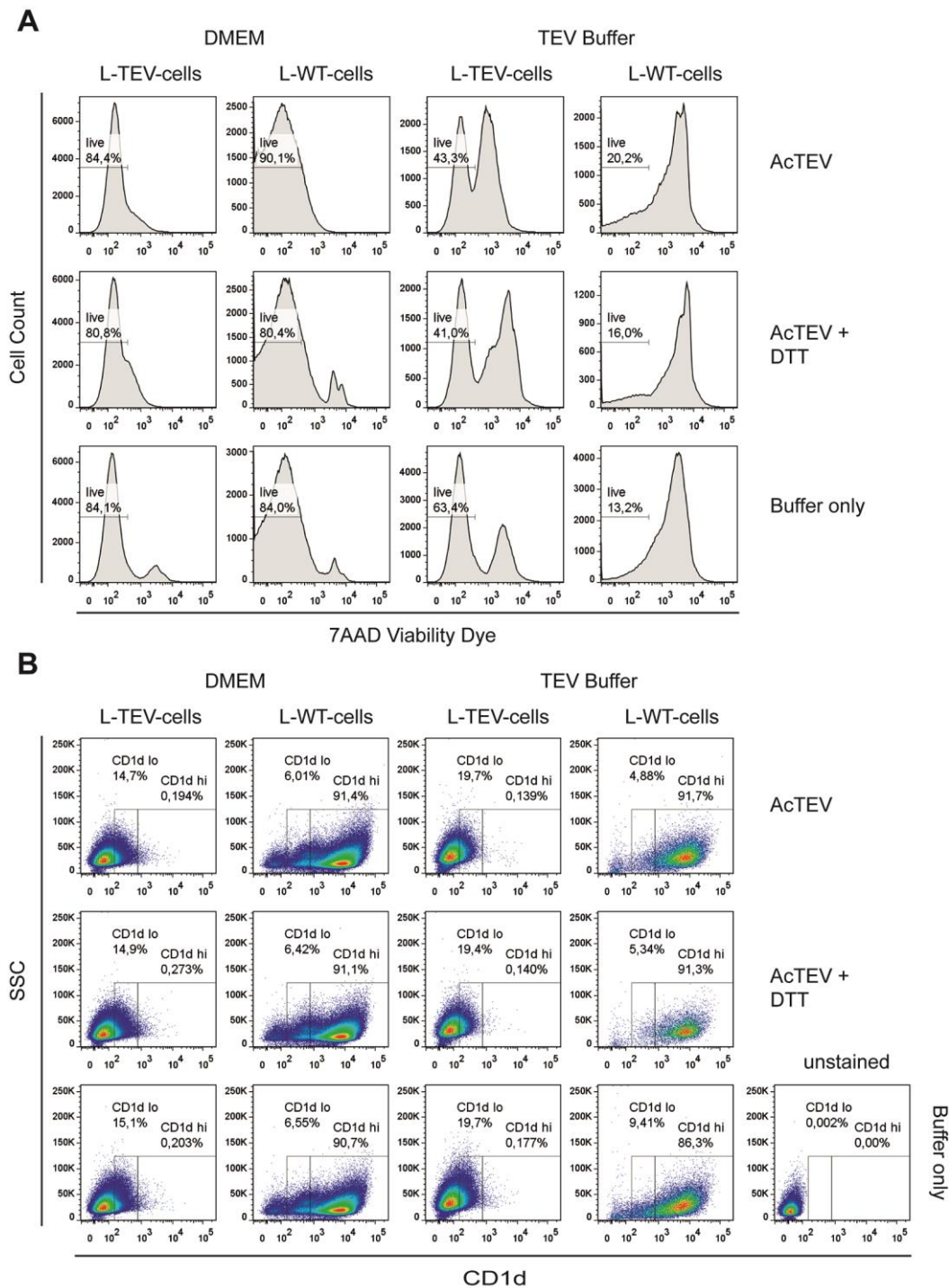


**Figure 9: TEV Protease Fails to Cleave  $h\beta_2m\_mCD1d\_TEV$ , While TEV Buffer Affects Cell Viability**

Cells stably transfected with  $h\beta_2m\_mCD1d\_TEV$  (L-TEV-cells) or with WT  $mCD1d$  (L-WT-cells) were incubated in DMEM or TEV buffer with or without DTT and active enzyme as indicated. (A) Representative histograms showing the viability of cells 24 h after transfection (B) Representative dot plots depicting the frequency of CD1d low ( $CD1d^{lo}$ ) and high ( $CD1d^{hi}$ ) expressing live cells as determined by flow cytometry. This experiment was performed once in duplicates.

Regardless of limited CD1d expression, flow cytometric analysis of L cells stably transduced with h $\beta_2$ m\_mCD1d\_TEV or WT\_mCD1d demonstrated that the use of TEV buffer, even in the absence of TEV protease, significantly affected cell viability (Figure 9). Furthermore, no evidence of TEV-protease-mediated cleavage of h $\beta_2$ m\_mCD1d\_TEV was detected, as indicated by unaltered cell surface expression of CD1d in all conditions (Figure 9).

The secretion of mCD1d into the SN was analyzed by ELISA. Treatment of stably h $\beta_2$ m\_mCD1d\_TEV-transfected L cells with TEV buffer plus AcTEV (+ DTT) resulted in the highest concentration of mCD1d in the culture supernatant (0.5 ng/ml), followed by DMEM with DTT and AcTEV, as well as AcTEV buffer plus DTT (0.26 ng/ml). However, analysis of the supernatants of L-WT-cells, which express WT CD1d without a TEV cleavage site and thus should not release mCD1d into the SN, revealed mCD1d levels of up to 3 ng/ml after exposure to TEV buffer and only 0.3 ng/ml after exposure to DMEM (Figure 10). These data, together with flow cytometric data showing decreased viability upon AcTEV buffer exposure, suggest that treatment of eukaryotic cells with AcTEV buffer results in cell lysis and thereby uncontrolled release of mCD1d into the supernatant.

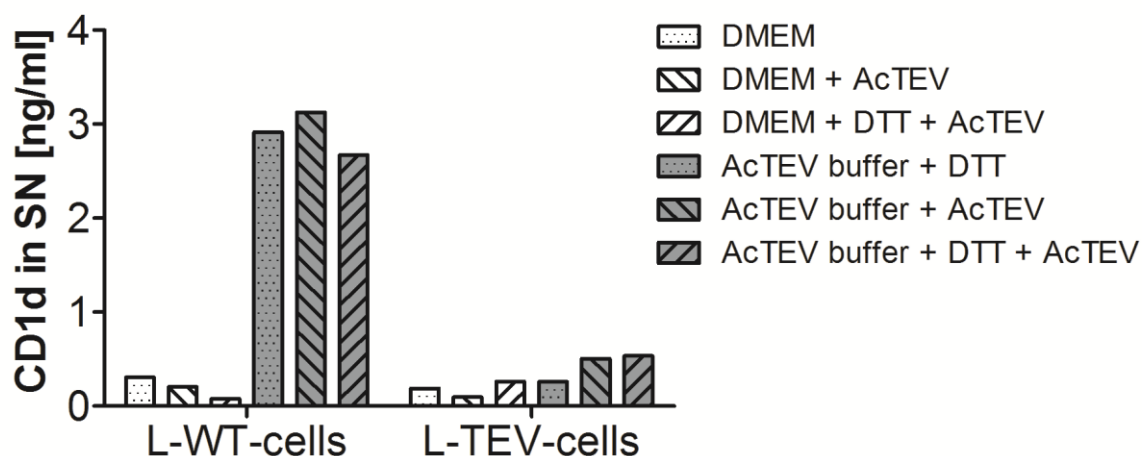


**Figure 10: mCD1d ELISA of Supernatants of Mouse Fibroblast Cells Stably Transfected with h $\beta_2$ m\_mCD1d\_TEV or WT mCD1d**

Mean mCD1d concentrations in the supernatant of L cells stably transfected with h $\beta_2$ m\_mCD1d\_TEV (L-TEV-cells) or with WT mCD1d (L-WT-cells) upon the indicated treatment, as determined by ELISA. mCD1d levels were slightly increased in L cells treated with AcTEV + TEV buffer, but even more so in Ld cells, which should not respond to TEV digestion. The experiment was performed once and mean values of triplicates are shown.

### 4.3 Investigation of different buffer systems and alternative TEV proteases

The previous experiment with stably transfected L-TEV-cells and L-WT-cells led to the conclusion that the use of TEV buffer was detrimental to cell integrity and should thus be avoided. However, the experiment also demonstrated that the use of DMEM as reaction buffer for TEV cleavage of h $\beta_2$ m\_mCD1d\_TEV did not allow for detectable CD1d release. DMEM complete is supplemented with fetal calf serum (FCS), which contains a range of proteins and organic compounds. While FCS helps maintain cell viability during incubation, it may contain substances which are inhibitory to TEV protease. Thus, we investigated potential alternative buffers compatible with TEV protease. HBSS is commonly used in the isolation of primary cells from tissues but does not contain FCS and was therefore considered an adequate substitute for DMEM with fewer components that might inhibit TEV activity.

Additionally, to ensure that the concentration of TEV protease was sufficient for CD1d cleavage, the TEV protease concentration was doubled in subsequent experiments. Furthermore, TEV protease from a different distributor, ProTEV (Promega), was used alongside the previously used AcTEV (Invitrogen) protease.

Given that HeLa cells, a cell line generated from human cervical cancer cells<sup>88</sup>, exhibited increased CD1d expression after transfection with h $\beta_2$ m\_mCD1d\_TEV, subsequent experiments were performed 24 h after transient transfection of HeLa cells instead of L cells. Cells were treated with Brefeldin A for three hours and then either incubated in HBSS or the TEV buffer provided by the respective TEV manufacturer, with and without active protease. One sample in DMEM only was added as a control. As for the previous experiments, cleavage was performed at 30° C for 1 h according to manufacturer's protocols.

Flow cytometric analysis revealed that the cells were more sensitive to the Invitrogen TEV buffer than they were to the Promega TEV buffer or HBSS, as indicated by a population shift in the FSC/SSC scatter (Figure 11 A, upper panel). More importantly, however, TEV protease-mediated proteolytic release of CD1d at the cell surface was not observed in any of the conditions (Figure 11 A lower panel and B).

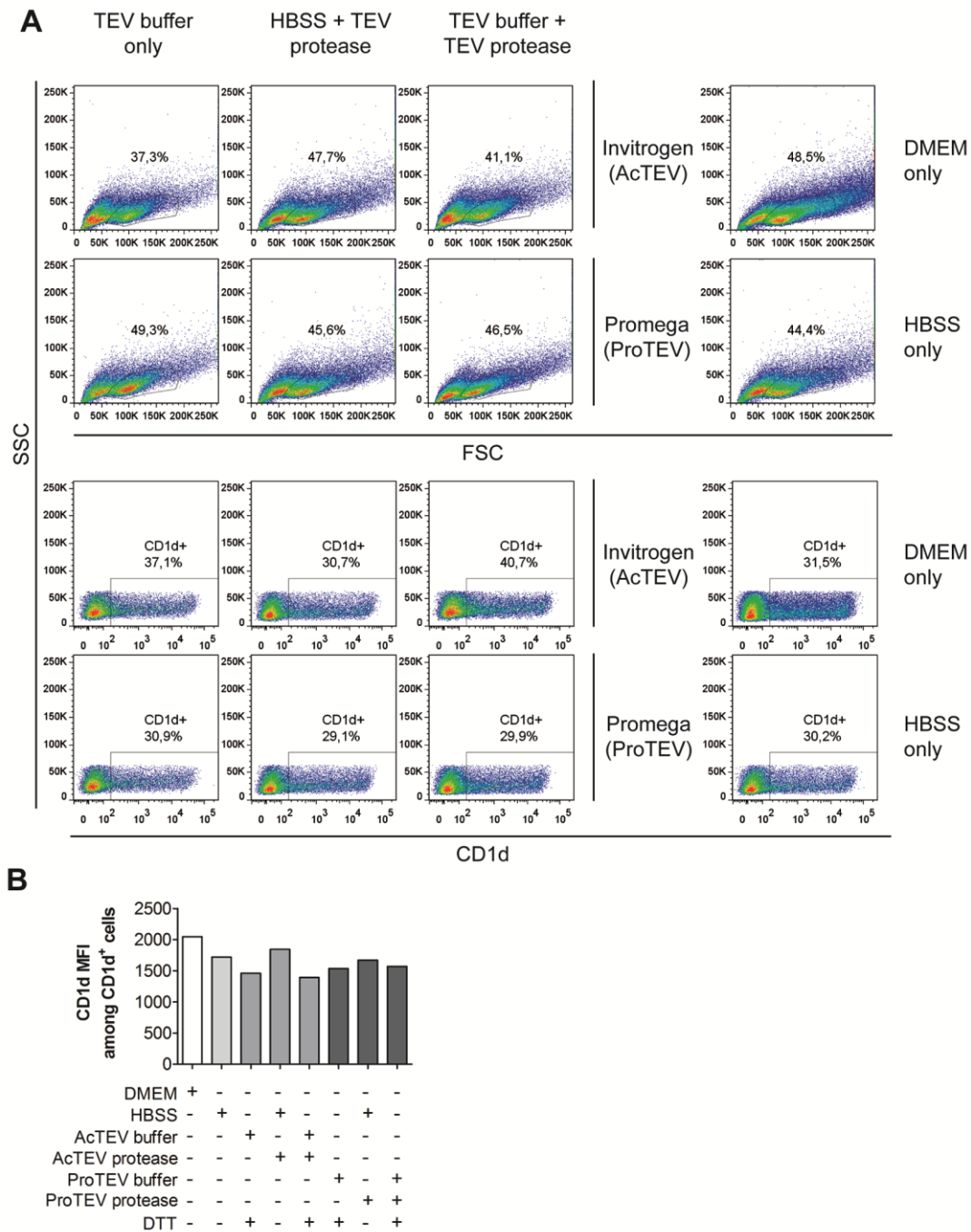


**Figure 11: Alternative Buffer Systems and TEV Proteases for Enzymatic Release of CD1d**

(A) Flow cytometric analysis of HeLa cells transiently transfected with  $h\beta_2m\_mCD1d\text{-TEV}$  treated with AcTEV or ProTEV protease, either with the appropriate TEV buffer or HBSS. DMEM and HBSS alone were used as negative controls. Upper panel: HeLa cells were more sensitive to Invitrogen TEV buffer, as indicated shifts in the FSC scatter (top panels). Lower panel: Relative frequency of CD1d<sup>+</sup> cells among the FSC/SSC population gated as shown in the top panel. (B) mCD1d cell surface expression per cell, gated on CD1d<sup>+</sup> cells, as determined by mean fluorescence intensity (MFI). The experiment was performed once.



#### 4.4 Glycine-Serine Spacers Do Not Promote TEV Protease Dependent Cleavage of h $\beta$ <sub>2</sub>m\_mCD1d\_TEV

Based on the design of the h $\beta$ <sub>2</sub>m\_mCD1d\_TEV construct with the TEV recognition sequence close to the plasma membrane, we speculated that the lack of detectable surface shedding may be caused by inaccessibility of the cleavage site for TEV protease.

We therefore decided to insert three Gly-Ser spacers ((GGGS)<sub>3</sub>) between the TMD and the TEV cleavage site, to enhance accessibility. A similar hCD1d construct containing a Sortase A transpeptidase (SrtA) cleavage site (LPETG) separated from the TMD by three GGGS spacers (LPETG-hCD1d(GGGS)<sub>3</sub>), had previously been shown to be cleavable by Gijsbert Grotenbreg and colleagues (National University of Singapore, Singapore, Singapore) (unpublished data).

Instead of classic mutagenesis techniques, we performed PIPE mutagenesis, which enables the substitution of a DNA sequence with a mutagenized, longer sequence in just one PCR (see 3.1.1). PCR products were directly transformed into chemically competent *E. coli* and construct sequences were verified by Sanger sequencing. HeLa cells were then transiently transfected with the mutagenized construct (h $\beta$ <sub>2</sub>m\_mCD1d\_TEV(GGGS)<sub>3</sub>) and TEV protease cleavage was investigated as previously described using AcTEV and ProTEV protease with the appropriate buffers.

Flow cytometric analysis of the relative frequency of live CD1d<sup>+</sup> cells and also of the MFI of these CD1d expressing cells did not reveal any proteolytic release of CD1d from the cell surface (Figure 12 A, B).

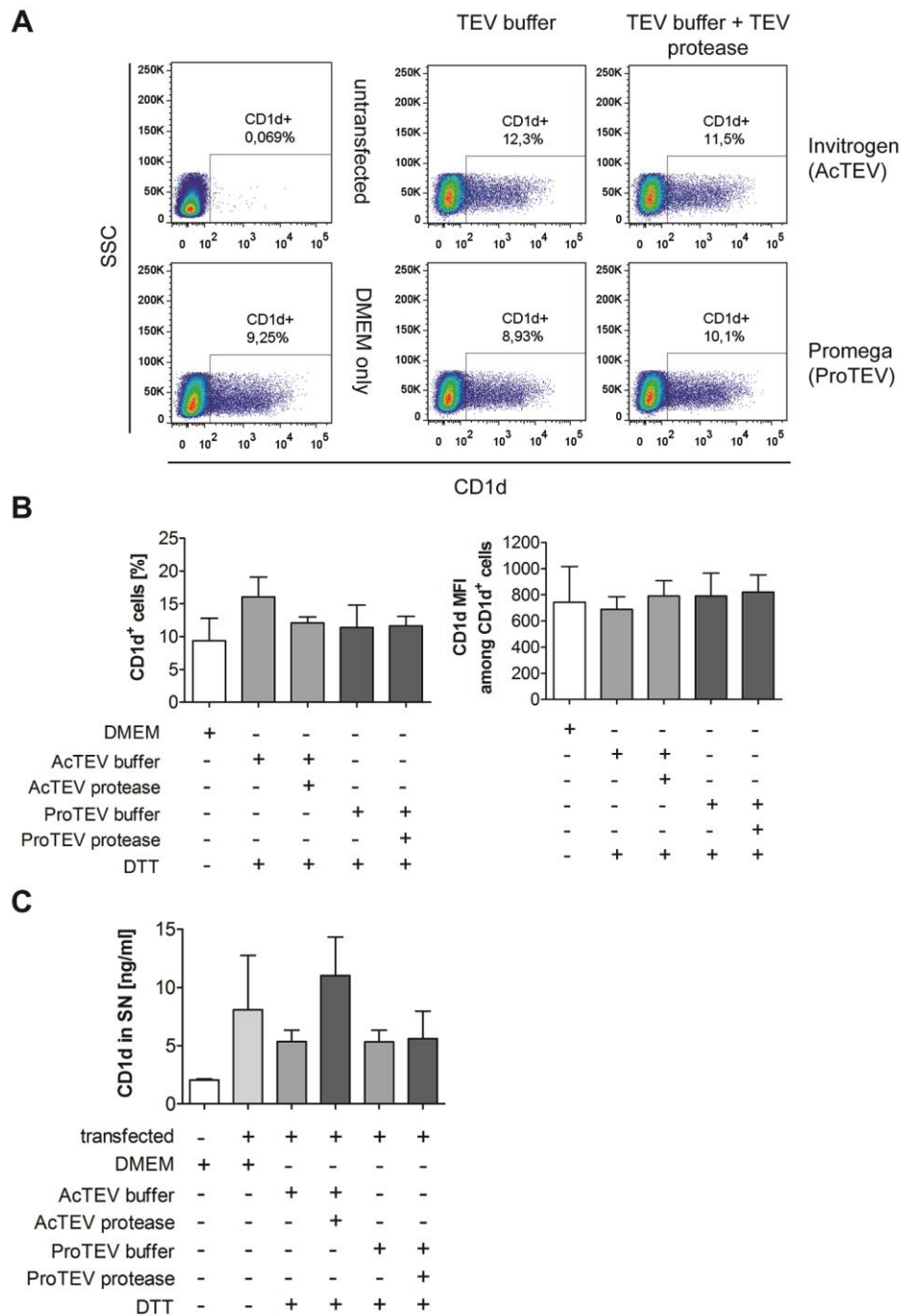


**Figure 12: Glycine-Serine Spacers Do Not Promote TEV Protease-Mediated Cleavage of CD1d.**

HeLa cells were transfected with  $h\beta_2m\_mCD1d\_TEV(GGGS)_3$  and analyzed 24 h after transfection. (A) Representative flow cytometry dot plots showing the cell surface expression of  $h\beta_2m\_mCD1d\_TEV(GGGS)_3$  before and after treatment as indicated. (B) Quantification of the relative percentage of live CD1d expressing cells (left) and CD1d expression per cell gated on CD1d<sup>+</sup> cells (MFI, right). Median and range of two individual experiments performed in duplicates are shown. (C) mCD1d ELISA from SN of cells treated as described in A. Median and range of two individual experiments performed in duplicates are shown.

ELISA results revealed that cells treated with AcTEV TEV buffer and AcTEV protease released more mCD1d into the supernatant than cells treated with AcTEV TEV buffer or ProTEV TEV buffer alone or ProTEV TEV buffer plus ProTEV protease. However, the concentration of mCD1d secreted by cells treated under the same conditions with DMEM only was in the same range (Figure 12 C). Thus, despite the introduction of glycine-serine spacers, no TEV-mediated cleavage of mCD1d from the cell surface could be detected.

In conclusion, TEV protease-based strategies did not allow for proteolytic release of CD1d at the cell surface. We therefore decided to pursue a different strategy for proteolytic CD1d cleavage.

#### 4.5 Sortase A for proteolytic release of CD1d

As an alternative for the h $\beta_2$ m\_mCD1d\_TEV construct, we investigated mCD1d constructs containing an LPETG sequence in the extracellular juxtamembrane domain of CD1d, which serves as a recognition site for *Staphylococcus aureus* sortase A (SrtA), a bacterial transpeptidase that cleaves the threonine-glycine bond within the LPETG sequence.<sup>85</sup> Constructs were engineered to contain none, one or two Gly-Ser spacers between the transmembrane domain and the LPETG cleavage site (pcep4\_LPETG\_mCD1d(GGGS)<sub>0-2</sub>), which itself was positioned between the TMD and the  $\alpha_3$  domain of mCD1d. Unlike the TEV constructs, the LPETG\_mCD1d constructs were not covalently linked to  $\beta_2$ m, as we observed that cellular  $\beta_2$ m expression and non-covalent binding to CD1d are not rate-limiting for CD1d expression (data not shown).

As done previously for h $\beta_2$ m\_mCD1d\_TEV, HeLa cells were transiently transfected using lipofection and analyzed 24 h after transfection. The cells were trypsinized and half of the cells of each well were incubated for 1 h at 37° C in DMEM with or without 50  $\mu$ M SrtA enzyme. The cells were then analyzed by flow cytometry and ELISA for mCD1d. THP-1 cells, a human leukemic monocyte cell line<sup>91</sup> stably transfected with a human CD1d construct containing three Gly-Ser spacers (pcep4\_LPETG\_hCD1d(GGGS)<sub>3</sub>) were previously shown to be amenable to sortase-mediated CD1d cleavage (personal communication, Gijsbert Grotenbreg, National University of Singapore, Singapore, Singapore) and were used as a positive control for SrtA activity.

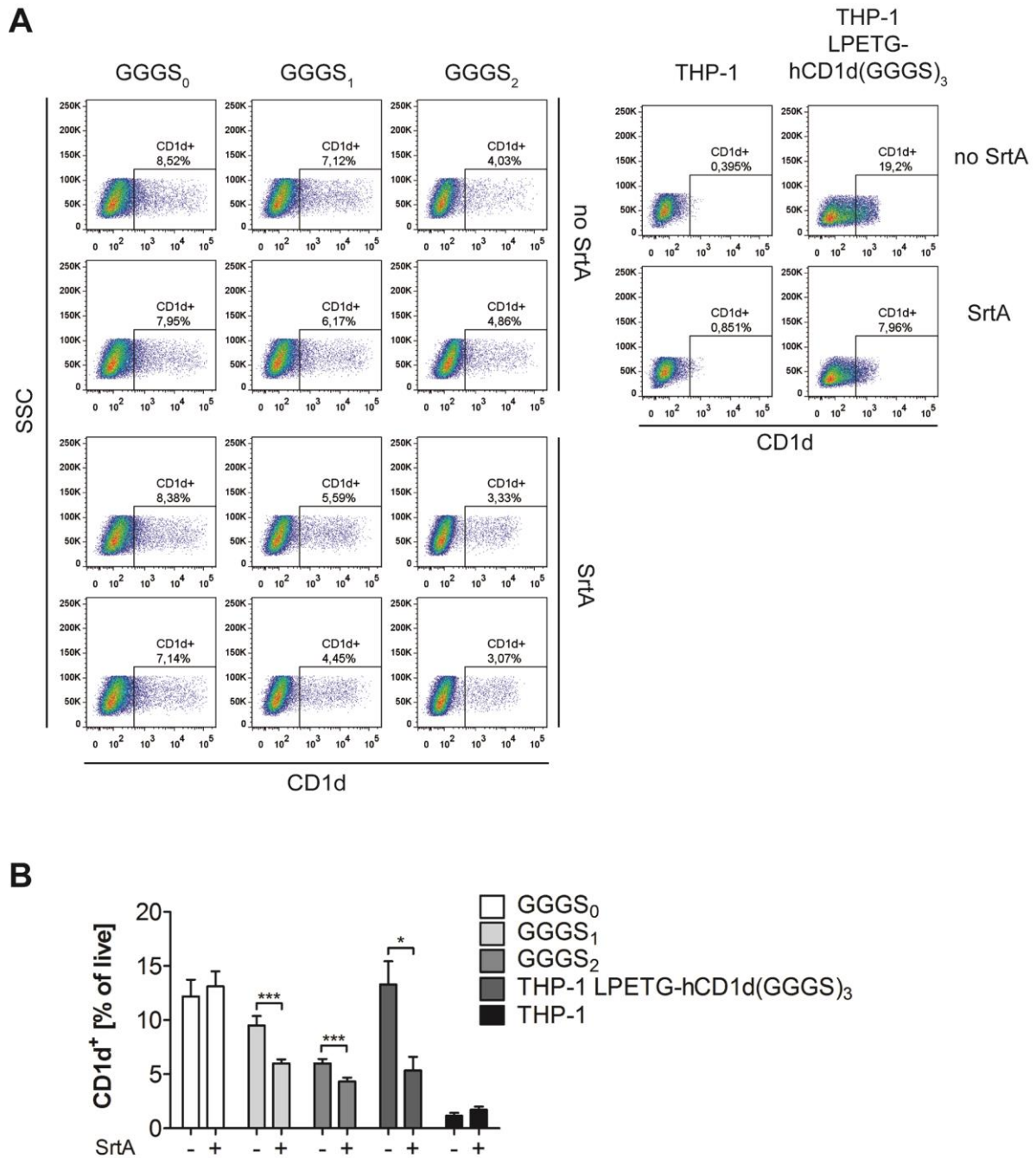


**Figure 13: SrtA Digest of HeLa Cells Transfected with LPETG\_mCD1d(GGGS)<sub>0-2</sub> or THP 1 Cells Stably Transfected with LPETG\_hCD1d\_(GGGS)<sub>3</sub>.**

HeLa cells were transfected with LPETG\_mCD1d(GGGS)<sub>0-2</sub> and subjected to SrtA digest 24 h after transfection. (A) Dot plots (duplicate samples) showing SrtA dependent reduction of CD1d expression on live cells representative of five individual experiments. Cleavage efficiency increases with the number of GGGS spacers while baseline expression decreases. (B) Quantification of the relative number of CD1d expressing cells. Mean  $\pm$  SEM of five individual experiments performed in duplicates is shown (Student's *t*-test; \*  $p < 0.05$ , \*\*\*  $p < 0.01$ ).

Cell surface expression of the constructs as determined in the absence of SrtA treatment decreased with the number of Gly-Ser spacers, whereas cleavage efficiency as determined in the presence of SrtA increased (A, B). While a SrtA-dependent reduction of CD1d expression was barely detectable for the GGGS<sub>0</sub> construct, SrtA-induced loss of CD1d cell surface expression was observed for 25 % and 33 % of cells expressing the GGGS<sub>1</sub> and GGGS<sub>2</sub> constructs, respectively ( ).

These results were confirmed by the analysis of the concentration of CD1d in the cell culture SN by ELISA (**Figure 14**). While an increase of CD1d in the SN was detected for all three constructs, the relative increase was substantially higher for the GGGS<sub>1</sub> and GGGS<sub>2</sub> constructs compared to the GGGS<sub>0</sub> construct. Up to 10 ng/ml of mCD1d were measured in the supernatant. This corresponds to 1 ng of mCD1d derived from  $5 \times 10^5$  cells, which is considered sufficient for MS analysis.

However, baseline release of CD1d in the absence of SrtA treatment also increased with each additional Gly-Ser spacer, suggesting that these spacers enhanced the accessibility of the CD1d protein for SrtA but also contributed to structural instability associated with spontaneous CD1d cleavage (**Figure 14**).

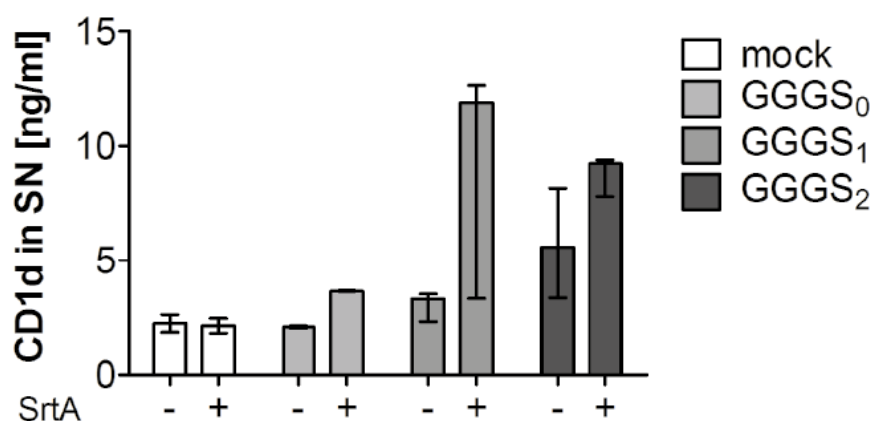


**Figure 14: mCD1d ELISA of HeLa Cells Transfected with LPETG\_mCD1d(GGGS)<sub>0-2</sub> after SrtA Digest**

HeLa cells were transfected with LPETG\_mCD1d(GGGS)<sub>0-2</sub> and subjected to SrtA digest 24 h after transfection. CD1d concentrations in SN taken from cells after SrtA digest as determined by ELISA (median values with range from two individual experiments performed in triplicates).

#### 4.6 Increased LPETG\_CD1d Expression Through Use of an Alternative Plasmid Backbone

Unlike  $h\beta_2m\_mCD1d\_TEV$ , LPETG\_mCD1d(GGGS)<sub>1</sub> and GGGS<sub>2</sub> could be cleaved from the cell surface of HeLa cells upon digestion with SrtA at considerable rates, resulting in the release of 1 ng of CD1d from  $5 \times 10^5$  cells. However, the transfection rate of the LPETG\_mCD1d constructs was quite low, compared to the rates achieved using  $h\beta_2m\_mCD1d\_TEV$  in HeLa cells. We speculated that this may relate to the fact that these constructs were on different vector backbones (pcep4 and pcDNA3.1, respectively). Thus, we sub-cloned the LPETG\_mCD1d constructs into pcDNA3.1 and investigated the transfection rates in HeLa cells after transient lipofection.

Using pcDNA3.1 instead of pcep4 increased the expression rate of all three LPETG\_mCD1d constructs by two- to three-fold, reaching close to 20 % transfected cells for GGGS<sub>0</sub> and GGGS<sub>1</sub>. As observed previously, GGGS<sub>2</sub> showed the lowest cell surface expression (Figure 15).

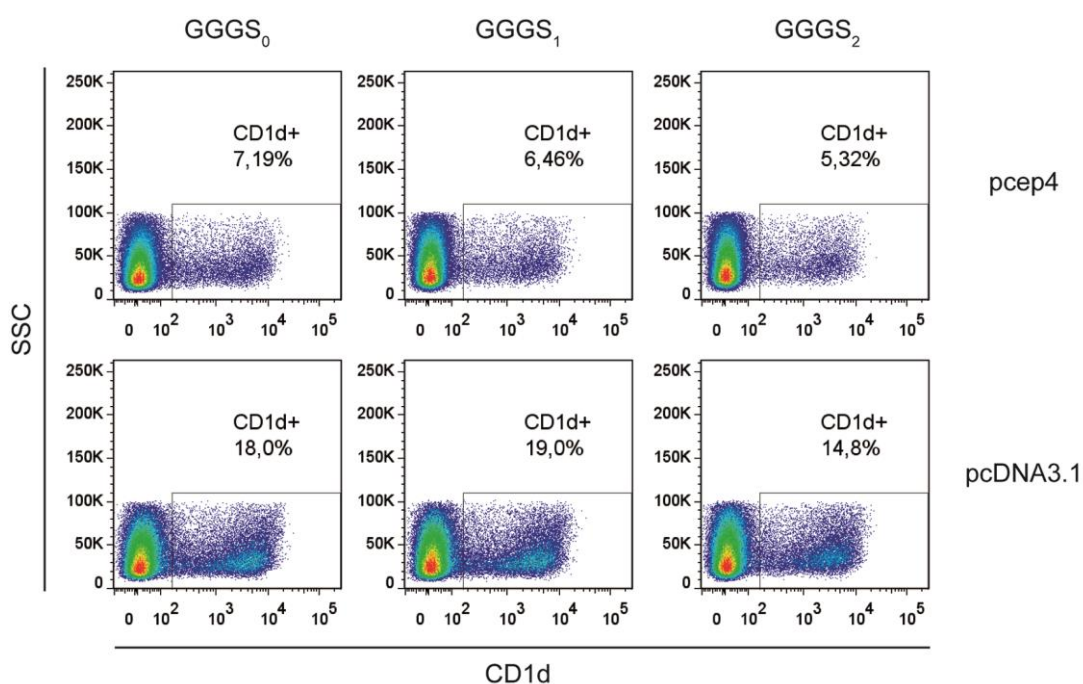


**Figure 15: Flow Cytometric Analysis of the Expression of LPETG\_mCD1d(GGGS)<sub>0-2</sub> using pcep4 and pcDNA3.1 Vector Backbones.**

HeLa cells were transfected with LPETG\_mCD1d(GGGS)<sub>0-2</sub> on either vector backbone in the same experiment and analyzed for CD1d cell surface expression by flow cytometry. Representative dot plots show the increase in CD1d expressing cells when using a pcDNA3.1 vector backbone.

When compared with WT mCD1d on a pcDNA3.1 backbone, LPETG\_mCD1d(GGGS)<sub>0</sub> had nearly the same surface expression (Figure 15). Again, baseline CD1d cell surface expression negatively correlated with the number of glycine-serine spacers. Conversely, SrtA digestion became more efficient. While the GGGS<sub>0</sub> construct was not cleaved at all, the number of GGGS<sub>1</sub> expressing cells was reduced by approximately 20 % and GGGS<sub>2</sub> expressing cells by close to 50 % (Figure 16 A). Likewise, CD1d expression per cell, as determined by MFI, showed the same trend (Figure 16 B).

While the reduction in the relative frequency of CD1d expressing cells was greater for LPETG\_mCD1d(GGGS)<sub>2</sub> compared to LPETG\_mCD1d(GGGS)<sub>1</sub>, the MFI of CD1d<sup>+</sup> cells was equally reduced by approximately 50 % for both constructs (Figure 16 B). Considering that LPETG\_mCD1d(GGGS)<sub>1</sub> shows a higher cell surface expression compared to LPETG\_mCD1d(GGGS)<sub>2</sub>, which was confirmed by the frequency of CD1d-positive cells and the MFI, protein yields from both constructs were anticipated to be similar, even with a lower cleavage efficiency of LPETG\_mCD1d(GGGS)<sub>1</sub>. This was indeed confirmed by ELISA, revealing mCD1d levels of more than 2 ng in the SN of  $5 \times 10^5$  HeLa cells transfected with either LPETG\_mCD1d(GGGS)<sub>2</sub> or LPETG\_mCD1d(GGGS)<sub>1</sub> and treated with SrtA (Figure 16 C). Again, however, increasing the number of spacers led to spontaneous cleavage of LPETG\_mCD1d (Figure 16 C).

Even though the digestion efficiency increased with the number of spacers, this positive effect was partially compensated by the observation that baseline expression and protein stability appeared to be negatively influenced by addition of GGGS spacers. Since the protein yield after SrtA treatment did not differ between the GGGS<sub>1</sub> and GGGS<sub>2</sub> constructs and since the LPETG\_mCD1d(GGGS)<sub>2</sub> construct underwent significant spontaneous cleavage, we considered pcDNA3.1\_LPETG\_mCD1d(GGGS)<sub>1</sub> the most suitable construct for proteolytic cleavage of cell surface CD1d and subsequent MS analysis of bound lipids. However, one essential factor still needed to be investigated: The capacity of any of the constructs tested to present antigen to CD1d-restricted T cells.

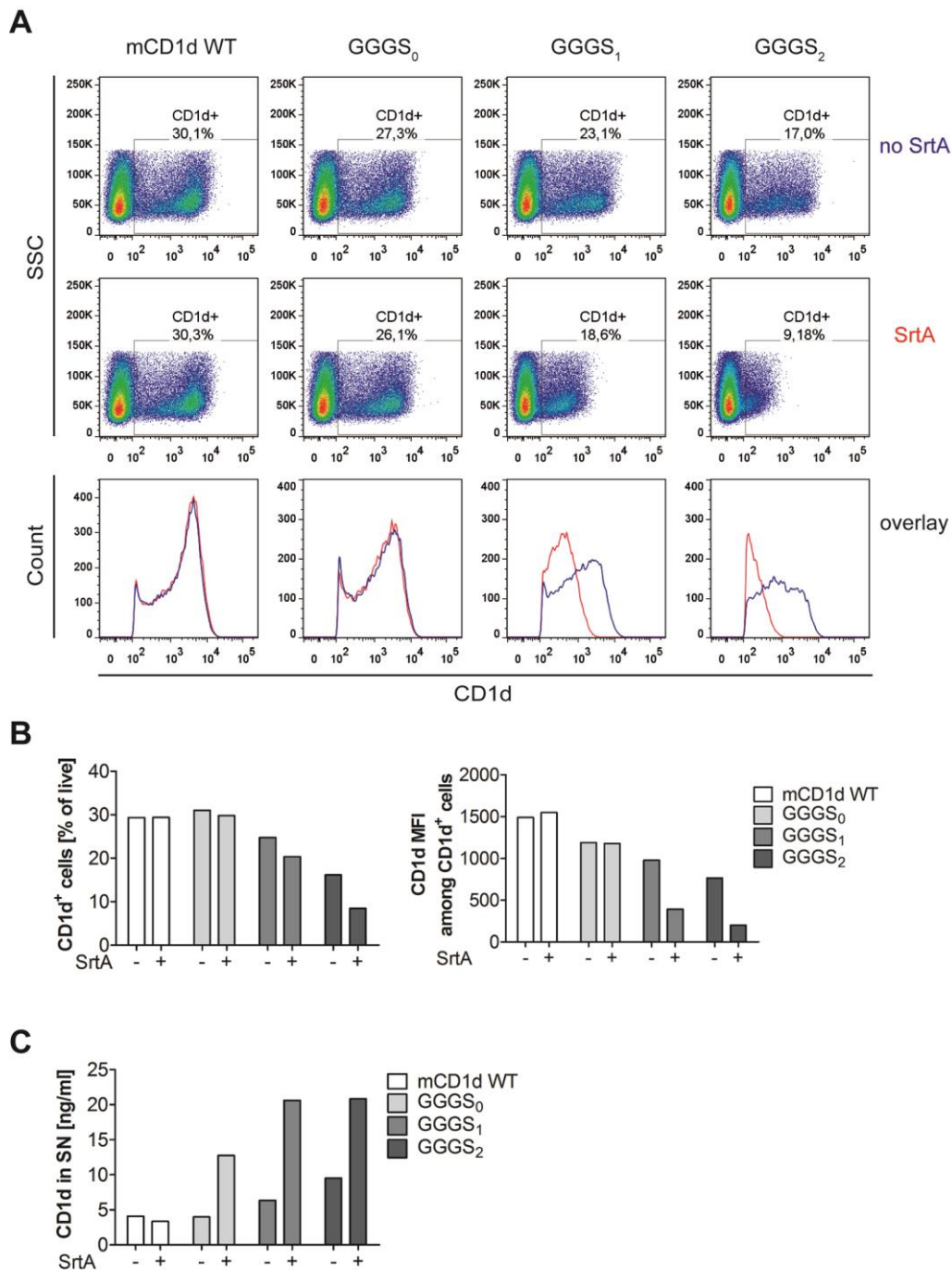


**Figure 16: SrtA Digest of HeLa cells Transfected with pcDNA\_LPETG\_mCD1d(GGGS)<sub>0-2</sub>.**

HeLa cells were transfected with pcDNA3.1\_LPETG\_mCD1d(GGGS)<sub>0-2</sub> and used for SrtA digest 24 h after transfection. (A) Dot plots depicting the relative expression rate of CD1d and histograms representing the expression per cell of the CD1d<sup>+</sup> subset of cells. Cells show decreasing expression rates of mCD1d, but increasing cleavage efficiency with increasing spacer number. (B) Quantification of the relative percentage of CD1d-positive cells (left) and CD1d expression per cell gated on CD1d<sup>+</sup> cells (MFI) with and without active enzyme (right). (C) Release of CD1d into the SN of cells incubated with or without SrtA, as determined by ELISA. A shows individual plots and B and C show the mean of duplicate values from one experiment.



#### 4.7 CD1d-Dependent Antigen Presentation Is Affected by Gly-Ser Spacers

CD1d-mediated antigen presentation is a complex process, which depends on CD1d trafficking, lipid loading and exchange as well as appropriate alignment of CD1d with the TCR. We therefore investigated whether the addition of Gly-Ser spacers or the SrtA motif itself altered the ability of CD1d to load and present lipid antigens.

HeLa cells were transfected with WT and LPETG\_mCD1d. 24 hours after transfection, the expression of mCD1d was determined by flow cytometry and cells were seeded into 96-well plates, in which they were co-cultured with the 24.7 iNKT cell hybridoma.<sup>78</sup> NKT cells recognize natural cellular lipids in the context of CD1d, which is associated with their activation and has been termed autoreactivity. Transfected HeLa cells were first co-cultured in the absence of exogenous lipids to test for the loading and presentation of endogenous lipids. Additionally, transfected HeLa cells were incubated with increasing concentrations of  $\alpha$ -galactosylceramide ( $\alpha$ GalCer) or galactosyl- $\alpha$ 1-2-galactosylceramide ( $\alpha$ GalGalCer), prior to addition of the 24.7 cells, to test for the loading and presentation of exogenous lipids.  $\alpha$ GalCer is a potent antigen for iNKT cells and is therefore often used as a positive control for the induction of iNKT cell activation.<sup>13,78</sup>  $\alpha$ GalGalCer needs to be processed to  $\alpha$ GalCer by lysosomal enzymes to induce CD1d-mediated activation of iNKT cells.<sup>65</sup> By using these two lipids, we could not only investigate the capacity of the mCD1d constructs to present antigen, but could also determine if they exhibited unimpaired endolysosomal trafficking. Activation of the iNKT cell hybridomas was assessed by secretion of mL-2.

For both  $\alpha$ GalCer and  $\alpha$ GalGalCer, the concentration of mL-2 in the SN of the co-cultured cells increased in a dose-dependent manner for all mCD1d constructs tested. WT\_mCD1d induced the strongest activation upon presentation of  $\alpha$ GalCer, while the GGGS<sub>0</sub> construct was associated with only slightly less iNKT cell activation (Figure 17 A). Addition of GGGS spacers reduced the ability of CD1d to activate iNKT cells, which was particularly evident for the LPETG\_mCD1d(GGGS)<sub>2</sub> construct (Figure 17 A).

$\alpha$ GalGalCer induced slightly stronger NKT cell responses compared to  $\alpha$ GalCer, indicating sufficient trafficking of all mCD1d constructs. Using  $\alpha$ GalGalCer, WT\_CD1d, LPETG\_mCD1d(GGGS)<sub>0</sub>, and LPETG\_mCD1d(GGGS)<sub>1</sub> showed largely

comparable iNKT cell activation, while LPETG-mCD1d(GGGS)<sub>2</sub> again induced a considerably weaker iNKT cell response (Figure 17 A).

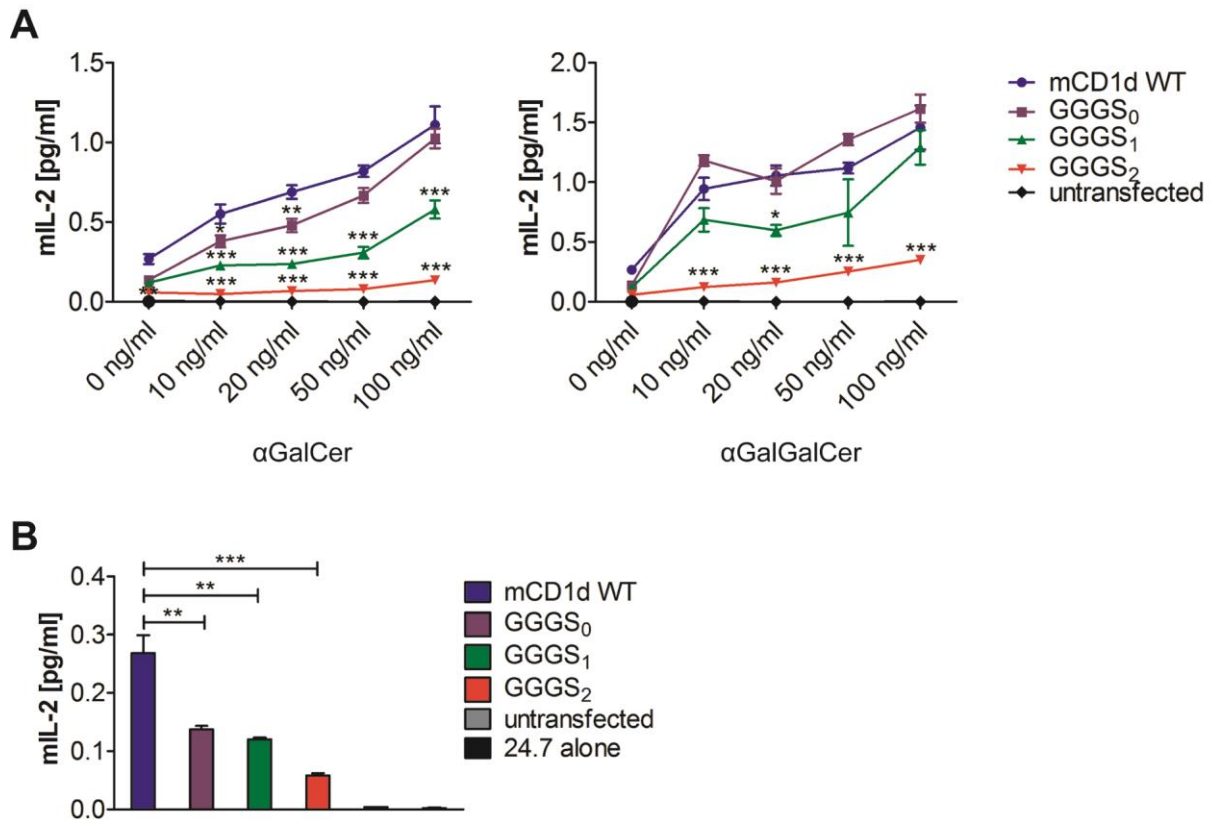


**Figure 17: Antigen Presentation by LPETG\_mCD1d(GGGS)<sub>0-2</sub> Expressing HeLa Cells.**

HeLa cells were transfected with the indicated mCD1d constructs. 24 h after transfection, the cells were either incubated over night with the implied concentrations of  $\alpha$ GalCer or  $\alpha$ GalGalCer or cultured without the addition of exogenous lipids. The following day, the cells were washed extensively and  $1 \times 10^5$  24.7 cells were added per well. Supernatants of the co-cultures were taken after 24 h. (A) mIL-2 ELISA of SN taken from HeLa cells previously incubated with  $\alpha$ GalCer or  $\alpha$ GalGalCer after 24 h of co-culture with 24.7 cells. The secretion of IL-2 represents the response of 24.7 cells to exogenous lipids presented by CD1d. (Two-way ANOVA with Bonferroni post-hoc analysis; \*  $p < 0.05$ , \*\*\*  $p < 0.01$ ; GGGS<sub>0-2</sub> compared with mCD1d WT) (B) mIL-2 ELISA of SN taken from the co-culture of HeLa and 24.7 cells without previous addition of exogenous antigen. The secretion of mIL-2 represents the response of 24.7 cells to endogenous antigen presentation (One-way ANOVA with Bonferroni post-hoc analysis; \*\*  $p \leq 0.01$ , \*\*\*  $p \leq 0.001$ ). (Mean values with SEM, all experiments were performed in triplicates.)

Similar to the data described for presentation of exogenous antigens, the addition of GGGS spacers to mCD1d reduced the response to the presentation of endogenous antigen. Surprisingly, the NKT hybridomas' response to WT\_mCD1d was nearly twice as strong compared to the construct only containing the LPETG sequence

(LPETG\_mCD1d(GGGS)<sub>0</sub>). A comparison of the three LPETG\_mCD1d constructs revealed that the addition of one GGGS spacer reduced iNKT cell activation only minimally, while the addition of two spacers again decreased it by approximately 50 % (Figure 17 B).

Of note, results on antigen presentation were not corrected for decreased cell surface expression of CD1d as observed for LPETG\_mCD1d(GGGS)<sub>1</sub> and LPETG\_mCD1d(GGGS)<sub>2</sub>. We therefore conclude that at least the mild alterations in antigen presentation observed for LPETG\_mCD1d(GGGS)<sub>1</sub> were likely related to slightly decreased cell surface expression.

Altogether, our data demonstrate that LPETG\_mCD1d(GGGS)<sub>1</sub> is an engineered CD1d molecule amenable to SrtA-mediated proteolytic release at the cell surface with minor effects on CD1d expression, trafficking, and antigen loading, as well as presentation. We thus report the establishment of a novel, enzymatically cleavable CD1d construct, which, alongside secreted CD1d, may provide the basis for the first comprehensive analysis of CD1d-associated lipid antigens *in vitro* and *ex vivo*.

## 5 Discussion

CD1d restricted, lipid-reactive NKT cells have been shown to play a crucial role in a range of immune responses, including antimicrobial immunity, tumor immunity, and inflammatory disorders, such as IBD or asthma.<sup>12</sup> Capable of rapidly secreting large amounts of various cytokines and chemokines, NKT cells can influence most cells of the innate and adaptive immune system and thus direct both pro- and anti-inflammatory immune reactions.<sup>11</sup> However, our knowledge of the antigens involved in CD1d-mediated activation of NKT cells is limited, which is largely due to technical limitations associated with the loss of CD1d-bound lipids during extraction and purification of CD1d. We therefore aimed to develop CD1d proteins which allow for enzymatic cleavage of CD1d at the cell surface lipids, while showing little impact on subcellular trafficking as well as antigen loading and presentation by CD1d. Such engineered proteins could serve as the basis for mass spectrometric analysis of CD1d-associated lipids and will provide new opportunities to identify these *in vitro* and *in vivo*. A better understanding of the CD1d lipidome may provide helpful information for the development of strategies towards therapeutic targeting of lipid antigen presentation in NKT cell-mediated diseases.

### 5.1 H $\beta$ <sub>2</sub>m\_mCD1d\_TEV Protease Does Not Allow for Proteolytic Release of Cell Surface CD1d

During the search for methods to facilitate the investigation of CD1d-associated lipids, different genetically modified CD1d constructs were developed recently. Experiments with these constructs have provided critical information on the importance of different cellular compartments for lipid loading and modification and also on a small number of lipid antigens capable of activating NKT cells.<sup>36,52,60–62,67,78</sup> However, most of the constructs amenable to CD1d collection and MS analysis do not undergo trafficking through the endolysosomal system but are restricted to secretory compartments. As an exception, *Muindi et al.*<sup>60</sup> described a mCD1d construct with an intact transmembrane and cytoplasmic domain and largely unaltered intracellular trafficking of CD1d, which was designed to be cleaved at the cell surface using exogenously added TEV protease. However, the authors observed similar release of CD1d in the presence or absence of TEV protease, suggesting spontaneous cleavage of the engineered CD1d molecule upon exposure to TEV buffer.<sup>60</sup> In an attempt to solve these issues, we first optimized the construct

sequence by removing one TEV cleavage site and substituting it with a Strep-tag ii for subsequent protein purification. In a second construct we replaced h $\beta_2m$  with m $\beta_2m$ , so that  $\beta_2m$  and CD1d were derived from the same species (h $\beta_2m\_mCD1d\_TEV$  and m $\beta_2m\_mCD1d\_TEV$ ). A secreted mCD1d construct lacking the TMD and C-terminus of CD1d originally published by *Gumperz* and colleagues (mCD1d-Fc) and also used by *Muindi* et al. was also modified.<sup>60,78</sup> Instead of the Fc region of mouse IgG<sub>2a</sub>, a Strep-tag ii and an 8 x His tag were added to the C-terminus of the  $\alpha_3$  domain of CD1d. A secreted CD1d construct associated with m $\beta_2m$  instead of h $\beta_2m$  was also generated (h $\beta_2m\_sol\_mCD1d$ , m $\beta_2m\_sol\_mCD1d$ ) (Figure 7). Interestingly, transfection of these constructs into mouse intestinal epithelial cells (MODE-K) revealed that the modified constructs associated with h $\beta_2m$  (h $\beta_2m\_mCD1d\_TEV$  and h $\beta_2m\_sol\_mCD1d$ ) had a higher relative expression than those associated with m $\beta_2m$  (Figure 8). Due to high sequence homology of both  $\beta_2m$  and class I receptor  $\alpha$ -chains in humans and mice, mouse  $\beta_2m$  can associate with human MHC class I (major histocompatibility complex I) receptors and human  $\beta_2m$  can dimerize with mouse MHC class I.<sup>98-101</sup> Studies have shown that heterodimers of h $\beta_2m$  with human or mouse MHC I are both more stable than heterodimers formed with m $\beta_2m$ , independent of species origin of MHC class I.<sup>99,100</sup> The molecular basis for these observations remains unclear, but our results indicate that the same principle holds true for  $\beta_2m$ -mCD1d heterodimers.

h $\beta_2m\_mCD1d\_TEV$  was well expressed in different mouse and human cell lines (MODE-K, L cells, HeLa cells), but we were not able to detect TEV-mediated release of cell surface CD1d in any of the experiments performed (Figure 9-Figure 12). Neither a different commercial source of TEV protease, nor an increase in the concentration of TEV protease or the addition of Brefeldin A to prevent replenishment with newly synthesized CD1d led to detectable TEV-dependent CD1d cleavage.

We also demonstrated that AcTEV buffer was detrimental to the cells, which may be related to the moderately basic pH of the buffer (Tris-HCl at pH 8.0) and the lack of proteins, electrolytes and nutrients which are normally contained in cell-culture medium. The TEV buffer provided by Promega was less detrimental, most likely because it consisted of 50 mM HEPES at neutral pH 7 (Figure 11). DMEM or HBSS provided a better environment for the cells, but contain sodium chloride, which may have adverse effects on TEV protease activity.<sup>102</sup> Additionally, DMEM contains fetal

calf serum, which is a natural product and thus contains a range of organic substances<sup>103</sup> that might affect TEV protease.

Furthermore, we considered that the lack of TEV-mediated CD1d shedding may be caused by inaccessibility of the cleavage site located in the juxtamembrane portion of the CD1d protein between the  $\alpha_3$  domain and the TMD. We therefore generated a construct with three GGGS spacers inserted between the TMD and the cleavage site (h $\beta_2$ m\_mCD1d\_TEV(GGGS)<sub>3</sub>). However, increasing the distance between the plasma membrane and the TEV recognition motif did not improve cleavage (Figure 12). Thus, we concluded that TEV-mediated shedding of the CD1d extracellular domain from the surface of eukaryotic cells cannot be achieved with the current constructs and further confirm recent data,<sup>60</sup> suggesting that the previously observed release of TEV-CD1d represents spontaneous rather than TEV-induced release of CD1d, possibly as a consequence of impaired cell viability in TEV buffer.

## 5.2 Sortase A-Mediated Release of Cell Surface CD1d

As an alternative for the TEV-cleavable CD1d construct, we began working with LPETG\_mCD1d. LPETG is an amino acid motif recognized by the *S. aureus* SrtA transpeptidase, which cleaves the threonine-glycine bond in this recognition sequence. Similar to the TEV-cleavable construct, the LPETG constructs had the SrtA cleavage site inserted between the TMD and  $\alpha_3$  domain of mCD1d, but were not covalently linked to  $\beta_2$ m. These constructs were either designed with none, one or two GGGS spacers just C-terminal of the cleavage site, thereby increasing the distance between the LPETG motif and the TMD.

All of the constructs were detectable at the cell surface of transfected HeLa cells, with cell surface expression inversely correlating with the number of Gly-Ser spacers added. Conversely, the efficiency of SrtA-mediated release of cell surface LPETG\_mCD1d improved with the addition of each GGGS spacer (Fig. 13). Because the relative expression of the LPETG\_mCD1d constructs in HeLa cells was lower than the expression previously seen for h $\beta_2$ m\_mCD1d\_TEV, we sub-cloned the constructs from their pcep4 vector backbone into pcDNA3.1. Changing the vector backbone to pcDNA3.1 increased the expression rate by two to three-fold compared to pcep4, even though both plasmids use the same CMV promoter/enhancer element for transcription initiation (Figure 15). This effect is likely due to the smaller plasmid

size of pcDNA3.1, which is nearly half the size of pcep4 and reflects the observation that vector size negatively affects transfection rates and promoter activity.<sup>104</sup>

We therefore continued working with the LPETG\_mCD1d(GGGS)<sub>0-2</sub> constructs on a pcDNA3.1 plasmid backbone. With a higher expression of the constructs, the protein yield from cleavage experiments also increased, resulting in as much as 2 ng of mCD1d released into the SN of  $5 \times 10^5$  HeLa cells transfected with LPETG\_mCD1d(GGGS)<sub>1</sub> and LPETG\_mCD1d(GGGS)<sub>2</sub> after incubation with SrtA (Figure 16). However, we also observed an increase in non-enzymatic, spontaneous shedding of the LPETG\_mCD1d constructs proportional to the spacer number. Gly-Ser spacers are a commonly used tool in the generation of fusion-proteins. Due to their small size and lack of complex side-chains, glycine and serine make up flexible linker elements, which have also been detected in naturally occurring proteins.<sup>105,106</sup> Another study investigating the properties of naturally occurring linker peptides stated that the majority of linkers consisted of more complex amino acids and were therefore more rigid. According to their analysis, the average length of a naturally occurring linker peptide is  $10 \pm 5.8$  amino acids.<sup>107</sup> Glycine-rich linkers are considered independent units that do not affect the functions of the linked domains, in part because glycine does not readily form  $\alpha$ -helices.<sup>105</sup> A study with poly-glycine linkers of different lengths (G<sub>n</sub>) added to the protein Rop demonstrated that an increase in linker length did not affect the protein's folding or capability to bind RNA, but a longer linker was associated with decreased protein stability in tests with thermal and chemical denaturation.<sup>108</sup> Though the linker peptides used in our constructs lie within the average length of naturally occurring linker peptides, it is possible that the high flexibility combined with the linker length destabilizes the protein, especially in the LPETG\_mCD1d(GGGS)<sub>2</sub> construct. Nevertheless, it is noteworthy that while no spontaneous shedding was detected for the LPETG\_mCD1d(GGGS)<sub>0</sub> construct, SrtA-induced release was also only detected at very low levels. It thus appears that the addition of the GGGS spacer(s) is required for SrtA binding to, and processing of, CD1d and at the same time leads to moderate spontaneous release of LPETG-CD1d.

To investigate whether the sortase motif or the Gly-Ser spacer(s) affect CD1d-restricted antigen presentation, HeLa cells transfected with WT\_mCD1d and the LPETG\_mCD1d constructs were either directly co-cultured with iNKT hybridoma

cells or incubated with exogenous lipid antigens before co-culture with iNKT cells. Independent of the presented antigen, the ability to activate iNKT cells in a CD1d-restricted manner negatively correlated with the presence and number of Gly-Ser spacers. While LEPTG\_mCD1d(GGGS)<sub>0</sub> and LEPTG\_mCD1d(GGGS)<sub>1</sub> exhibited only mild alterations in the presentation of endogenous and exogenous lipid antigens, possibly as a consequence of slightly decreased cell surface expression of these constructs, LEPTG\_mCD1d(GGGS)<sub>2</sub> exhibited significant defects in the presentation of self- and non-self-antigens (Figure 17). Given that two CD1d ligands with distinct subcellular processing and loading requirements yielded similar results for LEPTG\_mCD1d(GGGS)<sub>2</sub>, alterations in antigen presentation are unlikely to result from altered endolysosomal trafficking (Figure 17).

A more likely explanation for the obtained results is an altered positioning of the CD1d lipid binding groove relative to the iNKT TCR, induced by the addition of the LPETG cleavage site and/or the Gly-Ser spacer(s). The interaction of lipid-loaded CD1d with the NKT-TCR is different from the interaction of the TCR with MHC class I. Unlike the diagonal positioning, which is observed for the interaction between the TCR and MHC class I, the iNKT TCR docks over the F' pocket of CD1d, approximately parallel to the long axis of the CD1d antigen binding groove. The iNKT TCR hereby spans areas of the  $\alpha_1$  and  $\alpha_2$  domains of CD1d, with complementarity determining region (CDR) 2 $\beta$  and CDR3 $\alpha$  playing an important role in TCR-CD1d-antigen interaction.<sup>109-111</sup> The affinity of the interaction is not just dependent on the positioning of the TCR relative to CD1d, but also on the antigen presented. In crystallization studies of the synergy between the V $\alpha$ 14 TCR and CD1d either loaded with the exogenous antigen  $\alpha$ GalCer or the endogenous antigen iGb3, a much lower affinity for the endogenous antigen was measured.<sup>111,112</sup> Considering the complexity of CD1d-TCR interactions, it seems conceivable that a slight alteration in the positioning of CD1d relative to the TCR, due to the insertion of a cleavage site or a flexible linker, could be disruptive for CD1d-TCR interactions.

Taken together, we present an engineered CD1d protein, LPETG\_mCD1d(GGGS)<sub>1</sub>, which exhibited substantial SrtA-mediated release at the cell surface and yields amounts of CD1d predicted to be sufficient for MS-based analysis. Further, this construct showed limited spontaneous release in the absence of SrtA and exhibited



only minor alterations in CD1d expression and antigen loading as well as presentation.

### 5.3 Conclusion and Outlook

Here, we present novel CD1d proteins engineered to contain the recognition site for SrtA to allow for SrtA-mediated enzymatic cleavage of CD1d at the cell surface. These constructs shall provide the basis for future, systematic analyses of CD1d-associated lipids *in vivo* and *in vitro*.

To avoid interference with the folding and antigen binding of CD1d, the SrtA recognition site was integrated into the juxtamembrane region of CD1d, in between the TMD and the extracellular  $\alpha 3$  domain. Insertion of the SrtA recognition motif into CD1d had only minor effects on protein expression and antigen presentation. However, the positioning of the LPETG motif in close proximity to the plasma membrane did not allow for sufficient enzyme-mediated CD1d cleavage at the cell surface, most likely due to inaccessibility of the cleavage site. We therefore integrated Gly-Ser spacers between the TMD and the sortase motif and observed that the addition of one or more Gly-Ser spacers promoted the access of SrtA to the LPETG motif and allowed for cleavage of CD1d at the cell surface. The concentration of CD1d released upon SrtA treatment is predicted to be sufficient for lipidomics-based characterization of CD1d-associated lipids. However, addition of the spacers also promoted spontaneous, non-enzymatic release of CD1d. Further, addition of the Gly-Ser spacer(s) negatively affected CD1d-restricted antigen presentation, presumably resulting from spontaneous CD1d cleavage as well as altered interactions with the NKT TCR due to increased flexibility of the engineered CD1d protein. Considering these observations, adding one GGGS spacer to the SrtA motif served as an optimal compromise allowing for sufficient SrtA-mediated CD1d cleavage, while limiting spontaneous shedding and alterations in CD1d-restricted antigen presentation.

In future studies, SrtA-cleavable CD1d proteins as engineered in this work will be used to investigate the spectrum of CD1d-associated lipids *in vitro* and *in vivo*. Comparison of CD1d-associated lipids isolated from cells transfected with LPETG\_mCD1d and a secreted form of CD1d will provide important information on differences between lipids loaded while trafficking along the secretory pathway and

lipids loaded within the endolysosomal compartments. Also, treatment of LPETG\_CD1d-transfected cells with stimuli resembling inflammatory conditions or using cells representative of different developmental stages of cancer<sup>113</sup>, may allow the investigation of potentially disease-associated changes in the CD1d lipid repertoire. By means of hydrodynamic injection<sup>114</sup> or transgenic expression, it may further be possible to express genetically engineered CD1d *in vivo* to directly investigate differences between CD1d-associated lipids under healthy and inflammatory conditions.

Thus, LPETG\_mCD1d may provide the basis for novel strategies to identify CD1d-restricted antigens involved in protective and pathogenic NKT cell responses *in vivo*.

## 6 Summary

CD1d is an atypical MHC class I molecule which is expressed by a range of professional and non-professional antigen presenting cells (APCs). Unlike classical MHC receptors, CD1d does not present peptide antigens to conventional T cells but presents lipid antigens to natural killer T (NKT) cells. NKT cells are involved in a multitude of immune responses and play a key role in the development of the human inflammatory bowel disease ulcerative colitis (UC).

The search for CD1d-restricted lipid antigens involved in the activation of intestinal NKT cells is therefore critical for a better understanding of the mechanisms responsible for the initiation of NKT cell-dependent intestinal inflammation in UC. However, the identification of lipids associated with CD1d is laborious and technically challenging, as isolation of CD1d from the plasma membrane through classical isolation methods has previously been associated with inevitable dissociation of CD1d-bound lipids. Genetically engineered CD1d proteins lacking the transmembrane domain (TMD) and cytoplasmic domain are secreted and thus do not require extraction from the plasma membrane. However, these proteins undergo incomplete subcellular trafficking and fail to survey endolysosomal compartments, thus providing limited information on the range of CD1d-associated lipids.

Here, we present genetically engineered CD1d proteins, which undergo unimpaired trafficking through secretory and endolysosomal compartments and can be enzymatically cleaved at the cell surface of eukaryotic cells. To this end, CD1d was engineered to contain amino acid motifs in its extracellular juxtamembrane region, which are recognized by TEV protease (h $\beta_2$ m\_mCD1d\_TEV) or Sortase A (SrtA) transpeptidase (LPETG\_mCD1d). While TEV protease-dependent enzymatic cleavage of h $\beta_2$ m\_mCD1d\_TEV could not be achieved, SrtA allowed for proteolytic release of CD1d from the plasma membrane. However, SrtA-dependent release of CD1d was only possible after the addition of glycine-serine spacers between the TMD and the SrtA recognition motif. This likely promoted access of SrtA to its cleavage site but also facilitated spontaneous release of CD1d in the absence of SrtA. CD1d engineered to contain only one glycine-serine spacer, however, allowed for substantial SrtA-dependent cleavage with limited spontaneous release of CD1d and only minor alterations in CD1d expression and antigen loading as well as presentation.

In conclusion, we present CD1d proteins amenable to proteolytic release at the cell surface, which may provide the basis for future analyses of the repertoire of CD1d-associated lipids in health and disease.

## 7 Zusammenfassung

CD1d ist ein atypisches MHC I Molekül, das von einer Reihe professioneller, sowie nicht professioneller Antigen präsentierender Zellen exprimiert wird. Anders als klassische MHC I Moleküle präsentiert CD1d keine Peptid-Antigene an konventionelle T Zellen, sondern Lipid-Antigene an Natürliche Killer T (NKT) Zellen. NKT Zellen sind an einer Vielzahl von Immunreaktionen beteiligt und spielen eine zentrale Rolle in der Pathogenese der Colitis ulcerosa.

Um ein besseres Verständnis für die NKT Zell-abhängigen Mechanismen intestinaler Entzündung in der Colitis ulcerosa zu erlangen, ist es von zentraler Bedeutung mehr über die Lipid-Antigene zu erfahren, die zur Aktivierung intestinaler NKT Zellen beitragen. Die Identifikation CD1d-assoziiierter Lipid-Antigene ist jedoch ein technisch anspruchsvolles Unterfangen. Klassische, Detergenzien-abhängige Isolierungsmethoden für Transmembranproteine können für CD1d nicht angewandt werden, da diese mit einem unvermeidbaren Verlust der gebundenen Lipide einhergehen. Eine Lösung für diese Problematik stellen genetisch modifizierte CD1d Proteine dar, die aufgrund fehlender Transmembran- und cytoplasmatischen Domänen sezerniert werden und somit nicht aus der Plasmamembran isoliert werden müssen. Allerdings werden diese Moleküle lediglich durch die sekretorischen Kompartimente (endoplasmatisches Retikulum, Golgi-Apparat) transportiert und liefern somit keine Informationen zu Lipid-Antigenen, die innerhalb der endolysosomalen Kompartimente von CD1d gebunden werden.

In dieser Arbeit präsentieren wir genetisch modifizierte CD1d Proteine, deren intrazellulärer Transport nicht beeinträchtigt ist und die durch enzymatische Spaltung an der Oberfläche eukaryotischer Zellen isoliert werden können. Zwei kurze Peptide, die als Erkennungssequenzen für TEV Protease (h $\beta$ <sub>2</sub>m\_mCD1d\_TEV) oder Sortase A Transpeptidase (LPETG\_mCD1d) dienen, wurden in die extrazelluläre juxtamembranäre Domäne des CD1d Moleküls integriert. Während eine effiziente Spaltung des Proteins durch TEV Protease nicht erreicht werden konnte, ließ sich das Sortase-spaltbare Protein erfolgreich isolieren. Voraussetzung für eine erfolgreiche Spaltung war jedoch die vorherige Integration von Glycin-Serin Peptiden zwischen der Transmembrandomäne und der Sortase A Schnittstelle. Diese Spacer Peptide machten die Sortase A Schnittstelle vermutlich zugänglicher, förderten aber auch die Enzym-unabhängige Spaltung des Proteins. Das Einfügen eines einzelnen

Glycin-Serin Peptids resultierte in einer verbesserten Spaltbarkeit von CD1d mit minimaler Enzym-unabhängiger Freisetzung. Zudem wurden die Beladung und Präsentation von Lipid-Antigenen durch die Integration eines Glycin-Serin Peptids nur marginal beeinflusst.

Zusammengefasst präsentieren wir CD1d Proteine, die in Enzym-spezifischer Weise an der Oberfläche eukaryotischer Zellen proteolytisch gespalten und freigesetzt werden können und somit die Grundlage für zukünftige Untersuchungen des CD1d-assoziierten Lipidspektrums *in vitro* und *in vivo* bilden sollen.

## 8 Bibliography

1. Kaser, A., Zeissig, S. & Blumberg, R. S. Inflammatory Bowel Disease. *Annu. Rev. Immunol.* **28**, 573–621 (2010).
2. Liao, C.-M., Zimmer, M. I. & Wang, C.-R. The Functions of Type I and Type II Natural Killer T Cells in Inflammatory Bowel Diseases: *Inflamm. Bowel Dis.* **19**, 1330–1338 (2013).
3. Clara Abraham & Judy H. Cho. Inflammatory Bowel Disease. *N Engl J Med* 2066–2078 (2009).
4. Zeissig, S. & Blumberg, R. S. Commensal microbial regulation of natural killer T cells at the frontiers of the mucosal immune system. *FEBS Lett.* **588**, 4188–4194 (2014).
5. Fuss, I. J. *et al.* Nonclassical CD1d-restricted NK T cells that produce IL-13 characterize an atypical Th2 response in ulcerative colitis. *J. Clin. Invest.* **113**, 1490–1497 (2004).
6. Fuss, I. J. *et al.* IL-13R $\alpha$ 2-bearing, type II NKT cells reactive to sulfatide self-antigen populate the mucosa of ulcerative colitis. *Gut* **63**, 1728–1736 (2014).
7. Makino, Y., Kanno, R., Ito, T., Higashino, K. & Taniguchi, M. Predominant expression of invariant V alpha 14+ TCR alpha chain in NK1.2+ T cell populations. *Int Immunol* **7**, 1157–61 (1995).
8. Matsuda, J. L. *et al.* Tracking the response of natural killer T cells to a glycolipid antigen using CD1d tetramers. *J. Exp. Med.* **192**, 741–754 (2000).
9. van Dieren, J. M. *et al.* Roles of CD1d-restricted NKT cells in the intestine: *Inflamm. Bowel Dis.* **13**, 1146–1152 (2007).
10. Bendelac, A., Savage, P. B. & Teyton, L. The Biology of NKT Cells. *Annu. Rev. Immunol.* **25**, 297–336 (2007).

11. Matsuda, J. L., Mallevaey, T., Scott-Browne, J. & Gapin, L. CD1d-restricted iNKT cells, the 'Swiss-Army knife' of the immune system. *Curr. Opin. Immunol.* **20**, 358–368 (2008).
12. Dowds, C. M., Kornell, S.-C., Blumberg, R. S. & Zeissig, S. Lipid antigens in immunity. *Biol. Chem.* **395**, (2014).
13. Burdin, N. *et al.* Selective Ability of Mouse CD1 to Present Glycolipids:  $\alpha$ -Galactosylceramide Specifically Stimulates V $\alpha$ 14+ NK T Lymphocytes. *J. Immunol.* **161**, 3271–3281 (1998).
14. Godfrey, D. I., MacDonald, H. R., Kronenberg, M., Smyth, M. J. & Kaer, L. V. NKT cells: what's in a name? *Nat. Rev. Immunol.* **4**, 231–237 (2004).
15. The majority of CD1d-sulfatide-specific T cells in human blood use a semiinvariant V $\delta$ 1 TCR - Bai - 2012 - European Journal of Immunology - Wiley Online Library. at <<http://onlinelibrary.wiley.com/doi/10.1002/eji.201242531/full>>
16. Heller, F., Fuss, I. J., Nieuwenhuis, E. E., Blumberg, R. S. & Strober, W. Oxazolone colitis, a Th2 colitis model resembling ulcerative colitis, is mediated by IL-13-producing NK-T cells. *Immunity* **17**, 629–638 (2002).
17. Wingender, G. *et al.* Intestinal Microbes Affect Phenotypes and Functions of Invariant Natural Killer T Cells in Mice. *Gastroenterology* **143**, 418–428 (2012).
18. O'Keeffe, J. *et al.* Diverse populations of T cells with NK cell receptors accumulate in the human intestine in health and in colorectal cancer. *Eur. J. Immunol.* **34**, 2110–2119 (2004).
19. Boirivant, M., Fuss, I. J., Chu, A. & Strober, W. Oxazolone Colitis: A Murine Model of T Helper Cell Type 2 Colitis Treatable with Antibodies to Interleukin 4. *J. Exp. Med.* **188**, 1929–1939 (1998).



20. Schiechl, G. *et al.* Tumor development in murine ulcerative colitis depends on MyD88 signaling of colonic F4/80+CD11b<sup>high</sup>Gr1<sup>low</sup> macrophages. *J. Clin. Invest.* **121**, 1692–1708 (2011).
21. Saubermann, L. J. *et al.* Activation of natural killer T cells by  $\alpha$ -galactosylceramide in the presence of CD1d provides protection against colitis in mice. *Gastroenterology* **119**, 119–128 (2000).
22. Wirtz, S., Neufert, C., Weigmann, B. & Neurath, M. F. Chemically induced mouse models of intestinal inflammation. *Nat. Protoc.* **2**, 541–546 (2007).
23. Burdin, N., Brossay, L. & Kronenberg, M. Immunization with  $\alpha$ -galactosylceramide polarizes CD1-reactive NK T cells towards Th2 cytokine synthesis. *Eur J Immunol* 2014–2025 (1999).
24. Mandal, M. *et al.* Tissue distribution, regulation and intracellular localization of murine CD1 molecules. *Mol. Immunol.* **35**, 525–536 (1998).
25. Saenz, S. A., Taylor, B. C. & Artis, D. Welcome to the neighborhood: epithelial cell-derived cytokines license innate and adaptive immune responses at mucosal sites. *Immunol. Rev.* **226**, 172–190 (2008).
26. Kaser, A. *et al.* XBP1 Links ER Stress to Intestinal Inflammation and Confers Genetic Risk for Human Inflammatory Bowel Disease. *Cell* **134**, 743–756 (2008).
27. Colgan, S. P., Hershberg, R. M., Furuta, G. T. & Blumberg, R. S. Ligation of intestinal epithelial CD1d induces bioactive IL-10: critical role of the cytoplasmic tail in autocrine signaling. *Proc. Natl. Acad. Sci.* **96**, 13938–13943 (1999).
28. Colgan, S. P. *et al.* Intestinal heat shock protein 110 regulates expression of CD1d on intestinal epithelial cells. *J. Clin. Invest.* **112**, 745–754 (2003).
29. Olszak, T. *et al.* Protective mucosal immunity mediated by epithelial CD1d and IL-10. *Nature* **509**, 497–502 (2014).

30. Saraiva, M. & O'Garra, A. The regulation of IL-10 production by immune cells. *Nat. Rev. Immunol.* **10**, 170–181 (2010).
31. Neufert, C. *et al.* Activation of epithelial STAT3 regulates intestinal homeostasis. *Cell Cycle* **9**, 652–655 (2010).
32. Pickert, G. *et al.* STAT3 links IL-22 signaling in intestinal epithelial cells to mucosal wound healing. *J. Exp. Med.* **206**, 1465–1472 (2009).
33. Bollrath, J. *et al.* gp130-Mediated Stat3 Activation in Enterocytes Regulates Cell Survival and Cell-Cycle Progression during Colitis-Associated Tumorigenesis. *Cancer Cell* **15**, 91–102 (2009).
34. Grivennikov, S. *et al.* IL-6 and Stat3 Are Required for Survival of Intestinal Epithelial Cells and Development of Colitis-Associated Cancer. *Cancer Cell* **15**, 103–113 (2009).
35. Hodge, D., Hurt, E. & Farrar, W. The role of IL-6 and STAT3 in inflammation and cancer. *Eur J Cancer* **41**, 2502–12 (2005).
36. Fox, L. M. *et al.* Recognition of Lyso-Phospholipids by Human Natural Killer T Lymphocytes. *PLoS Biol.* **7**, e1000228 (2009).
37. Zeissig, S. *et al.* Hepatitis B virus-induced lipid alterations contribute to natural killer T cell-dependent protective immunity. *Nat. Med.* **18**, 1060–1068 (2012).
38. Rhost, S. *et al.* Identification of novel glycolipid ligands activating a sulfatide-reactive, CD1d-restricted, type II natural killer T lymphocyte: Cellular immune response. *Eur. J. Immunol.* **42**, 2851–2860 (2012).
39. Jahng, A. Prevention of Autoimmunity by Targeting a Distinct, Noninvariant CD1d-reactive T Cell Population Reactive to Sulfatide. *J. Exp. Med.* **199**, 947–957 (2004).
40. Zhou, D. Lysosomal Glycosphingolipid Recognition by NKT Cells. *Science* **306**, 1786–1789 (2004).

41. Facciotti, F. *et al.* Peroxisome-derived lipids are self antigens that stimulate invariant natural killer T cells in the thymus. *Nat. Immunol.* **13**, 474–480 (2012).
42. Iyer, A. K., Liu, J., Gallo, R. M., Kaplan, M. H. & Brutkiewicz, R. R. STAT3 promotes CD1d-mediated lipid antigen presentation by regulating a critical gene in glycosphingolipid biosynthesis. *Immunology* n/a–n/a (2015). doi:10.1111/imm.12521
43. Ly, D. & Moody, D. B. The CD1 size problem: lipid antigens, ligands, and scaffolds. *Cell. Mol. Life Sci.* **71**, 3069–3079 (2014).
44. Kang, S.-J. Calnexin, Calreticulin, and ERp57 Cooperate in Disulfide Bond Formation in Human CD1d Heavy Chain. *J. Biol. Chem.* **277**, 44838–44844 (2002).
45. Cohen, N. R., Garg, S. & Brenner, M. B. in *Advances in Immunology* (ed. Alt, F. W.) **102**, 1–94 (Academic Press, 2009).
46. De Libero, G. & Mori, L. The Easy Virtue of CD1c. *Immunity* **33**, 831–833 (2010).
47. Zeng, Z.-H. *et al.* Crystal structure of mouse CD1: an MHC-like fold with a large hydrophobic binding groove. *Science* **277**, 339–345 (1997).
48. Paduraru, C. *et al.* An N-Linked Glycan Modulates the Interaction between the CD1d Heavy Chain and beta2-Microglobulin. *J. Biol. Chem.* **281**, 40369–40378 (2006).
49. Jayawardena-Wolf, J., Benlagha, K., Chiu, Y.-H., Mehr, R. & Bendelac, A. CD1d endosomal trafficking is independently regulated by an intrinsic CD1d-encoded tyrosine motif and by the invariant chain. *Immunity* **15**, 897–908 (2001).
50. Bonifacino, J. S. & Traub, L. M. SIGNALS FOR SORTING OF TRANSMEMBRANE PROTEINS TO ENDOSOMES AND LYSOSOMES \*. *Annu. Rev. Biochem.* **72**, 395–447 (2003).

51. Barral, D. C. & Brenner, M. B. CD1 antigen presentation: how it works. *Nat. Rev. Immunol.* **7**, 929–941 (2007).
52. Ya-Hui Chiu *et al.* Multiple defects in antigen presentation and T cell development by mice expressing cytoplasmic tail-truncated CD1d. *Nat. Immunol.* (2002). doi:10.1038/ni740
53. Cernadas, M. *et al.* Lysosomal Localization of Murine CD1d Mediated by AP-3 Is Necessary for NK T Cell Development. *J. Immunol.* **171**, 4149–4155 (2003).
54. Kunte, A. *et al.* Endoplasmic Reticulum Glycoprotein Quality Control Regulates CD1d Assembly and CD1d-mediated Antigen Presentation. *J. Biol. Chem.* **288**, 16391–16402 (2013).
55. Lawton, A. P. *et al.* The Mouse CD1d Cytoplasmic Tail Mediates CD1d Trafficking and Antigen Presentation by Adaptor Protein 3-Dependent and -Independent Mechanisms. *J. Immunol.* **174**, 3179–3186 (2005).
56. Zhou, D. Editing of CD1d-Bound Lipid Antigens by Endosomal Lipid Transfer Proteins. *Science* **303**, 523–527 (2004).
57. Dougan, S. K. Microsomal triglyceride transfer protein lipidation and control of CD1d on antigen-presenting cells. *J. Exp. Med.* **202**, 529–539 (2005).
58. Brozovic, S. *et al.* CD1d function is regulated by microsomal triglyceride transfer protein. *Nat. Med.* **10**, 535–539 (2004).
59. Odyniec, A. N. *et al.* Regulation of CD1 Antigen-presenting Complex Stability. *J. Biol. Chem.* **285**, 11937–11947 (2010).
60. Muindi, K. *et al.* Activation state and intracellular trafficking contribute to the repertoire of endogenous glycosphingolipids presented by CD1d. *Proc. Natl. Acad. Sci.* **107**, 3052–3057 (2010).

61. Yuan, W., Kang, S.-J., Evans, J. E. & Cresswell, P. Natural Lipid Ligands Associated with Human CD1d Targeted to Different Subcellular Compartments. *J. Immunol.* **182**, 4784–4791 (2009).
62. Cox, D. *et al.* Determination of Cellular Lipids Bound to Human CD1d Molecules. *PLoS ONE* **4**, e5325 (2009).
63. Yuan, W. *et al.* Saposin B is the dominant saposin that facilitates lipid binding to human CD1d molecules. *Proc. Natl. Acad. Sci.* **104**, 5551–5556 (2007).
64. Kang, S.-J. & Cresswell, P. Saposins facilitate CD1d-restricted presentation of an exogenous lipid antigen to T cells. *Nat. Immunol.* **5**, 175–181 (2004).
65. Prigozy, T. I. *et al.* Glycolipid antigen processing for presentation by CD1d molecules. *Science* **291**, 664–667 (2001).
66. Gadola, S. D. *et al.* Impaired selection of invariant natural killer T cells in diverse mouse models of glycosphingolipid lysosomal storage diseases. *J. Exp. Med.* **203**, 2293–2303 (2006).
67. De Silva, A. D. *et al.* Lipid Protein Interactions: The Assembly of CD1d1 with Cellular Phospholipids Occurs in the Endoplasmic Reticulum. *J. Immunol.* **168**, 723–733 (2002).
68. Brennan, P. J. *et al.* Invariant natural killer T cells recognize lipid self antigen induced by microbial danger signals. *Nat. Immunol.* **12**, 1202–1211 (2011).
69. Kain, L. *et al.* The Identification of the Endogenous Ligands of Natural Killer T Cells Reveals the Presence of Mammalian  $\alpha$ -Linked Glycosylceramides. *Immunity* **41**, 543–554 (2014).
70. Kain, L. *et al.* Endogenous ligands of natural killer T cells are alpha-linked glycosylceramides. *Mol. Immunol.* (2015). doi:10.1016/j.molimm.2015.06.009
71. De Libero, G. *et al.* Bacterial Infections Promote T Cell Recognition of Self-Glycolipids. *Immunity* **22**, 763–772 (2005).

72. Salio, M. *et al.* Modulation of human natural killer T cell ligands on TLR-mediated antigen-presenting cell activation. *Proc. Natl. Acad. Sci.* **104**, 20490–20495 (2007).
73. Tatituri, R. V. *et al.* Recognition of microbial and mammalian phospholipid antigens by NKT cells with diverse TCRs. *Proc. Natl. Acad. Sci.* **110**, 1827–1832 (2013).
74. Fischer, K. *et al.* Mycobacterial phosphatidylinositol mannoside is a natural antigen for CD1d-restricted T cells. *Proc. Natl. Acad. Sci. U. S. A.* **101**, 10685–10690 (2004).
75. Kinjo, Y. *et al.* Invariant natural killer T cells recognize glycolipids from pathogenic Gram-positive bacteria. *Nat. Immunol.* **12**, 966–974 (2011).
76. Lotter, H. *et al.* Natural Killer T Cells Activated by a Lipopeptidophosphoglycan from *Entamoeba histolytica* Are Critically Important To Control Amebic Liver Abscess. *PLoS Pathog.* **5**, e1000434 (2009).
77. Wolf, B. J. *et al.* Identification of a Potent Microbial Lipid Antigen for Diverse NKT Cells. *J. Immunol.* (2015). doi:10.4049/jimmunol.1501019
78. Gumperz, J. E. *et al.* Murine CD1d-restricted T cell recognition of cellular lipids. *Immunity* **12**, 211–221 (2000).
79. Carrington, J. C. & Dougherty, W. G. Small nuclear inclusion protein encoded by a plant potyvirus genome is a protease. *J. Virol.* **61**, 2540–2548 (1987).
80. T. Dawn Parks, Kerstin K. Leuther, Eric D. Howard, Stephen A. Johnston & William G. Dougherty. Release of Proteins and Peptides from Fusion Proteins Using a Recombinant Plant Virus Proteinase. *Anal. Biochem.* 413–417 (1994).
81. Kapust, R. B. & Waugh, D. S. Controlled Intracellular Processing of Fusion Proteins by TEV Protease. *Protein Expr. Purif.* **19**, 312–318 (2000).

82. Waugh, D. S. An overview of enzymatic reagents for the removal of affinity tags. *Protein Expr. Purif.* **80**, 283–293 (2011).
83. Sarkis K. Mazmanian, Gewn Liu, Hung Ton-That & Olaf Schneewind. Staphylococcus aureus Sortase, an Enzyme that Anchors Surface Proteins to the Cell Wall. *Science* (1999).
84. Hung Ton-That, Gewn liu, Sarkis K. Mazmanian, Kym F. Faull & Olaf Schneewind. Purification and characterization of sortase, the transpeptidase that cleaves surface proteins of Staphylococcus aureus at the LPXTG motif. *PNAS* 12424–12429 (1999).
85. Marraffini, L. A., DeDent, A. C. & Schneewind, O. Sortases and the Art of Anchoring Proteins to the Envelopes of Gram-Positive Bacteria. *Microbiol. Mol. Biol. Rev.* **70**, 192–221 (2006).
86. Popp, M. W.-L., Antos, J. M. & Ploegh, H. L. in *Current Protocols in Protein Science* (eds. Coligan, J. E., Dunn, B. M., Speicher, D. W. & Wingfield, P. T.) (John Wiley & Sons, Inc., 2009). at <<http://doi.wiley.com/10.1002/0471140864.ps1503s56>>
87. Guimaraes, C. P. *et al.* Site-specific C-terminal and internal loop labeling of proteins using sortase-mediated reactions. *Nat. Protoc.* **8**, 1787–1799 (2013).
88. Gey, G.O., Coffman, W.D. & Kubicek, M.T. Tissue culture studies of the proliferative capacity of cervical carcinoma and normal epithelium. *Cancer Res.* **12**, 264–265 (1952).
89. Sanford, KK, Earle, WR & Likely, GD. The growth of single isolated tissue cells. *J Natl Cancer Inst* **9**, 229–46 (1948).
90. Vidal, K, Grosjean, I, Evillard, J.P., Gespach, C. & Kaiserlian, D. Immortalization of mouse intestinal epithelial cells by the SV40-large T gene. Phenotypical and

- immune characterization of the MODE-K cell line. *J Immunol Methods* 63–73 (1993).
91. Tsuchiya, S *et al.* Establishment and characterization of a human acute monocytic leukemia cell line (THP-1). *Int J Cancer* **26**, 171–6 (1980).
92. *High Throughput Protein Expression and Purification*. **498**, (Humana Press, 2009).
93. Huang, S. *et al.* Discovery of deoxyceramides and diacylglycerols as CD1b scaffold lipids among diverse groove-blocking lipids of the human CD1 system. *Proc. Natl. Acad. Sci.* **108**, 19335–19340 (2011).
94. Kim, H. S. *et al.* Biochemical Characterization of CD1d Expression in the Absence of  $\beta$ 2-microglobulin. *J. Biol. Chem.* **274**, 9289–9295 (1999).
95. Klausner, R. D., Donaldson, J. G. & Lippincott-Schwartz, J. Brefeldin A: insights into the control of membrane traffic and organelle structure. *J. Cell Biol.* **116**, 1071–1080 (1992).
96. Kim, M., O’Callaghan, P. M., Droms, K. A. & James, D. C. A mechanistic understanding of production instability in CHO cell lines expressing recombinant monoclonal antibodies. *Biotechnol. Bioeng.* **108**, 2434–2446 (2011).
97. Krishnan, M. *et al.* Effects of epigenetic modulation on reporter gene expression: implications for stem cell imaging. *FASEB J.* **20**, 106–108 (2006).
98. Gates, F. T., Coligan, J. E. & Kindt, T. J. Complete amino acid sequence of murine beta 2-microglobulin: structural evidence for strain-related polymorphism. *Proc. Natl. Acad. Sci.* **78**, 554–558 (1981).
99. Wang, Z. *et al.* Differential Effect of Human and Mouse  $\beta$ 2-Microglobulin on the Induction and the Antigenic Profile of Endogenous HLA-A and-B Antigens Synthesized by  $\beta$ 2-Microglobulin Gene-null FO-1 Melanoma Cells. *Cancer Res.* **53**, 4303–4309 (1993).



100. Pedersen, L. Ø. *et al.* The interaction of beta 2-microglobulin ( $\beta$ 2m) with mouse class I major histocompatibility antigens and its ability to support peptide binding. A comparison of human and mouse  $\beta$ 2m. *Eur. J. Immunol.* **25**, 1609–1616 (1995).
101. Tysoe-Calnon, V. A., Grundy, J. E. & Perkins, S. J. Molecular comparisons of the beta2-microglobulin-binding site in Class I major-histocompatibility-complex alpha-chains and proteins of related sequences. *Biochem J* **277**, 359–369 (1991).
102. Truman, A. & Hook, B. A TEV Protease Compatible with Inhibitory Compounds from Protein Purification. (2013). at <<http://www.promega.de/resources/pubhub/a-tev-protease-compatible-with-inhibitory-compounds-from-protein-purification>>
103. Lindl, T. in *Zell- und Gewebekultur* (2002).
104. Yin, W., Xiang, P. & Li, Q. Investigations of the effect of DNA size in transient transfection assay using dual luciferase system. *Anal. Biochem.* **346**, 289–294 (2005).
105. Reddy Chichili, V. P., Kumar, V. & Sivaraman, J. Linkers in the structural biology of protein-protein interactions. *Protein Sci.* **22**, 153–167 (2013).
106. Argos, P. An Investigation of Oligopeptides Linking Domains in Protein Tertiary Structures and Possible Candidates for General Gene Fusion. *J Mol Biol* **211**, 943–958 (1990).
107. George, R. A. & Heringa, J. An analysis of protein domain linkers: their classification and role in protein folding. *Protein Eng.* **15**, 871–879 (2002).
108. Nagi, A. D. & Regan, L. An inverse correlation between loop length and stability in a four-helix-bundle protein. *Fold. Des.* **2**, 67–75 (1997).

109. Pellicci, D. G. *et al.* Differential Recognition of CD1d- $\alpha$ -Galactosyl Ceramide by the V $\beta$ 8.2 and V $\beta$ 7 Semi-invariant NKT T Cell Receptors. *Immunity* **31**, 47–59 (2009).
110. Rossjohn, J., Pellicci, D. G., Patel, O., Gapin, L. & Godfrey, D. I. Recognition of CD1d-restricted antigens by natural killer T cells. *Nat. Rev. Immunol.* **12**, 845–857 (2012).
111. Godfrey, D. I. *et al.* Antigen recognition by CD1d-restricted NKT T cell receptors. *Semin. Immunol.* **22**, 61–67 (2010).
112. Zajonc, D. M., Savage, P. B., Bendelac, A., Wilson, I. A. & Teyton, L. Crystal Structures of Mouse CD1d-iGb3 Complex and its Cognate V $\alpha$ 14 T Cell Receptor Suggest a Model for Dual Recognition of Foreign and Self Glycolipids. *J. Mol. Biol.* **377**, 1104–1116 (2008).
113. Whitehead, R. H., VanEeden, P. E., Noble, M. D., Ataliotis, P. & Jat, P. S. Establishment of conditionally immortalized epithelial cell lines from both colon and small intestine of adult H-2Kb-tsA58 transgenic mice. *Proc. Natl. Acad. Sci.* **90**, 587–591 (1993).
114. Suda, T. & Liu, D. Hydrodynamic Gene Delivery: Its Principles and Applications. *Mol. Ther.* **15**, 2063–2069 (2007).

## 9 Appendix

### 9.1 Figure Index

Figure 1: NKT Cells Secrete Various Cytokines Upon Activation.....	3
Figure 2: Schematic Depiction of the Antigen-Binding Grooves of the CD1 Isoforms .....	27
Figure 3: Trafficking of mCD1d.....	29
Figure 4: Antigenic Self-Lipids.....	30
Figure 5: Schematic Depiction of TEV Protease- and Sortase A-Mediated Protein Cleavage.....	33
Figure 6: Schematic Depiction of the h $\beta_2$ m_mCD1d_TEV(GGGS) <sub>3</sub> PIPE Substitution PCR.....	45
Figure 7: Schematic overview of mCD1d constructs.....	59
Figure 8: Comparison of the Expression of Different Genetically Modified mCD1d Constructs in MODE-K cells.....	60
Figure 9: TEV Protease Fails to Cleave h $\beta_2$ m_mCD1d_TEV, While TEV Buffer Affects Cell Viability.....	62
Figure 10: mCD1d ELISA of Supernatants of Mouse Fibroblast Cells Stably Transfected with h $\beta_2$ m_mCD1d_TEV or WT mCD1d.....	63
Figure 11: Alternative Buffer Systems and TEV Proteases for Enzymatic Release of CD1d.....	65
Figure 12: Glycine-Serine Spacers Do Not Promote TEV Protease-Mediated Cleavage of CD1d.....	67
Figure 13: SrtA Digest of HeLa Cells Transfected with LPETG_mCD1d(GGGS) <sub>0-2</sub> or THP 1 Cells Stably Transfected with LPETG_hCD1d_(GGGS) <sub>3</sub> .....	69
Figure 14: mCD1d ELISA of HeLa Cells Transfected with LPETG_mCD1d(GGGS) <sub>0-2</sub> after SrtA Digest.....	70
Figure 15: Flow Cytometric Analysis of the Expression of LPETG_mCD1d(GGGS) <sub>0-2</sub> using pcep4 and pcDNA3.1 Vector Backbones.....	71
Figure 16: SrtA Digest of HeLa cells Transfected with pcDNA_LPETG_mCD1d(GGGS) <sub>0-2</sub> .....	73
Figure 17: Antigen Presentation by LPETG_mCD1d(GGGS) <sub>0-2</sub> Expressing HeLa Cells.....	75
Figure 18: pcDNA3.1_h $\beta_2$ m_sol_mCD1d plasmid map.....	102
Figure 19: pcDNA3.1_m $\beta_2$ m_sol_mCD1d plasmid map.....	103

Figure 20: pcDNA3.1_h $\beta_2$ m_mCD1d_TEV plasmid map .....	104
Figure 21: pcDNA3.1_m $\beta_2$ m_mCD1d_TEV plasmid map .....	105
Figure 22: pcDNA3.1 h $\beta_2$ m_mCD1d_TEV(GGGS) <sub>3</sub> plasmid map .....	106
Figure 23: pcDNA3.1_LPETG_mCD1d(GGGS) <sub>0</sub> plasmid map .....	107
Figure 24: pcDNA3.1_LPETG_mCD1d(GGGS) <sub>1</sub> plasmid map .....	108
Figure 25: pcDNA3.1_LPETG_mCD1d(GGGS) <sub>2</sub> plasmid map .....	109

## 9.2 Table Index

Table 1: Antibodies.....	35
Table 2: Primer Sequences .....	44
Table 3: Composition of a PIPE-PCR Reaction .....	46
Table 4: Reaction Conditions for PIPE-PCR .....	46
Table 5: Restriction Digest of Plasmid DNA .....	47
Table 6: Restriction Digest of PCR Products.....	47
Table 7: Reaction Conditions for TEV-Mediated Cleavage of CD1d .....	50
Table 8: Reaction Conditions For Transfection Using Lipofectamine .....	52
Table 9: Reaction Conditions for Transfection Using Turbofect .....	53

## 9.3 Plasmid Maps

Created with SnapGene®

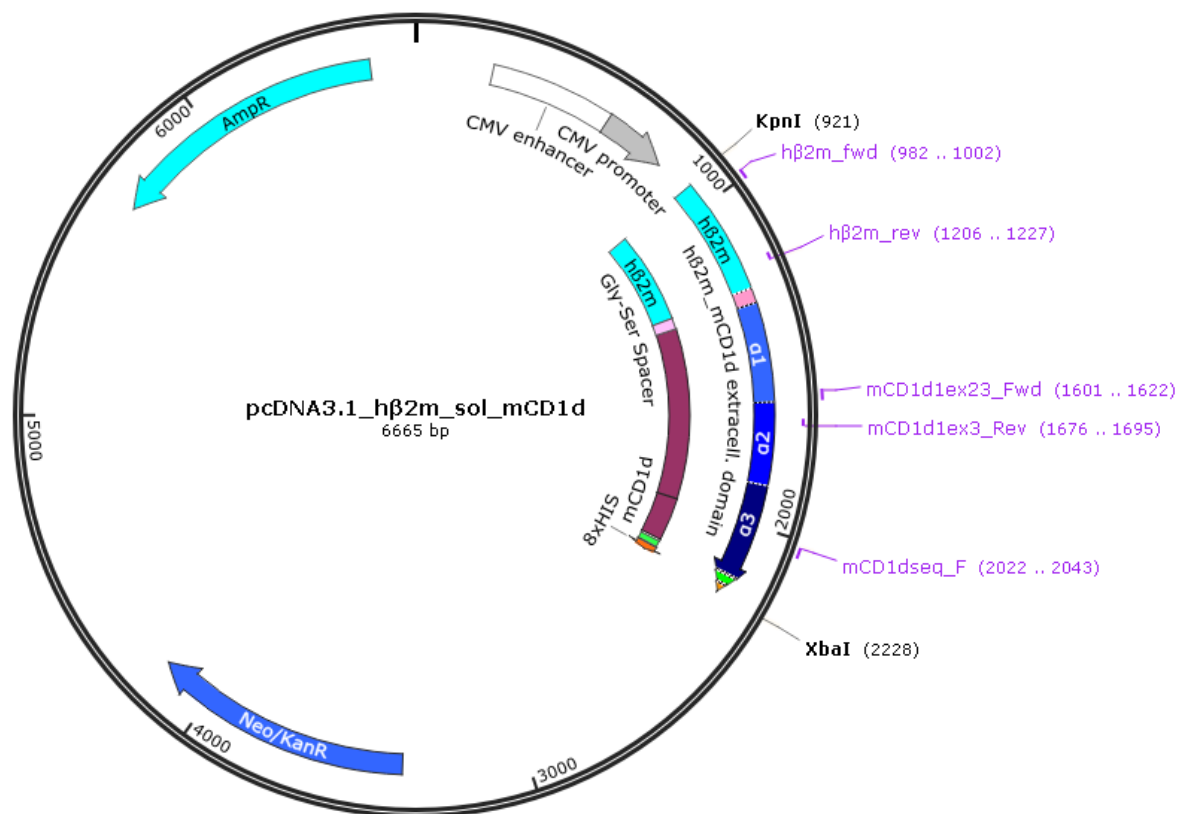
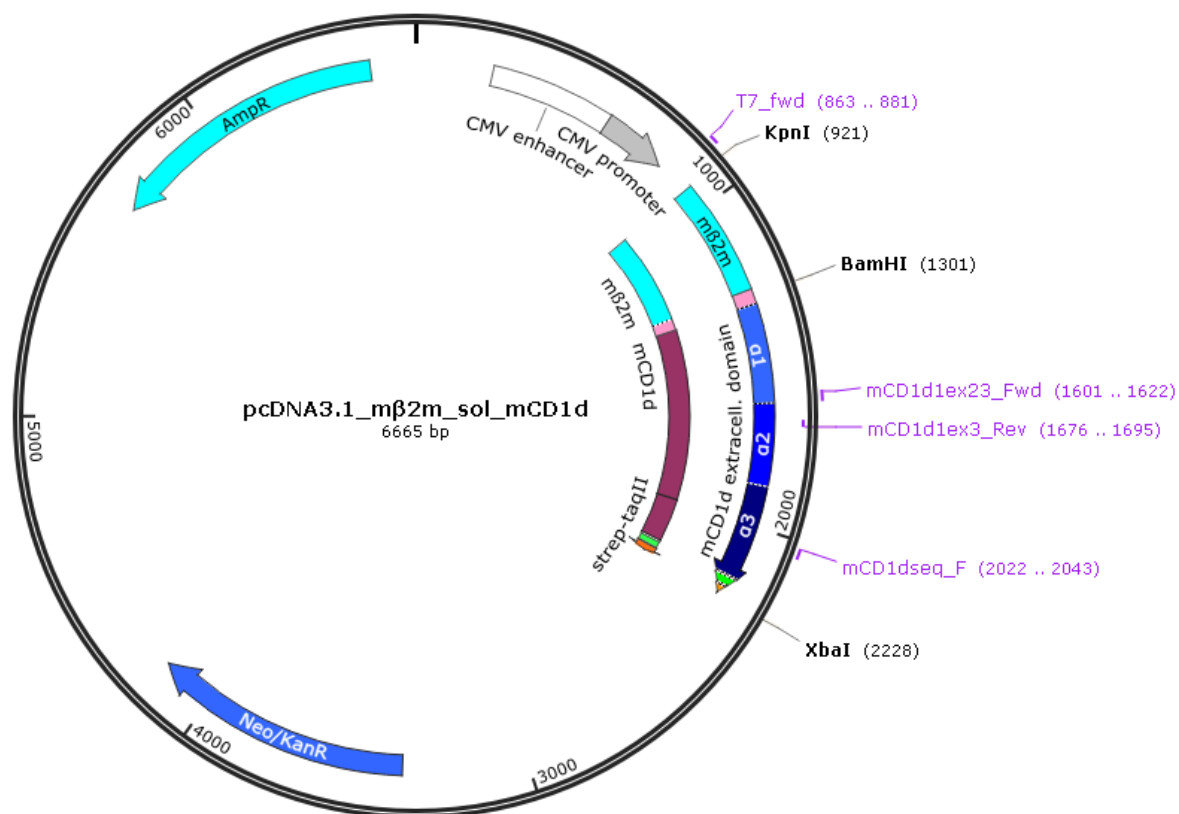


Figure 18: pcDNA3.1\_hβ<sub>2</sub>m\_sol\_mCD1d plasmid map



**Figure 19: *pcDNA3.1\_mβ2m\_sol\_mCD1d* plasmid map**

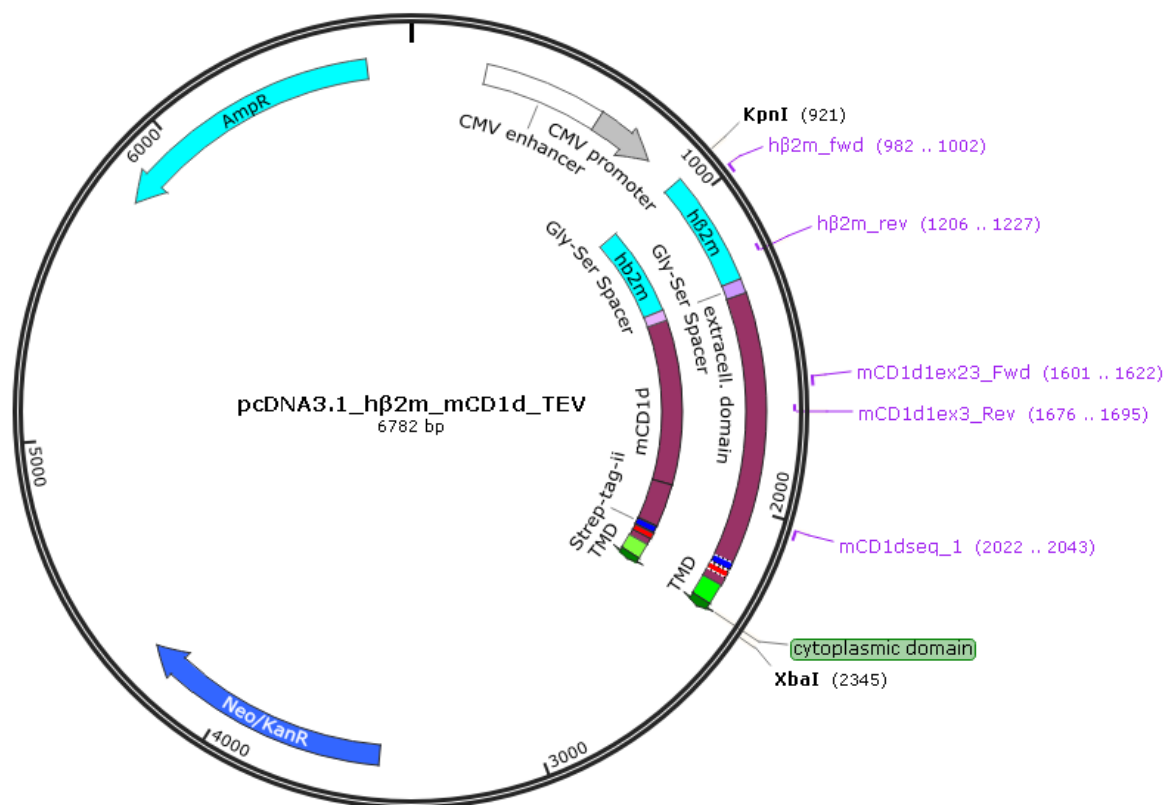


Figure 20: pcDNA3.1\_hβ<sub>2</sub>m\_mCD1d\_TEV plasmid map

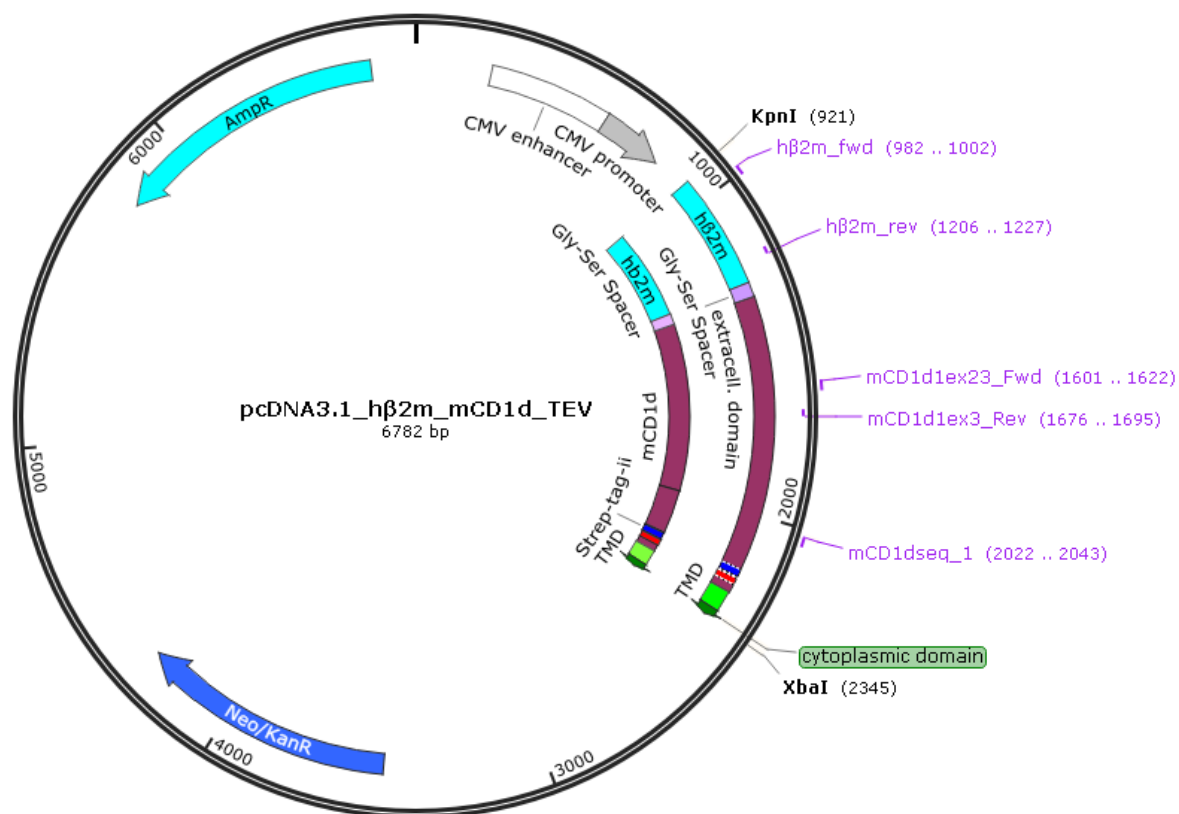


Figure 21: pcDNA3.1\_mβ<sub>2</sub>m\_mCD1d\_TEV plasmid map



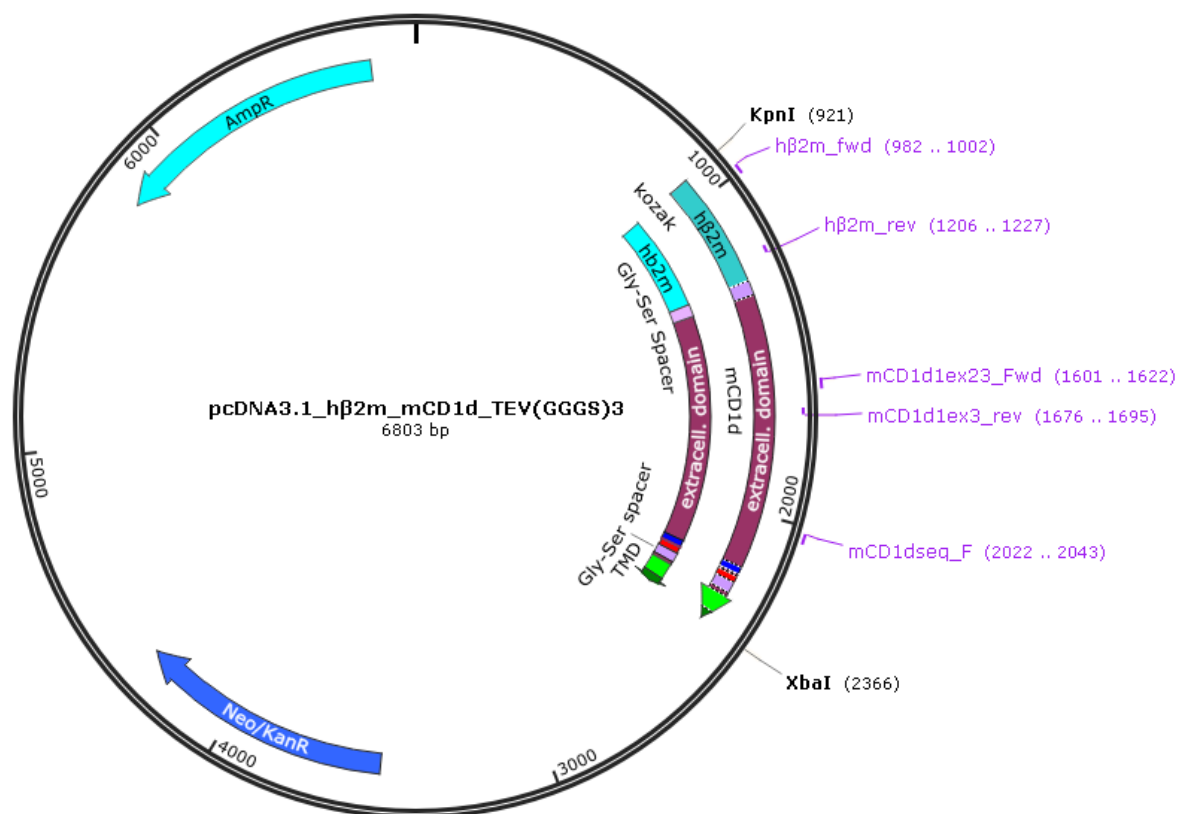
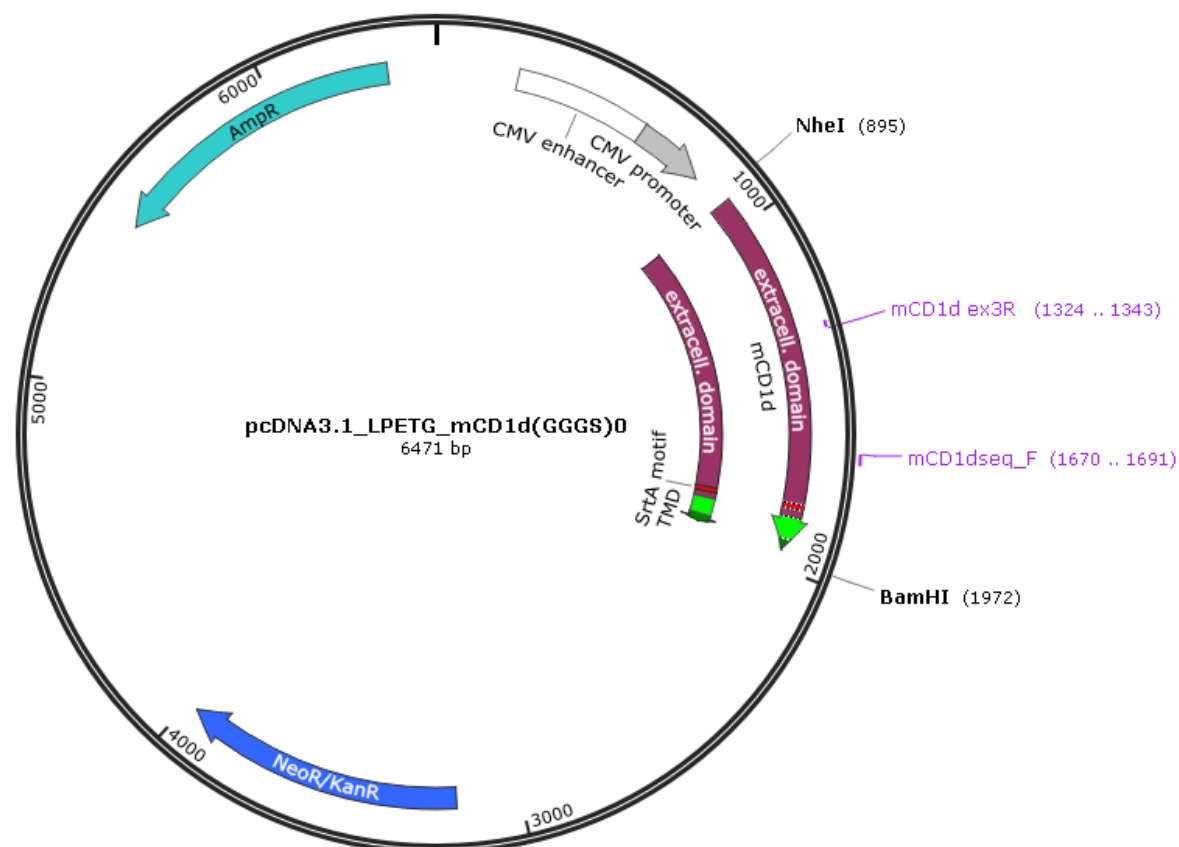
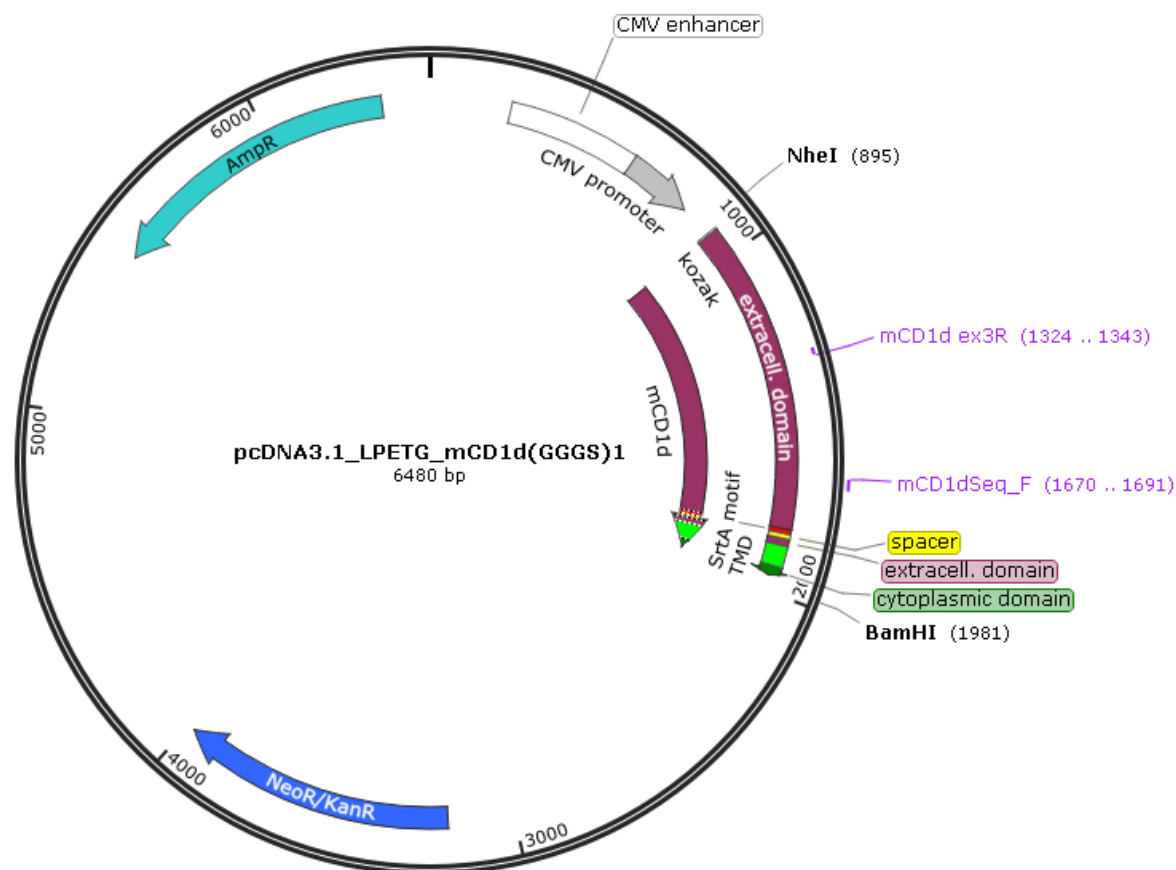


Figure 22: pcDNA3.1 hβ<sub>2</sub>m\_mCD1d\_TEV(GGGS)<sub>3</sub> plasmid map



**Figure 23: pcDNA3.1\_LPETG\_mCD1d(GGGS)<sub>0</sub> plasmid map**



**Figure 24: pcDNA3.1\_LPETG\_mCD1d(GGGS)<sub>1</sub> plasmid map**

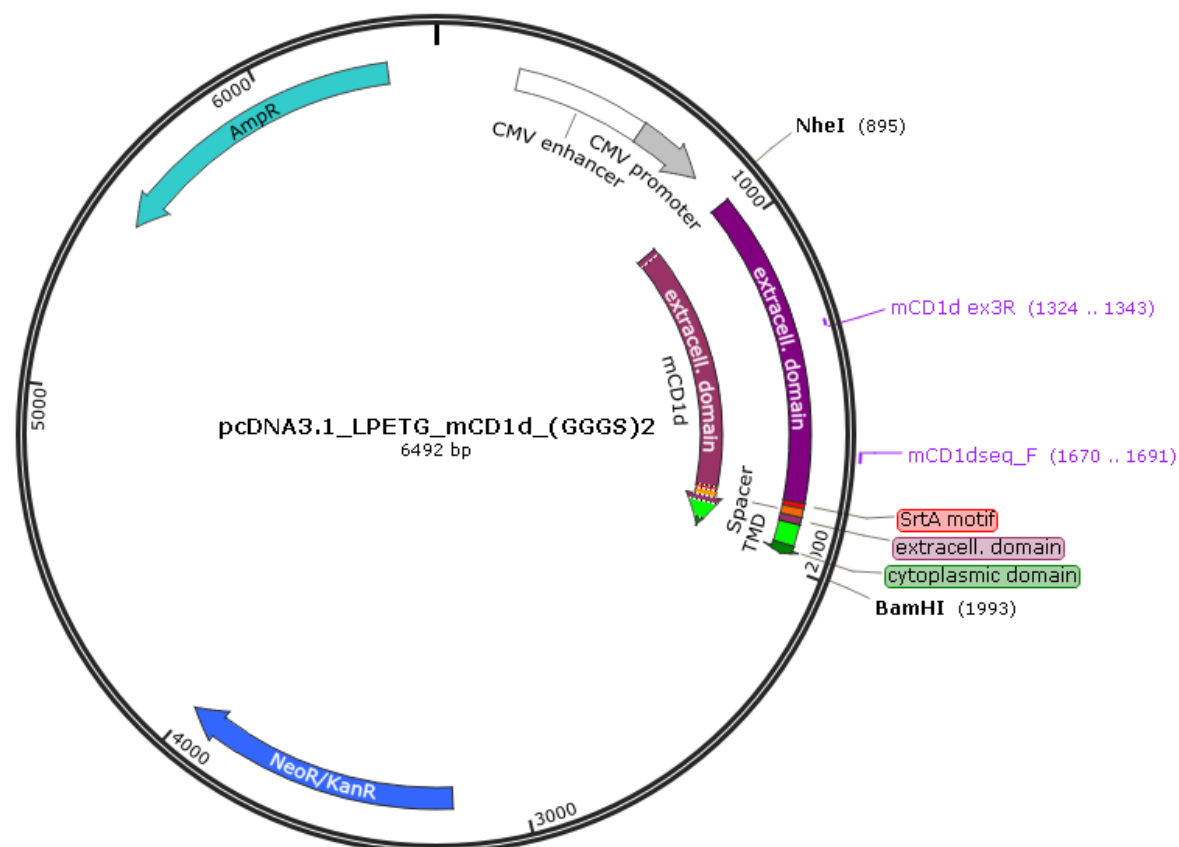


Figure 25: *pcDNA3.1\_LPETG\_mCD1d(GGGS)<sub>2</sub>* plasmid map

## **Acknowledgments**

First of all I would like to thank Prof. Dr. Sebastian Zeiig for giving me the opportunity to prepare my thesis in his lab. Working on different projects has taught me a lot and I want to thank you for many fruitful discussions and your constant enthusiasm.

A great Thank you to Prof. Dr. Thomas Roeder for providing a second opinion on my thesis.

I would also like to thank Prof. Dr. Richard S. Blumberg, Dr. Torsten Olszak and Dr. Joana F. Neves, as well as Dr. Gijsbert Grotenbreg for insightful discussions and helpfull suggestions.

Lab life would be boring and sometimes quite frustrating without great colleagues, so thanks to everyone from the AG Zeiig for nice lunch breaks in the sun, "Feierabend" talks in the lab and fun activities outside work. A special Thank you to Esther for showing me the ropes when I first started and for accepting me into her group of friends immediately. Thank you to all of you who helped with big experiments, especially Esther, Mirko, Kerstin and Sabin. Emilie, Mirko, thank you for your support with the CD1d project and many helpful discussions.

A big thank you to anyone who gave me their time reading parts of this thesis: Emilie, Angelika, Matti – I very much appreciate it!

To all my friends, especially Heike and Verena, who offered fun and distraction when I needed it and pushed me to stay positive, even through rough patches – thank you guys!

Matti, you are my calm in the storm. Thanks for being the ever-positive you and sticking with me through all the Ups and Downs of the past couple of years.

And most importantly: my family. Your endless love, support and encouragement has gotten me to where I am today and it means the world to me. Thank you for always pushing me to be my best and always being there for me.

## Curriculum Vitae

### Personal Information

---

Date of Birth	04/28/1987
Place of Birth	Frederick, Maryland (USA)
Citizenship	German, American
Current residence	Muhliusstr. 77, 24103 Kiel

### Education

---

Since 09/2015	Research assistant in the group of Prof. Dr. Dietrich Kabelitz, University Medical Center Kiel, Germany
Since 05/2012	PhD student in the group of Prof. Dr. Sebastian Zeißig, University Medical Center Kiel, Germany
12/2011	Master's Degree;  Thesis title: "APP and LRP1 Traffic in Common Transport Vesicles" (Final Grade 1,2)  Awarded the GBM-Master-/Diplomaprize 2012
10/2010 - 12/2011	Student at the Technical University of Kaiserslautern, Department of Biology, Study programme 'Biosciences'
08/2010	Bachelor's Degree;  Thesis title: 'Investigation of the Sub-Cellular Localization of APP Dimers' (Final Grade 2,3)
08/2008 - 01/2009	ERASMUS Semester at the University of Gothenburg, Sweden
10/2006 - 08/2010	Student at the Technical University of Kaiserslautern, Department of Biology, Study programme 'Biowissenschaften'

**School Career**

---

1999 - 03/2006 Elisabeth Langgässer Gymnasium, Alzey, Germany  
Abitur (Final Grade 2,1)

1997 - 1999 Lina Hilger Gymnasium, Bad Kreuznach, Germany

## Erklärung

Hiermit erkläre ich, dass...

...die vorliegende Dissertation nach den Regeln guter wissenschaftlicher Praxis der deutschen Forschungsgemeinschaft von mir eigenständig verfasst wurde.

...bis auf die angegebenen Quellen und die wissenschaftliche Beratung durch meinen Doktorvater Prof. Dr. Sebastian Zeißig keine weiteren Hilfsmittel in Anspruch genommen wurden.

...Teile dieser Dissertation veröffentlicht im Rahmen der Publikation

Olszak, T., Neves, JF., **Dowds, CM.** *et al.* Protective mucosal immunity mediated by epithelial CD1d and IL-10. *Nature* **509**, 497–502 (2014)

veröffentlicht wurden.

...diese Dissertation weder komplett, noch teilweise an anderer Stelle im Rahmen eines Prüfungsverfahrens vorgelegen hat.

Kiel, Oktober 2015

Marie Dowds